*Russian Chemical Reviews* **71** (8) 619 – 650 (2002) © 2002 Russian Academy of Sciences and Turpion Ltd

DOI 10.1070/RC2002v071n08ABEH000728

# Complex phosphates containing mono- and trivalent cations

L N Komissarova, M G Zhizhin, A A Filaretov

## Contents


| | | |
|---|---|---|
| I. | Introduction | 619 |
| II. | Double phosphates containing mono- and trivalent cations | 619 |
| III. | Hydrogen phosphates containing mono- and trivalent cations | 625 |
| IV. | Fluoride phosphates containing mono- and trivalent cations | 633 |
| V. | Hydroxide phosphates containing mono- and trivalent cations | 641 |
| VI. | Other complex phosphates containing mono- and trivalent cations | 646 |
| VII. | Conclusion | 648 |


**Abstract. The review surveys the data on the synthesis, structures, thermal stability and physical properties of complex phosphates containing $M^I$ and $M^{III}$ cations generated from double phosphates by the partial replacement $M^I \rightarrow H^+$ or $PO_4^{3-} \rightarrow X^{n-}$ [$X^{n-} = F^-$, $OH^-$, $EO_4^{n-}$ ($VO_4^{3-}$, $MoO_4^{2-}$) or $S_2O_3^{2-}$]. The sizes of the $M^I$ and $M^{III}$ cations and their ratio have a dominant role in the structure formation of complex phosphates. The prospects of the use of complex phosphates as polyfunctional materials are discussed. The bibliography includes 161 references.**

## I. Introduction

In the last two decades, an extensive search has been carried out for new ferroelectric, piezoelectric, laser, luminescent and other materials, which can be applied in quantum electronics and fibre optics and used as sorbents and catalysts. In this connection, complex phosphates containing mono- and trivalent cations, in particular, compounds of the $M^I_3M^{III}(PO_4)_2$ and $M^I_3M^{III}_2(PO_4)_3$ types ($M^I$ are alkali metals), attract considerable interest.[1] These compounds exhibit ionic conductivity as well as nonlinear optical and other interesting properties. Numerous luminophores possessing excellent technical characteristics have been already prepared on the basis of inorganic phosphates.[2, 3]

The classical approach to the design of new materials involves the construction of more compositionally complex compounds and composites. Presently, new methods for the preparation of phosphates containing different combinations of mono- and polyvalent cations as well as procedures for the synthesis of complex phosphates in which the $PO_4^{3-}$ anions are combined with the $F^-$, $OH^-$, $VO_4^{3-}$, $MoO_4^{2-}$ or $S_2O_3^{2-}$ anions attract considerable attention.

Purposeful changes in the compositions of the cationic and anionic components of complex phosphates allow one to vary the dimensional characteristics of framework structures and interlayer spaces in layered phases thus influencing various properties of complex phosphates containing $M^I$ and $M^{III}$ cations, in particular, the ionic mobility, ion-exchange processes, catalytic properties and sensor characteristics (gas detection). Complex hydrogen phosphates containing the $H^+$ ions and polyvalent cations are of obvious interest. The data on these types of complex phosphates have not been generalised. Such complex orthophosphates involving the $H^+$ ions and anions of different nature along with $M^I$ and $M^{III}$ cations are the subject of the present review. Both the data published in the literature and the results of our studies are surveyed. The review also surveys the data on double orthophosphates containing mono- and trivalent cations. The latter compounds along with hydrogen orthophosphates with trivalent cations are parent compounds of complex phosphates under consideration.

Each group of complex phosphates containing $M^I$ and $M^{III}$ cations is characterised by different compositions. The targeted synthesis of new complex phosphates containing variable combinations of cations and anions and predictions of their physicochemical characteristics require revealing the composition – structure – property relationships for different types of compounds, in particular, for complex double and hydrogen phosphates containing $M^I$ and $M^{III}$ cations, fluoride phosphates, hydroxide phosphates and phosphates containing other tetrahedral groups.

## II. Double phosphates containing mono- and trivalent cations

Studies of the phase formation in the $M^I_3PO_4 - M^{III}PO_4$ systems ($M^I$ = Na, K; $M^{III}$ = REE, Y, In, Sc)[4–8] were started in 1970s in connection with a search for new laser, luminescent and other materials. Two types of compounds, *viz.*, $M^I_3M^{III}(PO_4)_2$ (**1**) and $M^I_3M^{III}_2(PO_4)_3$(**2**), were found.† Compounds **1** are known for all rare-earth (Y, La – Lu) and some other (Sc, In, Fe) elements,

**L N Komissarova, M G Zhizhin** Department of Chemistry, M V Lomonosov Moscow State University, Leninskie Gory, 119992 Moscow, Russian Federation. Fax (7-095) 932 88 46. Tel. (7-095) 939 58 56 E-mail: komissarova@inorg.chem.msu.ru (L N Komissarova). Tel. (7-095) 939 52 48. E-mail: zhizhin@tech.chem.msu.ru (M G Zhizhin)
**A A Filaretov** N S Kurnakov Institute of General and Inorganic Chemistry, Russian Academy of Sciences, Leninsky prosp. 31, 119991 Moscow, Russian Federation. Fax (7-095) 954 12 79. Tel. (7-095) 939 58 56. E-mail: andfil@lamar.colostate.edu

Received 24 April 2002
*Uspekhi Khimii* **71** (8) 707 – 740 (2002); translated by T N Safonova

† Data on double phosphates with more complex compositions, *viz.*, $Na_6M^{III}_3(PO_4)_5$ (**3**), where $M^{III}$ = Dy, Ho or Tm, are limited to the conditions of their formation in the $Na_3PO_4 - M^{III}PO_4$ binary systems.[4]

whereas compounds **2** are typical only of trivalent cations with the ionic radii $r_{M^{III}} \leqslant 0.85$ Å. In studies of these compounds, primary attention has been given to their structures, polymorphic transformations, ionic conductivity and luminescent properties.

## 1. Synthesis

Phosphates with compositions $M^I_3M^{III}(PO_4)_2$ and $M^I_3M^{III}_2(PO_4)_3$ are generally prepared by the solid-phase synthesis from stoichiometric amounts of oxide $M^{III}_2O_3$, carbonate $M^I_2CO_3$ and alkali-metal and ammonium hydrogen orthophosphates characterised by different degrees of replacement at temperatures from 400 to 1100 °C.[9–11] Different types of dielectric ceramics with such compositions are produced by hot pressing.[12] The synthesis from aqueous solutions of the corresponding salts at normal[13] or high[14] pressure (hydrothermal method) is used more rarely. There are also procedures, which, strictly speaking, cannot be considered as preparative. As an example we refer to the reactions of cerium(IV) oxide with sodium and potassium hydrogen phosphates or diphosphates[15] accompanied by oxygen liberation. Another procedure for the preparation of double phosphates involves calcination of mixtures of REE hydrogen phosphates with composition $H_3M^{III}(PO_4)_2 \cdot 2H_2O$ with alkali-metal hydroxides or carbonates.[16] Single crystals of $M^I_3M^{III}(PO_4)_2$ were grown under the hydrothermal conditions at high temperatures ($T = 600-900$ °C)[14] or prepared by crystallisation from flux using an excess of alkali-metal halides (for example, KF).[17]

## 2. Structures and properties

Compounds with composition $M^I_3M^{III}(PO_4)_2$ containing different metal cations are similar in structure and physicochemical characteristics. The main structural feature common to all compounds of this group is the fact that they belong to the glaserite [$K_3Na(SO_4)_2$], arcanite (β-$K_2SO_4$), sodium chromate ($Na_2CrO_4$) or NASICON ‡ [$NaZr_2(PO_4)_3$] structural types (Fig. 1).

The $K_3Na(SO_4)_2$ (space group $P\bar{3}m1$, $a_1 = b_1 = 5.680$, $c_1 = 7.309$ Å),[18] β-$K_2SO_4$ (space group *Pnam*, $a_2 = 7.456$, $b_2 = 10.080$, $c_2 = 5.776$ Å)[19] and $Na_2CrO_4$ (space group *Cmcm*, $a_3 = 5.862$, $b_3 = 9.251$, $c_3 = 7.145$ Å)[20] structural types are widespread among inorganic salts with the $PO_4^{3-}$ tetrahedral anions.[1,21,22] All these salts belong to layered structures. In the crystals of these salts, the $PO_4$ tetrahedra have different orientations with respect to the cation positions (denoted as *M*, *X* and *Y*, see Fig. 1)[21] and can combine with each other to form numerous subtypes. The relationship between the parent structural types can be represented as the relation between the unit cell parameters of glaserite ($a_1$, $b_1$, $c_1$) and those of arcanite ($a_2$, $b_2$, $c_2$) and sodium chromate ($a_3$, $b_3$, $c_3$): $a_2 \approx c_1$, $b_2 \approx a_1\sqrt{3}$, $c_2 \approx a_1$ and $a_3 \approx a_1$, $b_3 \approx a_1\sqrt{3}$, $c_3 \approx c_1$.

It is assumed that the ratio between the radii of the cations is the governing factor responsible for the formation of glaserite- or arcanite-like structures.[21] The glaserite-like structures are stable for compounds in which the difference between the radii of the $M^+$ and $M^{3+}$ cations [$\Delta r_{(M^+-M^{3+})}$][23] occupying the *M*, *X* and *Y* positions is in the range $0.59 \leqslant \Delta r_{(M^+-M^{3+})} \leqslant 0.89$ Å.[21,24–27] However, compounds that are characterised by $\Delta r_{(M^+-M^{3+})} < 0.59$ Å and have glaserite-like structures are also known. Thus, $\Delta r_{(M^+-M^{3+})}$ for $Na_3Fe(PO_4)_2$ (glaserite structural type) is 0.38 Å.[24] At $\Delta r_{(M^+-M^{3+})} < 0.59$ Å, compounds generally crystallise in the arcanite structural type.[19–22]

‡ NASICON stands for Na Super Ionic Conductors.

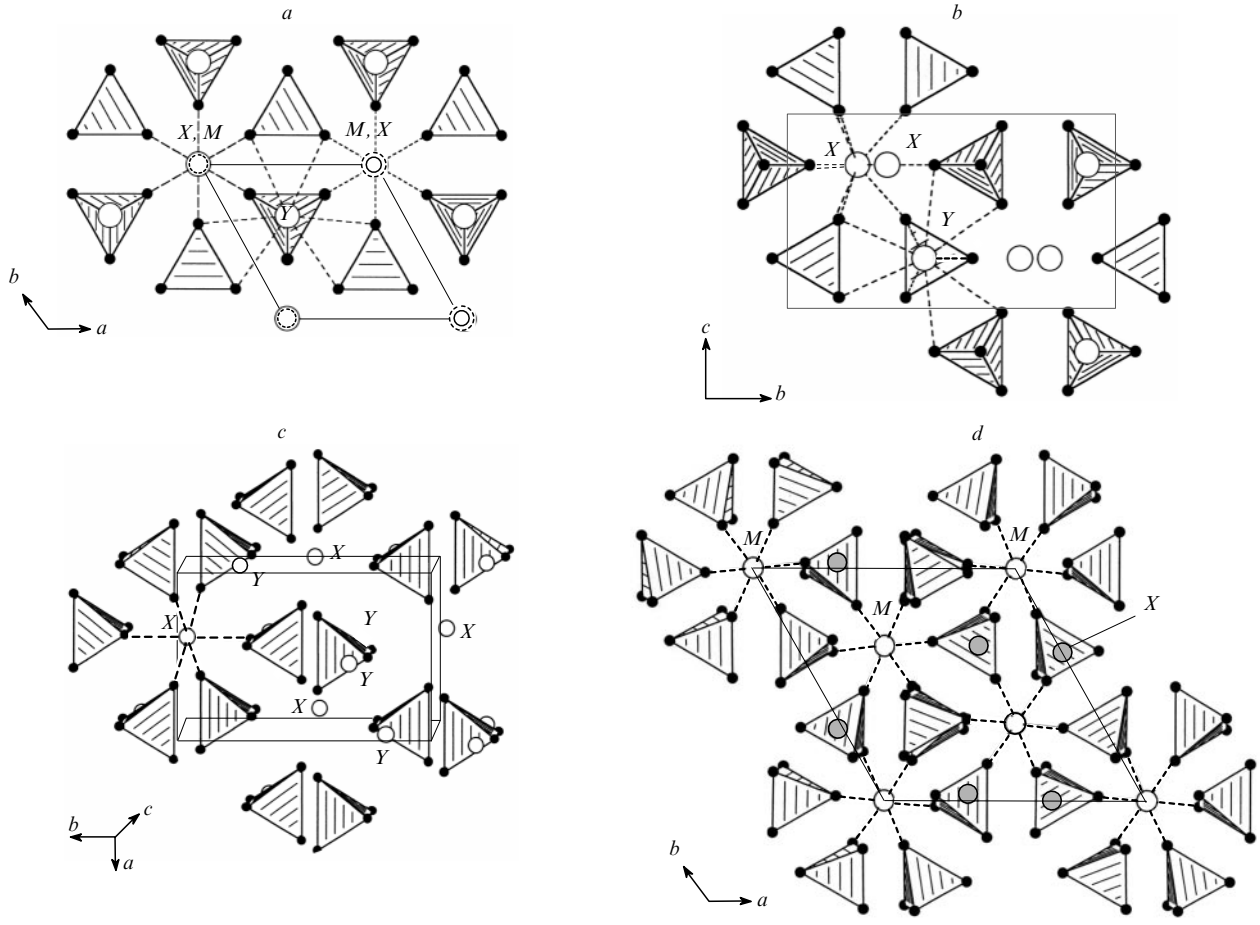



**Figure 1.** Projections of the $K_3Na(SO_4)_2$ (*a*), β-$K_2SO_4$ (*b*), $Na_2CrO_4$ (*c*), and $NaZr_2(PO_4)_3$ (NASICON) (*d*) structures. Hereinafter, the structures are drawn using the atomic coordinates published in the original studies.

The majority of representatives of the $M^{I}_{3}M^{III}(PO_4)_2$ group have structures of arcanite (β-$K_2SO_4$) or structures of an intermediate type (combinations of the β-$K_2SO_4$ and $Na_2CrO_4$ structures). In particular, the former structural type is typical of $K_3M^{III}(PO_4)_2$ ($M^{III}$ = La – Yb)[1, 17, 28] and the latter type is characteristic of $K_3In(PO_4)_2$ (see Ref. 29) and β-$Na_3M^{III}(PO_4)_2$ ($M^{III}$ = La – Lu, In).[13, 14, 30–33] These compounds belong to 'arcanite-like phosphates'.

In the structures of glaserite- and arcanite-like phosphates $M^{I}_{3}M^{III}(PO_4)_2$, the $M^{I}$ and $M^{III}$ cations occupy the *X* positions in an ordered fashion. The *Y* positions are occupied only by monovalent cations. However, the coordination polyhedra of the cations in the structures of $M^{I}_{3}M^{III}(PO_4)_2$ differ from those in the parent structural types due to distortions of the ideal β-$K_2SO_4$- and $Na_2CrO_4$-type crystal structures caused by displacements of the cations from the ideal positions and rotation of the $PO_4$ tetrahedra. For example, the coordination sphere about potassium in the structures of $K_3M^{III}(PO_4)_2$ ($M^{III}$ = Y, La – Yb) involves nine or ten oxygen atoms, whereas the coordination spheres about the REE atoms are formed by seven oxygen atoms. In $Na_3M^{III}(PO_4)_2$, the coordination numbers of both $Na^+$ and $M^{III}$ vary from 6 to 8 – 12.

The NASICON structural type can be described as the $\{[M^{III}_{2-x}\square_x(PO_4)_3]^{3-}\}_{3\infty}$ framework whose channels are occupied by alkali-metal cations.[21] The $NaZr_2(PO_4)_3$ (NASICON) structural type is widespread among superionic conductors, whereas double phosphates with composition $Na_3M^{III}(PO_4)_2$ containing only REE of the end of the series ($M^{III}$ = Tm, Yb, Lu) belong to this structural type. According to the stoichiometry of the framework, the structures of the latter compounds should be described by the $Na_{4.5}M^{III}_{1.5}(PO_4)_3$ formula.[34]

Most of the sodium-containing phosphates $Na_3M^{III}(PO_4)_2$ ($M^{III}$ = Y, La – Lu, In) have two or three crystal modifications each (Fig. 2, Table 1), *viz.*, monoclinic low-temperature β and γ modifications based on the arcanite structure (**A** type) or a combination of the β-$K_2SO_4$ and $Na_2CrO_4$ structures (arcanite-like structures, $\mathbf{A_1}$ – $\mathbf{A_5}$ subtypes) and high-temperature α modifications derived from the structures of glaserite (**G** type) or NASICON (**N** structural type).[20, 34]

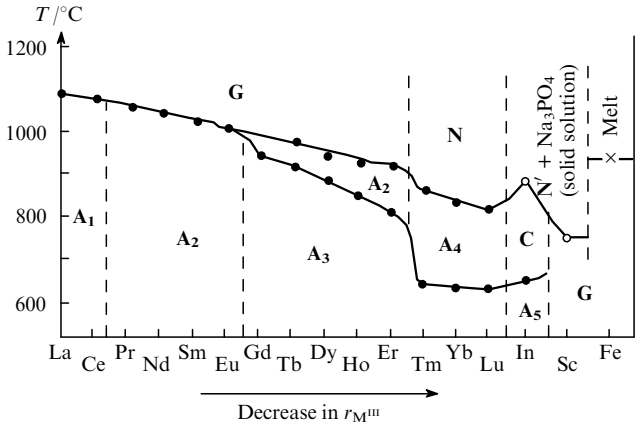



**Figure 2.** Occurrence of the structural types of the $Na_3M^{III}(PO_4)_2$ compounds depending on the temperature and nature of the $M^{III}$ cation. $\mathbf{A_1}$ – $\mathbf{A_5}$, arcanite-like subtypes (a combination of the β-$K_2SO_4$ and $Na_2CrO_4$ structures; **G**, **N** and **C**, the structural types of glaserite, NASICON and sodium chromate; **N′**, the NASICON-like phase with variable composition $Na_{3(1+x)}M^{III}_{(2-x)}(PO_4)_3$ ($0 \leqslant x \leqslant 0.2$).
Solid and empty circles denote polymorphic transformations and decomposition, respectively; the cross indicates incongruent melting.

The polymorphism of sodium-containing phosphates is, apparently, associated with a small difference in the ionic radii of sodium and trivalent REE. In arcanite-like structures of β-$Na_3M^{III}(PO_4)_2$, the proportion of the sodium-chromate structural motif in a combination of the β-$K_2SO_4$ and $Na_2CrO_4$ structures increases on going from lanthanum [$r_{VIII}(La^{3+})$ = 1.18 Å] to lutetium [$r_{VI}(Lu^{3+})$ = 0.85 Å] and indium

**Table 1**. Crystallographic characteristics of the $M^{I}_{3}M^{III}(PO_4)_2$ compounds.

| Compound | $M^{III}$ | Subtype (structural type) | Crystal system | Space group | $Z$[a] | Unit cell parameters | | | | Ref. |
|---|---|---|---|---|---|---|---|---|---|---|
| | | | | | | *a* /Å | *b* /Å | *c* /Å | β /deg | |
| β-$Na_3M^{III}(PO_4)_2$ | La – Ce | $Na_3La(PO_4)_2$ (**$A_1$**) | ortho-rhombic | $Pc2_1b$ | 8 | 5.34 (Ce) | 18.67 (Ce) | 14.05 (Ce) | – | 30 |
| | Pr – Eu | $Na_3Nd(PO_4)_2$ (**$A_2$**) | " | $Pbc2_1$ | 24 | 15.89 (Pr) – 15.88 (Eu) | 13.97 (Pr) – 13.96 (Eu) | 18.51 (Pr) – 18.47 (Eu) | – | 33 |
| | Y, Gd – Lu | $Na_3Nd(VO_4)_2$ (**$A_3$**) | mono-clinic | $Cc$ | 12 | 27.59 (Gd) – 27.27 (Lu) | 5.35 (Gd) – 5.28 (Lu) | 13.92 (Gd) – 13.88 (Lu) | 91.2 (Gd) – 91.3 (Lu) | 13 |
| | In | $Na_3In(PO_4)_2$ (**$A_5$**) | " | $P2_1/c$ | 4 | 7.127 | 18.220 | 8.616 | 143.36 | 14, 32 |
| γ-$Na_3M^{III}(PO_4)_2$ | Y, Nd – Er | $Na_3Nd(PO_4)_2$ (**$A_2$**) | ortho-rhombic | $Pbc2_1$ | 24 | 15.87 (Nd) – 15.86 (Er) | 13.95 (Nd) – 13.93 (Er) | 18.47 (Nd) – 18.31 (Er) | – | 33 |
| | Tm – Lu | $Na_3Tm(PO_4)_2$ (**$A_4$**) | " | $Pnmm$ ($Pnm2_1$) | 12 | 18.43 (Tm) – 18.33 (Lu) | 6.97 (Tm) – 6.95 (Lu) | 15.82 (Tm) – 15.80 (Lu) | – | 13 |
| α-$Na_3M^{III}(PO_4)_2$ | La – Er | $K_3Na(SO_4)_2$ (**G**) | trigonal | $P\bar{3}m1$ | 1 | 5.47 (La) – 5.37 (Er) | – | 7.69 (La) – 7.56 (Er) | – | 27 |
| | Tm – Lu | $NaZr_2(PO_4)_3$ (**N**) | " | $R\bar{3}c$ | 6 | 9.15 (Tm) – 9.11 (Lu) | – | 21.88 (Tm) – 21.80 (Lu) | – | 34 |
| | In | $Na_2CrO_4$ (**C**) | mono-clinic | $P2_1/m$ | 2 | 8.634 | 5.455 | 7.048 | 90.30 | 32 |
| | Fe | $K_3Na(CrO_4)_2$ (**G**) | " | $C2/c$ | 4 | 9.074 | 5.034 | 13.873 | 91.44 | 24 |
| $K_3M^{III}(PO_4)_2$ | Y, La – Yb | $K_3Nd(PO_4)_2$ (**A**) | " | $P2_1/m$ | 2 | 9.632 (La) – 9.324 (Yb) | 5.660 (La) – 5.613 (Yb) | 7.514 (La) – 7.417 (Yb) | 90.55 (Lu) – 90.92 (Yb) | 28 |
| | Lu | $K_3Na(SO_4)_2$ (**G**) | trigonal | $P\bar{3}$ | 3 | 9.611 | – | 7.731 | – | 26 |
| | In | $K_3In(PO_4)_2$ (**$A_6$**) | mono-clinic | $C2/c$ | 8 | 15.643 | 11.193 | 9.700 | 91.44 | 29 |
| | Sc | $K_3Na(SO_4)_2$ (**G**) | trigonal | $P\bar{3}$ | 3 | 9.424 | – | 7.619 | – | 25 |

[a] $Z$ is the number of formula units per unit cell.

[$r_{VI}(In^{3+}) = 0.76$ Å] to form new subtypes in the temperature range $T < 700-900$ °C. This is in agreement with the general principle consisting in the fact that trivalent cations in arcanite-like structures [for example, in β-$Na_3La(PO_4)_2$] occupy the $XO_8$ polyhedra corresponding to the $XO_9$ polyhedra in the structure of β-$K_2SO_4$, whereas these cations with smaller ionic radii tend to reduce their environment to octahedral, which corresponds to the $XO_6$ polyhedron in the structure of sodium chromate.[30,33] The $Na_3Sc(PO_4)_2$ and $Na_3Fe(PO_4)_2$ compounds with the $Sc^{3+}$ or $Fe^{3+}$ cations possessing smaller ionic radii [$r_{VI}(Sc^{3+}) = 0.745$ Å, $r_{VI}(Fe^{3+}) = 0.645$ Å] than $In^{3+}$ do not show polymorphism and crystallise in the glaserite structural type.[24]

As the temperature is increased ($T > 900$ °C), sodium-containing phosphates $Na_3M^{III}(PO_4)_2$ ($M^{III}$ = La–Er) are transformed from the β and γ modifications into the α modification corresponding to the higher-symmetry glaserite structural type. The high-temperature α modifications of $Na_3M^{III}(PO_4)_2$ ($M^{III}$ = Tm–Lu) belong to the NASICON structural type.[34] At high temperatures, α-$Na_3In(PO_4)_2$ would also be expected to transform into the NASICON-like modification. Instead, this compound decomposes at $T = 910$ °C to give a NASICON-like phase with variable composition $Na_{3(1+x)}In_{(2-x)}(PO_4)_3$ ($0 \leqslant x \leqslant 0.2$) and a solid solution based on α-$Na_3PO_4$. Analogous processes were observed upon heating of the $Na_3Sc(PO_4)_2$ and $Na_3Fe(PO_4)_2$ compounds above 790 and 975 °C, respectively.[24,31]

The nature and size of the REE ion have only a slight effect on the formation of a particular structural type of double potassium-containing phosphates $K_3M^{III}(PO_4)_2$.[28] However, a decrease in the ionic radius of the trivalent cation on going from ytterbium to lutetium also leads to the transformation from an arcanite-like to glaserite-like structure, which is accompanied by an increase in the symmetry of the crystal lattice from monoclinic [$K_3M^{III}(PO_4)_2$ compounds with large $M^{III}$ cations (Y, La–Yb)[27,28]] to trigonal [typical of $K_3M^{III}(PO_4)_2$, where $M^{III}$ = Lu or Sc[1,26]].

In the structures of $K_3M^{III}(PO_4)_2$ ($M^{III}$ = La–Yb), two of three potassium atoms are surrounded by ten oxygen atoms each, whereas the third potassium atom is surrounded by nine oxygen atoms. Due to distortion of the initial arcanite structure, the $X^{[6+3]}O_9$ polyhedra are transformed into $M^{III}O_7$ seven-vertex polyhedra, *viz.*, trigonal monocapped prisms with the $M^{III}-O$ distances in the range of 2.20–2.60 Å. In the virtually non-distorted glaserite-like structures of $K_3M^{III}(PO_4)_2$ ($M^{III}$ = Lu, Sc), the $M^{III}$ cations have an octahedral environment formed by oxygen atoms. Apparently, the transformation from an arcanite-like to glaserite-like structure is associated not only with an increase in the difference between the $M^{III}$ and $K^+$ radii but also with the effect of the electronic structure of the $M^{III}$ atom. Thus the $K_3Lu(PO_4)_2$ compounds [$\Delta r_{(K^+-Lu^{3+}_{VIII})} = 0.58$ Å] would be expected to have arcanite-like structures stable at $\Delta r_{(M^+-M^{3+})} < 0.59$ Å. However, $\Delta r_{(K^+-Lu^{3+}_{VI})}$ is actually equal to 0.69 Å and the glaserite-like structural type is realised. Because of the larger ionic radius of ytterbium [$\Delta r_{(K^+-Yb^{3+})} = 0.57$ Å] as compared to that of lutetium and the more labile *f* shell, the ytterbium cation tends to expand the nearest environment. As a consequence, $K_3Yb(PO_4)_2$ crystallises in the β-$K_2SO_4$ structural type. However, the arcanite-like structure of $K_3Yb(PO_4)_2$ is unstable and is readily destabilised under the action of different factors, in particular, upon the partial replacement of the $PO_4^{3-}$ ions by the bulkier $VO_4^{3-}$ anions.[28]

The $K_3In(PO_4)_2$ compound may be assigned to a new subtype of arcanite-like phosphates (**$A_6$**) characterised by a combination of the β-$K_2SO_4$ and $Na_2CrO_4$ structural motifs (Fig. 3).[29] Analysis of the crystal structure of $K_3In(PO_4)_2$ demonstrated that the potassium cations displace the indium cations from the *X* positions to the *Y* positions corresponding to the *Y* positions in the structure of sodium chromate (see Fig. 1 *c*), as distinct from double phosphate $Na_3In(PO_4)_2$ in which the *Y* positions are occupied exclusively by the $Na^+$ cations. Hence, the larger potassium cation (compared to sodium) causes the indium ions to change an octahedral environment formed by the oxygen atoms

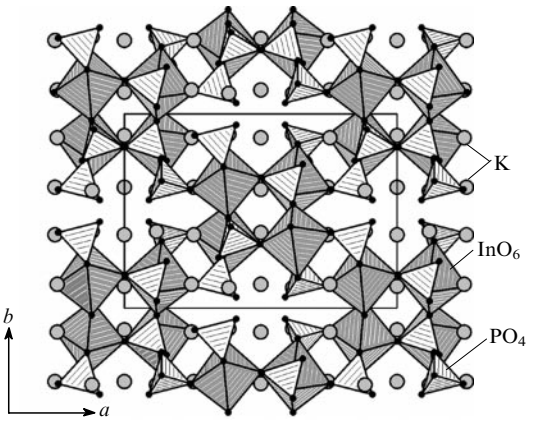



**Figure 3.** Structure of $K_3In(PO_4)_2$ projected onto the *ab* plane.

from six $PO_4$ tetrahedra for an octahedral environment formed by the oxygen atoms belonging to five $PO_4$ tetrahedra. In the structures of arcanite-like double phosphates $Na_3M^{III}(PO_4)_2$ ($M^{III}$ = La–Lu), the co-existence of the β-$K_2SO_4$ and $Na_2CrO_4$ motifs is achieved due to the presence of REE with different coordination numbers (6–8), whereas the co-existence of these motifs in the $K_3In(PO_4)_2$ structure is, apparently, associated with a substantial distortion of the polyhedra about the potassium atoms. Like the $K_3M^{III}(PO_4)_2$ compounds ($M^{III}$ = REE), $K_3In(PO_4)_2$ does not possess polymorphism below 1000 °C. The only difference is that the REE compounds decompose prior to melting ($T = 800-1000$ °C), whereas $K_3In(PO_4)_2$ melts congruently at a temperature above 1200 °C.[35] Taking into account the difference in the $K_3In(PO_4)_2$ and $K_3M^{III}(PO_4)_2$ structures ($M^{III}$ = Lu, Sc) and considering that the radii of the $M^{III}$ cations decrease in the series Lu–In–Sc, it can be assumed that the size of the $M^{III}$ cation is of secondary importance in the formation of a particular structural type in the group of the $M^I_3M^{III}(PO_4)_2$ compounds.

Double phosphates with composition $M^I_3M^{III}_2(PO_4)_3$ (type **2**, $M^I$ = Li, Na, K; $M^{III}$ = Fe, Sc, In, Cr) (Table 2) are typical of small $M^{III}$ cations ($r_{M^{3+}} < 0.8$ Å).[36–48] The crystallographic characteristics of such compounds in which $M^{III}$ is an REE atom (Ce–Gd) are available in the literature.[10,11] For these compounds, the unit cell parameters were calculated assuming of trigonal system. However, these data are in doubt. Composites of the general formula $M^I_{3(1+x)}M^{III}_{2-x}(PO_4)_3$ ($0.07 \leqslant x \leqslant 0.5$) are known. These composites belong to the region of solid solutions on the basis of high-temperature α modifications of $Na_{4.5}M^{III}_{1.5}(PO_4)_3$ ($M^{III}$ = Tm, Yb, Lu).[34]

The crystal structures of most of the $M^I_3M^{III}_2(PO_4)_3$ compounds were established, which made it possible to assign these compounds to the NASICON type. Complex phosphates of the general formula $M_xM'_2(PO_4)_3$, where $M = M^+$ (Li, Na) or $M^{2+}$ (Sr, Ba) and $M' = M^{2+}$ (Mg), $M^{3+}$ (Sc, In, Fe), $M^{4+}$ (Zr, Ti) or $M^{5+}$ (Ta, Nb), belong to this structural type. The occupancies of the *M* positions can vary over a wide range ($0 \leqslant x \leqslant 4$). The exception is the low-temperature β modification of $Na_3In_2(PO_4)_3$, which has an unusual structure.[45]

Depending on the combination of the cations, the symmetry of the unit cell in the $M^I_3M^{III}_2(PO_4)_3$ compounds changes from trigonal to monoclinic. All structures have framework structures built from the $M^{III}O_6$ and $PO_4$ polyhedra in a ratio of 2 : 3. The cavities in the framework are occupied by alkali-metal cations ($Li^+$, $Na^+$). The frameworks of the structures are penetrated by channels of two types, *I* and *II*, extended along the *b* axis of the unit cell (Fig. 4 *a*). The channel of type *III* are perpendicular to the channels *I* and *II* and intersect these channels. The smallest cross-sections of the channels *I*, *II* and *III* are 1.0, 1.1 and 0.9 Å, respectively. The large cavities in these channels (at the intersections of the channels *I* and *III* and of the channels *II* and *III*) are

**Table 2**. Crystallographic characteristics of the $M^I_3M^{III}_2(PO_4)_3$ compounds.

| Compound | $M^{III}$ | Crystal system | Space group | $Z$ | Unit cell parameters | | | | Ref. |
|---|---|---|---|---|---|---|---|---|---|
| | | | | | $a$ /Å | $b$ /Å | $c$ /Å | β /deg | |
| β-$Li_3M^{III}_2(PO_4)_3$ | Fe | monoclinic | $P2_1/n$ | 4 | 8.562 | 8.612 | 12.005 | 90.5 | 37 |
| | Sc | " | $P2_1/n$ | 4 | 8.853 | 8.802 | 12.273 | 90.0 | 38 |
| | In | " | $P2_1/n$ | 4 | 8.592 | 8.908 | 12.290 | 90.0 | 39 |
| α-$Li_3M^{III}_2(PO_4)_3$ | Fe [a] | trigonal | $R\bar{3}c$ | 6 | 8.316 | – | 22.459 | – | 40 |
| | Sc | orthorhombic | $Pbcn$ | 4 | 12.400 | 8.835 | 8.827 | – | 41 |
| | In [a] | trigonal | $R\bar{3}c$ | 6 | 8.432 | – | 23.268 | – | 42 |
| β-$Na_3M^{III}_2(PO_4)_3$ | Fe [a] | " | $R\bar{3}c$ | 6 | 8.727 | – | 21.808 | – | 40 |
| | Sc [a] | " | $R\bar{3}c$ | 6 | 8.927 | – | 22.340 | – | 47 |
| | In | monoclinic | $C2/c$ | 4 | 12.439 | 12.772 | 6.583 | 114.16 | 31, 45 |
| α-$Na_3M^{III}_2(PO_4)_3$ | Cr [a] | trigonal | $R\bar{3}c$ | 6 | 8.643 | – | 21.619 | – | 46 |
| | Fe [a] | monoclinic | $C2/c$ | 4 | 15.070 | 8.740 | 8.724 | 125.1 | 43 |
| | Sc [a] | " | $Bb$ | 4 | 16.100 | 9.109 | 8.928 | 127.2 | 44 |
| | In [a] | trigonal | $R\bar{3}c$ | 6 | 8.966 | – | 22.100 | – | 31, 48 |
| | Ce – Gd | " | see [b] | 6 | 9.18 (Ce) – 8.86 (Gd) | – | 14.44 (Ce) – 14.20 (Gd) | – | 10, 11 |
| $K_3M^{III}_2(PO_4)_3$ | Ce – Gd | trigonal | see [b] | 3 | 9.30 (Ce) – 8.86 (Gd) | – | 14.41 (Ce) – 14.27 (Gd) | – | 10, 11 |
| | Fe | monoclinic | $C2/c$ | 8 | 16.303 | 9.463 | 16.691 | 118.4 | 36 |

[a] The NASICON structural type. [b] The space groups were not unambiguously established.

occupied by alkali-metal cations located in two positions, *viz*., $M(1)$ and $M(2)$ (Fig. 4 *b*). The analysis of the number of the polyhedra and their coordination environments demonstrated that the general crystal-chemical formula of the NASICON structural type can be written as $[M(1),M(2)]_3M(3)_2(PO_4)_3$.

Taking the space group $R\bar{3}c$ (the highest symmetry for the compounds under consideration) as the basis, the $M(1)O_6$ polyhedron can be described as an elongated antiprism with the M(1) – O distances to the nearest six oxygen atoms equal to ~2.6 Å (the other six O atoms are at considerable distances from the metal atom, *viz*., at ~3.7 Å). The metal atom in the $M(2)$ position is surrounded by ten oxygen atoms eight of which are involved in the nearest environment, whereas the remaining two O atoms are somewhat remote. The analysis of the cross-sections of the channels showed that the cations with the radii of ~1 Å (for example, $Na^+$) could migrate within these channels. The cations can also pass through narrower regions, *viz*., through the ABC and ABD faces (see Fig. 4 *b*),[47] due to thermal displacements of the oxygen atoms. This fact is responsible for superionic conductivity of the $M^I_3M^{III}_2(PO_4)_3$ compounds.[49] The cations can occupy the $M(1)$ and $M(2)$ positions in different fashions: (1) these positions are completely occupied [$Na_{4.5}M^{III}_{1.5}(PO_4)_3$ or $M^I_3M^{III}(PO_4)_2$, where $M^{III}$ = Tm, Yb, Lu];[34] (2) only the $M(2)$ position is completely occupied (together with vacancies), for example, in β-$Na_3Sc_2(PO_4)_3$;[44] (3) the $M(1)$ and $M(2)$ positions are statistically occupied (together with vacancies), for example, in α-$Na_3M^{III}_2(PO_4)_3$, where $M^{III}$ = Sc, In.[47,48]

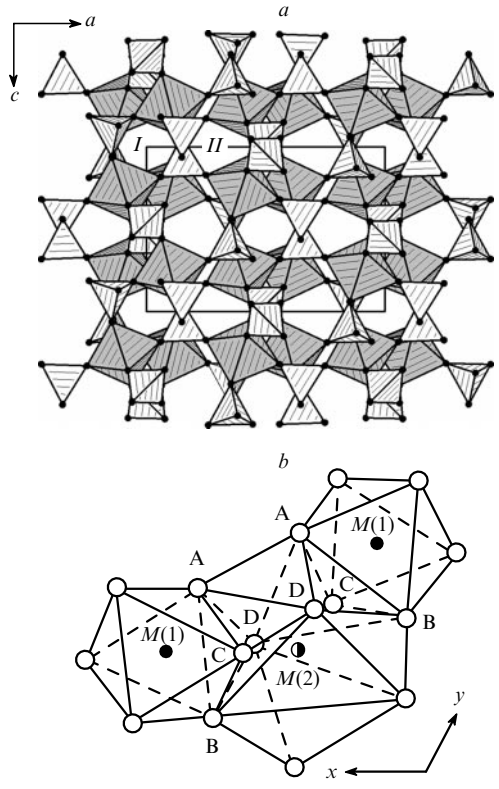



**Figure 4.** Structure of $M^I_3M^{III}_2(PO_4)_3$ projected onto the *ac* plane (*a*) and the oxygen environment about the $M(1)$ and $M(2)$ positions occupied by alkali-metal cations (*b*). The $M(3)$ position is omitted.

The low-temperature β modification of $Na_3In_2(PO_4)_3$ is described by the crystal-chemical formula $X(2)X(1)M(1).M(2)_2(PO_4)_3$. Alluaudite-like phosphates have analogous structures [the mineral alluaudite has the formula $Na_{0.6}Mn^{2+}_{1.2}Ca_{0.1}.Fe^{3+}_2Mg_{0.1}(PO_4)_3$]. The structures of indium compounds are characterised by the presence of the $In_2O_{10}$ dimers (bioctahedra) (Fig. 5 *a*), which form a framework structure together with the tetrahedral $PO_4$ groups (Fig. 5 *b*). The analysis of the polyhedra in the crystal structure of β-$Na_3In_2(PO_4)_3$ led one to the conclusion that the complete occupancy of the $M(2)$ position by a double- or triple-charged cation according to the crystal-chemical formula $X(2)X(1)M(1)M(2)_2(PO_4)_3$ is a necessary condition for crystallisation of double phosphates in the alluaudite structural type. It should be noted that the ionic radius of the cation in the dimer [$M(2)$ position] must be in the strictly specified range $0.74 \leqslant r \leqslant 0.76$ Å. The radii $r$ of the $Fe^{2+}$ and $In^{3+}$ cations fall within this range. Actually, the data on alluaudite-like phosphates $Na_2Fe^{3+}\underline{Fe}^{2+}_2(PO_4)_3$, $NaCaMn^{2+}\underline{Fe}^{2+}_2(PO_4)_3$ and $NaCd.\underline{In}^{3+}_2(PO_4)_3$ are available in the literature.[50] The fact is that the occurrence of alluaudite-like structures is determined by the size of the $PO_4$ tetrahedron. Two of ten $PO_4$ groups in the dimer are bridging and fix the distances between the vertices of the octahedra [$d(O\cdots O) \approx 2.5$ Å], which are equal to the length of the edge of the tetrahedron. As a result, this distance $d$[M(2)···M(2)] in the

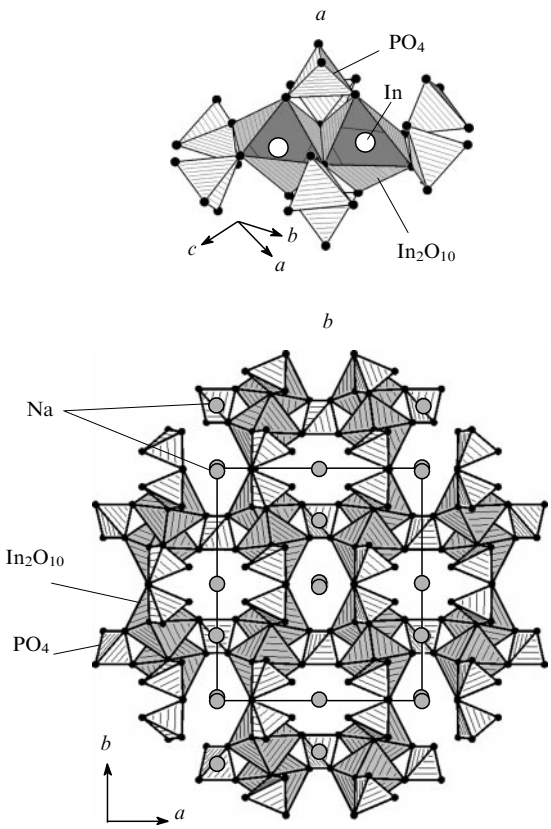



**Figure 5.** The $In_2O_{10}$ bioctahedron (*a*) and the structure of β-$Na_3In_2(PO_4)_3$ projected onto the *ab* plane (*b*).

dimer must be approximately equal to 3.0 Å. Due to repulsion between the cations, this distance increases to 3.19 Å in $Na_2Fe^{3+}Fe^{2+}_2(PO_4)_3$, 3.35 Å in β-$Na_3In_2(PO_4)_3$ and 3.38 Å in $NaCdIn_2(PO_4)_3$. The larger or smaller size of the cation as compared to $In^{3+}$ and (*i.e.*, $r < 0.74$ and $r > 0.76$ Å) will lead to destruction of the dimer as the structural block, which is confirmed by the lack of information on alluaudite-like phases with composition $M^I_3M^{III}_2(PO_4)_3$, where $M^{III}$ = REE, Sc, Fe, Cr.

From the crystal-chemical viewpoint, the transformation of the alluaudite-like β phase into the NASICON-like α phase [which was established from the analysis of the structures of both modifications of $Na_3In_2(PO_4)_3$] involves the radical rearrangement of the atoms. It was demonstrated that the transformation from the β phase to the α phase is accompanied by an increase in the distance between the indium atoms, destruction of the $In_2O_{10}$ dimers and formation of the isolated $InO_6$ octahedra. This rearrangement leads to an increase in 'porosity' [$\Delta(V/Z)_{\beta\to\alpha} = 8.1\%$] of the crystal structure due to the formation of rather large channels, which are statistically occupied by alkali-metal cations. The irreversibility of the polymorphic transformation β-$Na_3In_2(PO_4)_3$ → α-$Na_3In_2(PO_4)_3$ at $T = 820$ °C was confirmed by the DTA data.

Hence, compounds with two compositions, *viz.*, $M^I_3M^{III}(PO_4)_2$ and $M^I_3M^{III}_2(PO_4)_3$, are most widespread among double phosphates containing mono- and trivalent cations. The structural types of these compounds are determined by the nature and size of the $M^{III}$ cation as well as by the difference in the radii of the $M^I$ and $M^{III}$ cations, which is most pronounced for indium compounds (Table 3).

Investigations of the luminescence properties of REE phosphates showed that the $M^I_3M^{III}(PO_4)_2$ compounds ($M^I$ = Na, K; $M^{III}$ = Y, La, Nd, Gd) are promising laser materials.[27,51–54] Due to the unique luminescence properties (large absorption and luminescence cross-sections, rather large radiative lifetimes, weak concentration quenching of luminescence, low thresholds of generation, *etc.*), these crystals are quite competitive even with the recognised leader of this class of materials, *viz.*, yttrium–aluminium garnet YAG : $Nd^{3+}$, which is traditionally used in compact lasers. Luminophores based on $M^I_3M^{III}(PO_4)_2$ have the linear current characteristic of luminance at the cathode excitation in the current-density range of 0.1–50 μA $cm^{-2}$ (for the known $Zn_2SiO_4$–Mn luminophore, the saturation of luminance takes place at the current load of 5–10 μA $cm^{-2}$). The introduction of the second $M^{III}$ cation (diluent) into these materials leads to a noticeable increase in the line width resulting in deterioration of the optical characteristics. This was observed for the $Na_3Nd_{1-x}M^{III}_x(PO_4)_2$ ($M^{III}$ = Gd, Lu, Y) solid solutions.[52] The introduction of the $Ce^{3+}$ and $Tb^{3+}$ cations into a matrix of the β-$K_2SO_4$ type leads to an increase in the quantum yield due to the energy transfer from $Ce^{3+}$ to $Tb^{3+}$.[53]

The sizes of the polyhedra in the structures of NASICON-like phosphates allow one to predict the positions of the cations in the lattice and their mobility. Thus, a decrease in the size of the structure-forming $M^{III}$ cation hinders the migration of mobile alkali-metal cations within the channels of the framework. It was experimentally found that the ionic conductivity of $Na_3M^{III}_2(PO_4)_3$ is weakened as the radius of the trivalent cation decreases. At 570 °C, $\sigma$ is equal to $5.0\times10^{-2}$, $9.8\times10^{-3}$ and $7.8\times10^{-3}$ S $cm^{-1}$ for $Na_3Sc_2(PO_4)_3$, $Na_3Fe_2(PO_4)_3$ and $Na_3Cr_2(PO_4)_3$, respectively.[21,51] The dependence of the ionic conductivity of NASICON-like REE-containing phases on the temperature and degree of replacement of Zr by $M^{III}$ was studied only for mixed phosphates $Na_{1+x}Zr_{2-x}M^{III}_x(PO_4)_3$ ($M^{III}$ = Gd, Tb, Dy, Y, Er, Yb, In; $0 \leqslant x \leqslant 2$).[55] For the $Na_{2.4}In_{1.4}Zr_{0.6}(PO_4)_3$ compound, the maximum $\sigma$ value ($10^{-1}$ S $cm^{-1}$) was found at

**Table 3**. Characterisation of the structures of different types of double phosphates containing mono- and trivalent cations.

| Compound | Ratio $M^I : M^{III}$ | Ratio $M^{III} : PO_4^{3-}$ | Crystal system | Space group | Building blocks | Structural type |
|---|---|---|---|---|---|---|
| $M^I_3M^{III}(PO_4)_2$ | 3 : 1 | 1 : 2 | | | | |
| $M^I$ = Na; $M^{III}$ = REE, In, Ga, Sc, Al, Fe, Cr | | | trigonal | $P\bar{3}m1$ | $[M^{III}O_{8(7,6)}] + [PO_4]$ | layered [$M^{III}$ = La–Er, In (α phase), Sc, Al, Fe, Cr] |
| | | | orthorhombic | $Pbc2_1$, $Pnmm$ | | |
| | | | monoclinic | $Cc$ | $[M^{III}O_6] + [PO_4]$ | framework [$M^{III}$ = Tm–Lu, In (β phase)] |
| $M^I$ = K; $M^{III}$ = REE, Sc, In, Fe | | | monoclinic | $P2_1/m$, $C2/c$ | $[M^{III}O_{7(6)}] + [PO_4]$ | layered ($M^{III}$ = La–Er, Sc, Fe), framework ($M^{III}$ = In) |
| $M^I_3M^{III}_2(PO_4)_3$ | 3 : 2 | 2 : 3 | | | | |
| $M^I$ = Li, Na; $M^{III}$ = Yb–Lu, Ga, Sc, Al, Fe Cr | | | monoclinic | $P2_1/n$, $C2/c$, $Bb$ | $[M^{III}O_6] + [PO_4]$ | framework |
| | | | trigonal | $R\bar{3}c$ | | |
| | | | orthorhombic | $Pbcn$ | | |
| $M^I$ = Na, $M^{III}$ = In | | | monoclinic | $C2/c$ | $[M^{III}_2O_{10}] + [PO_4]$ | framework [$M^{III}$ = In (β phase)] |

400 °C and the minimum value ($2 \times 10^{-5}$ S cm$^{-1}$) was observed at room temperature. Of REE-containing composites, the Yb-doped analogue $Na_{2.4}Yb_{1.4}Zr_{0.6}(PO_4)_3$ is the most competitive material ($\sigma$ is $8.5 \times 10^{-2}$ S cm$^{-1}$ at 400 °C).

## III. Hydrogen phosphates containing mono- and trivalent cations

Complex hydrogen phosphates containing mono- and trivalent cations are characterised by the presence of hydrogen bonds between the oxygen and hydrogen atoms of the $HPO_4$ groups. Although formally belonging to double phosphates containing mono- and trivalent cations, these compounds possess a series of specific features. Hence, it is reasonable to consider these compounds separately. Hydrogen phosphates containing mono- and trivalent cations are classified into four main types, *viz.*, $M^IM^{III}(HPO_4)_2 \cdot n\,H_2O$, $M^I_xM^{III}_y(HPO_4)_z(PO_4)_u \cdot n\,H_2O$, $M^I_xM^{III}_y(H_2PO_4)_z(HPO_4)_u \cdot n\,H_2O$ and $M^I_2M^{III}(H_2PO_4)(HPO_4)_2 \cdot (H_3PO_4) \cdot n\,H_2O$, where $M^I$ = Na, K, Rb, Cs, $H_3O$, $NH_4$ and $M^{III}$ = Al, V, Fe, Ga, In.

Phosphates $M^I_3M^{III}(OH)(HPO_4)(PO_4)$ containing the $HPO_4$ groups along with the OH groups, which serve as bridges linking the $M^{III}O_6$ polyhedra in infinite chains, are known only for Al and Ga in combination with Na. These compounds will be considered in Section V.

### 1. Synthesis

The hydrothermal synthesis is one of conventional procedures for the preparation of hydrogen phosphates containing the $M^I$ and $M^{III}$ cations.[56–75] The problems associated with the preparation of compounds with specified compositions consist in choosing the optimum conditions of the synthesis. The compositions of the resulting compounds depend substantially on the parameters of the synthesis (the temperature, the degree of filling of an autoclave or a tube, the concentrations of the starting reagents, the aggregate state, pH of the medium, duration of the synthesis). General procedures for the preparation of this group of compounds are lacking. One of the criteria for the existence of complex hydrogen phosphates containing different cations and anions is the presence of a strongly acidic medium (pH is no higher than 2–2.5). All the aforesaid refer equally to the conditions of the hydrothermal synthesis of hydrogen phosphates with compositions $M^IM^{III}(HPO_4)_2 \cdot n\,H_2O$ ($M^I$ = Na, K, Rb, Cs, $H_3O$, $NH_4$; $M^{III}$ = Al, Fe, V, In; $n$ = 0–18) and $M^I_xM^{III}_y(HPO_4)_z(PO_4)_u \cdot n\,H_2O$ ($M^I$ = Rb, Cs; $M^{III}$ = V, Ga, In; $n$ = 0.5–2). The $M^IM^{III}(HPO_4)_2 \cdot n\,H_2O$ compounds are prepared under rather mild conditions (145–240 °C, see Table 4).

In studies of the phase formation in the $In_2O_3 - M^IH_2PO_4 - H_3PO_4 - HF$ and $In_2O_3 - M^IHal - H_3PO_4$ systems under hydrothermal conditions ($T$ = 200 °C), a series of indium hydrogen phosphates with composition $M^IIn(HPO_4)_2$ ($M^I$= K, Rb, Cs, $NH_4$) were prepared. These compounds are stable at pH 0.5–1.5.[56] The $RbIn(HPO_4)_2$ compound was isolated as crystals of two forms (colourless prismatic and elongated bipyramidal) characterised by the same empirical formula. Crystals of hydrogen phosphate $Na_2In_2(HPO_4)_4 \cdot H_2O$ were prepared in the synthesis of microporous borophosphates.[57] Interestingly, the phosphate with the same composition was synthesised under analogous conditions in the absence of $Na_2B_4O_7 \cdot 10\,H_2O$. Attempts to prepare a gallium-containing analogue according to the same procedure failed and led to the formation of new borophosphate with composition $NaGaBP_2O_7(OH)_3$.[57] Attempts to synthesise mixed rubidium gallium hydrogen phosphate were also unsuccessful in spite of the fact that the initial reagent ratio was varied over a wide range. Hydrogen phosphate $Rb_2Ga_4(HPO_4)(PO_4)_4 \cdot 0.5\,H_2O$ crystallised simultaneously with $GaPO_4$ (see Ref. 58) due, apparently, to high stability and low solubility of $GaPO_4$ (the solubility product is $1 \times 10^{-21}$).

The field of chemistry dealing with the synthesis of porous compounds has been extensively developed in recent years. These compounds have inorganic frameworks built from the phosphate tetrahedra. The cavities in these frameworks can capture different positively charged groups, including organic groupings. The preparation of these compounds under hydrothermal conditions is often accompanied by the formation of complex hydrogen phosphates as by-products. For example, prismatic crystals of $NH_4(Al_{1-x}Ga_x)(HPO_4)_2$ ($x$ = 0.36) comprising ~5%–10% of the total weight of the product were obtained under mild conditions ($T$ = 130 °C) from a mixture consisting of aluminium and gallium chlorides, tetramethylammonium hydroxide and a cobalt complex with composition [Λ-Co(en)$_3$(H$_2$PO$_4$)$_3$] (en is ethylenediamine).[59] Two types of crystals were isolated from a mixture of $RbOH - FePO_4 \cdot 2\,H_2O - Me_2NH - MePO(OH)_2 - H_3PO_4$ at 230 °C, *viz.*, colourless elongated parallelepiped-shaped crystals of hydrogen phosphate $RbFe(HPO_4)_2$ (see Ref. 60) and prismatic crystals of unknown structure. It should be noted that a powdered product obtained in the course of the synthesis had the same nominal composition as that of the crystals of $RbFe(HPO_4)_2$ but was the low-symmetry modification.

Vanadium hydrogen phosphates $M^IV(HPO_4)_2$ ($M^I$ = Rb, $NH_4$) were synthesised under slightly modified conditions ($T$ = 240 °C).[61] Only triclinic crystals of α-$RbV(HPO_4)_2$ were isolated in pure form. Attempts to obtain their monoclinic analogues β-$RbV(HPO_4)_2$ and β-$(NH_4)V(HPO_4)_2$ in pure form failed even upon variation of the initial reagent ratio over a wide range. According to the results of chemical analysis, the composition of the impurity phase is identical to that of β-$(NH_4)V(HPO_4)_2$. This indicates that the phase formation of vanadium hydrogen phosphates, like that of indium hydrogen phosphates β$_1$- and β$_2$-$RbIn(HPO_4)_2$, is a complex process resulting in co-crystallisation of different modifications of a compound under the same conditions. Attempts to prepare hydrogen phosphates $M^IV(HPO_4)_2$ ($M^I$ = K or Cs) led to the formation of two phases, *viz.*, $K(V^{IV}O)V^{III}(HPO_4)_3(H_2O)_2$ and $CsV_2(PO_4).(HPO_4)_2(H_2O)_2$.[62] The caesium indium derivative $CsIn_2(PO_4).(HPO_4)_2(H_2O)_2$ (see Ref. 63) was isolated from aqueous solutions containing $InCl_3$, $H_3PO_4$, $CsVO_3$ and $Me_4NOH$ in a ratio of 2 : 6 : 1 : 1. It should be noted that mixed caesium indium hydrogen phosphate was not produced in the synthesis with the use of CsCl, CsOH and $Cs_2CO_3$ instead of $CsVO_3$. Hydrogen phosphates containing the $H_2PO_4^-$ and $HPO_4^{2-}$ anions were prepared from solutions containing high concentrations of $H_3PO_4$ ($\geqslant$3 M). The synthesis with the use of $CsGa(H_2PO_4)_4$ as the starting compound in the presence of $Cs_2CO_3$ and an excess of $H_3PO_4$ afforded $Cs_2Ga(H_2PO_4)(HPO_4)_2 \cdot H_3PO_4 \cdot 0.5\,H_2O$.[64]

### 2. Structures and properties

The $M^IM^{III}(HPO_4)_2$ compounds possess a series of interesting structural features. These compounds were prepared for the Al, V, Fe, Ga and In cations in combination with K, Rb and Cs[56, 60, 61, 65] as well as with the single-charged $NH_4^+$ and $H_3O^+$ cations.[56, 59, 61, 66–68] The composition of the unit cell of mixed indium sodium hydrogen phosphate does not correspond to the $M^IM^{III}(HPO_4)_2$ formula, which is associated with the incorporation of water molecules in the crystal lattice of this compound. Two compounds whose compositions correspond to the $Na_2In_2(HPO_4)_4 \cdot H_2O$ [57] and $Na_4In_8(HPO_4)_{14}(H_2O)_6 \cdot 12\,H_2O$ formulas were isolated.[69] The crystallographic characteristic of mixed-cation hydrogen orthophosphates $M^IM^{III}(HPO_4)_2$ and more complex sodium indium phosphates are given in Table 5.

All $M^IM^{III}(HPO_4)_2$ compounds have frameworks built from the vertex-sharing $M^{III}O_6$ octahedra and $PO_4$ tetrahedra. The cavities and channels of the frameworks are occupied by monovalent cations. Variations in the sizes of the $M^I$ and $M^{III}$ cations give rise to different structural types. Thus, different types of frameworks can be formed, the polyhedra are distorted and the sizes of the channels and cavities are changed. As a consequence, the crystal lattice can incorporate water molecules, which participate in structure formation. It seems essential that in all structures, the protonated vertices of the $PO_4$ tetrahedra are directed

**Table 4**. Hydrothermal synthesis of complex hydrogen phosphates.

| Compound | Characteristics of the crystals (colour) | Starting reagents (molar ratio) | Synthesis conditions | | | Ref. |
|---|---|---|---|---|---|---|
| | | | pH | $T$ /°C | $\tau$ /h | |
| $KAl(HPO_4)_2 \cdot H_2O$ | colourless prismatic | $Al(OH)_3$, 1M $KH_2PO_4$, 1M $H_3PO_4$ (K : P = 0.5) | – | 145 [a] | 720 | 65 |
| $NH_4(Al_{1-x}Ga_x)(HPO_4)_2$ | the same | $AlCl_3 \cdot 6H_2O$, $GaCl_3$, $H_3PO_4$, [Λ-Co(en)$_3$(H$_2$PO$_4$)$_3$], $Me_4NOH$, $H_2O$ [Co(en)$_3$ : Al : Ga : P : $Me_4NOH$ : $H_2O$ = 0.25 : 1 : 1 : 2.86 : 2 : 90] | – | 130 | 96 | 59 |
| $(H_3O)Fe(HPO_4)_2$ | pink needle-like | $Fe_3(PO_4)_2 \cdot 3H_2O$, $FePO_4$ | 2 | 227 | 168 | 67 |
| $RbFe(HPO_4)_2$ | colourless parallele-piped-shaped | $RbOH$, $FePO_4 \cdot 2H_2O$, $Me_2NH$, $MePO(OH)_2$, $H_3PO_4$ | – | 230 | 96 | 60 |
| β-$(NH_4)V(HPO_4)_2$ | yellow-green | [$V_2O_5$ : $V_{met}$ : $(NH_4)_2HPO_4$ : $H_3PO_4$ : $H_2O$ = = 1 : 1 : 2 : 10 : 190] | – | 240 | 48 | 61 |
| β-$RbV(HPO_4)_2$ | pale-green platelet-like | ($Rb_2V_2O_6$ : $V_{met}$ : $Bu_4NBr$ : $H_3PO_4$ : $H_2O$ = = 9 : 2 : 1 : 60 : 760) | – | 240 | 48 | 61 |
| α-$RbV(HPO_4)_2$ | yellow-green | ($Rb_2V_2O_6$ : $V_{met}$ : $PhMe_3NBr$ : $H_3PO_4$ : $H_2O$ = = 1 : 1 : 0.5 : 15 : 190) | – | 240 | 44 | 61 |
| $Na_2In_2(HPO_4)_4 \cdot H_2O$ | colourless platelet-like | $Na_2B_4O_7 \cdot 10H_2O$, $Na_2HPO_4 \cdot 12H_2O$, $In_{met}$, HCl (Na : In : P : B = 17 : 1 : 6 : 10) [b] | – | 80<br>130 | 168<br>336 | 57<br>57 |
| $Na_4In_8(HPO_4)_{14}(H_2O)_6 \cdot 12H_2O$ | colourless hexagonal-prismatic | $Na_2HPO_3 \cdot 5H_2O$, $In(NO_3)_3 \cdot 3H_2O$, $H_3PO_3$ | – | 125 | 50 | 69 |
| $KIn(HPO_4)_2$ | transparent colourless bipyramidal | $In_2O_3$, $KH_2PO_4$, $H_3PO_4$, HF (K : In : P : F = 4.8 : 1 : 6.2 : 3) [c] | 1.5 | 200 | 144 | 56 |
| $(NH_4)In(HPO_4)_2$ | white powder | $In_2O_3$, $NH_4Cl$, $H_3PO_4$ ($NH_4$ : In : P = 8 : 1 : 2) [c] | 1 | 200 | 144 | 56 |
| β$_2$-$RbIn(HPO_4)_2$ | transparent colourless bipyramidal | $In_2O_3$, $RbH_2PO_4$, $H_3PO_4$, HF (Rb : In : P : F = 4.65 : 1 : 6.15 : 3) [c] | 0.5 | 200 | 144 | 56 |
| $CsIn(HPO_4)_2$ | colourless needle-like | $In_2O_3$, CsF, $H_3PO_4$ (Cs : In : P = 3 : 1 : 6) [c] | 1 | 200 | 96 | 56 |
| $Rb_2Ga_4(HPO_4)(PO_4)_4 \cdot 0.5H_2O$ | the same | $Ga_2O_3$, 3M $RbH_2PO_4$, 3M $H_3PO_4$ (Rb : P = 0.5) | – | 600 [d] | 40 | 58 |
| $CsV_2(PO_4)(HPO_4)_2(H_2O)_2$ | green | $Cs_4V_2O_7$, $V_{met}$, $H_3PO_4$, $H_2O$, $PhMe_3NCl$ (1 : 2 : 46 : 800 : 1.1) | – | 200 | 48 | 62 |
| $CsIn_2(PO_4)(HPO_4)_2(H_2O)_2$ | pale-yellow | $InCl_3$, $H_3PO_4$, $CsVO_3$, $Me_4NOH$, $H_2O$ (2 : 6 : 1 : 1 : 125) | – | 200 | 48 | 63 |
| $KFe_3(H_2PO_4)_6(HPO_4)_2 \cdot 4H_2O$ | colourless hexagonal-prismatic | $Fe_2O_3$, $H_3PO_4$, $K_2CO_3$, $H_2O$ (Fe : P : K = 1 : 4 : 1) | – | 290 [e] | 1 | 75 |
| $Cs_2Ga(H_2PO_4)(HPO_4)_2 \cdot H_3PO_4 \cdot 0.5H_2O$ | colourless needle-like | $CsGa(H_2PO_4)_4$, $Cs_2CO_3$, $H_3PO_4$ ($Cs_2O$ : $Ga_2O_3$ = 7.5 : 1) | – | – | 1 | 64 |

[a] Slow cooling to 25 °C for 24 h; [b] the degree of filling of the autoclave was 30%; [c] the degree of filling of the autoclave was 75%; [d] slow cooling to 275 °C for 65 h; [e] slow cooling with a rate of 20 °C per hour.

**Table 5**. Crystallographic characteristics of the $M^IM^{III}(HPO_4)_2$ compounds.

| Compound | Crystal system | Space group | $Z$ | Unit cell parameters | | | | Ref. |
|---|---|---|---|---|---|---|---|---|
| | | | | $a$ /Å | $b$ /Å | $c$ /Å | $\beta$ (or α, β, γ) /deg | |
| $KAl(HPO_4)_2 \cdot H_2O$ | monoclinic | $P2_1/c$ | 8 | 10.040 | 9.107 | 16.254 | 100.98 | 65 |
| $KAl(DPO_4)_2 \cdot D_2O$ | " | $P2_1/c$ | 8 | 10.037 | 9.105 | 16.223 | 100.97 | 65 |
| $(H_3O)Fe(HPO_4)_2$ | " | $P2_1/c$ | 4 | 5.191 | 8.748 | 14.448 | 94.81 | 67 |
| $NH_4(Al_{0.64}Ga_{0.36})(HPO_4)_2$ | triclinic | $P\bar{1}$ | 3 | 7.109 | 8.695 | 9.252 | α = 65.01, β = 70.25, γ = 69.01 | 59 |
| α-$(NH_4)Fe(HPO_4)_2$ | " | $P\bar{1}$ | 6 | 9.838 | 7.185 | 14.159 | α = 93.46, β = 85.58, γ = 89.47 | 68 |
| $RbFe(HPO_4)_2$ | trigonal | $R\bar{3}c$ | 6 | 8.160 | – | 52.75 | – | 60 |
| β-$(NH_4)V(HPO_4)_2$ | monoclinic | $P2_1/c$ | 4 | 5.201 | 8.738 | 14.398 | 94.8 | 61 |
| α-$(NH_4)V(HPO_4)_2$ | triclinic | $P\bar{1}$ | 3 | 7.173 | 8.841 | 9.458 | α = 65.1, β = 70.7, γ = 69.6 | 66 |
| β-$RbV(HPO_4)_2$ | monoclinic | $P2_1/c$ | 4 | 5.210 | 8.789 | 14.330 | 94.4 | 61 |
| α-$RbV(HPO_4)_2$ | triclinic | $P\bar{1}$ | 3 | 8.831 | 9.450 | 7.188 | α = 109.6, β = 110.3, γ = 65.3 | 61 |
| $KIn(HPO_4)_2$ | monoclinic | $P2_1/c$ | 4 | 9.623 | 8.257 | 9.457 | 115.72 | 56 |
| $(NH_4)In(HPO_4)_2$ | " | $P2_1/c$ | 4 | 9.665 | 8.276 | 9.596 | 116.15 | 56 |
| β$_2$-$RbIn(HPO_4)_2$ | " | $P2_1/c$ | 4 | 9.705 | 8.367 | 9.528 | 116.60 | 56 |
| $CsIn(HPO_4)_2$ | " | $P2_1/c$ | 4 | 5.330 | 9.157 | 14.796 | 93.81 | 56 |
| $Na_2In_2(HPO_4)_4 \cdot H_2O$ | triclinic | $P\bar{1}$ | 2 | 9.3013 | 9.4976 | 9.2685 | α = 98.710, β = 98.953, γ = 60.228 | 57 |
| $Na_4In_8(HPO_4)_{14}(H_2O)_6 \cdot 12H_2O$ | trigonal | $P\bar{3}c1$ | 2 | 13.850 | – | 18.493 | – | 69 |

inside the channels. This arrangement of the protons has an effect on the shape of the channels and their presence compensates the negative charge of the frameworks of these compounds.

Two types of the $AlO_6$ octahedra and four crystallographically independent $PO_4$ tetrahedra are the main polyhedra in the structure of $KAl(HPO_4)_2 \cdot H_2O$.[65] The alternating $AlO_6$ and $HPO_4$ polyhedra are linked in chains along the *a* and *c* axis thus forming a framework (Fig. 6). The size and shape of the cavities in the framework are affected by the potassium cations and protons involved in the $HPO_4$ groups. The $Al(1)O_6$ octahedron, which is formed by four oxygen atoms belonging to four $HPO_4$ groups and two oxygen atoms of two *cis*-oriented water molecules, is strongly distorted. The $Al(2)O_6$ octahedron is less distorted and is formed only by the oxygen atoms of the $HPO_4$ groups. The $Al(1)O_6$ octahedra are arranged along the *a* axis, whereas the $Al(2)O_6$ octahedra are aligned along the *c* axis. The structure contains two types of the K cations. The coordination sphere about the K(1) cation is formed by the oxygen atoms of only the $HPO_4$ groups, whereas the coordination sphere about the K(2) cation involves the oxygen atom of the $H_2O$ molecule along with the oxygen atoms of the $HPO_4$ groups. The coordination numbers of the potassium atoms in both polyhedra are equal to 9. In the structure of the deuterated analogue $KAl(DPO_4)_2 \cdot D_2O$,[65] seven types of hydrogen bonds were revealed.

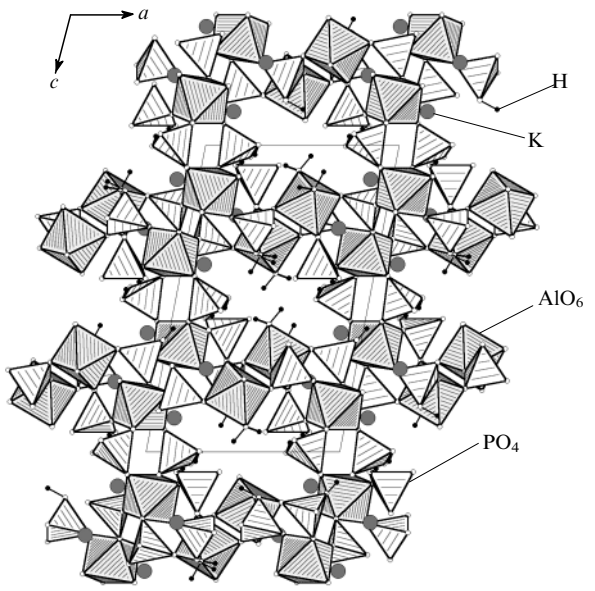



**Figure 6.** Structure of $KAl(HPO_4)_2 \cdot H_2O$ projected onto the *ac* plane.

The difference in the size of the $M^I$ and $M^{III}$ cations has a substantial effect on the structural features of hydrogen phosphates $M^IM^{III}(HPO_4)_2$ ($M^I$ = K, Rb, Cs, $H_3O$, $NH_4$; $M^{III}$ = Fe, V, In), which crystallise in the monoclinic system. This is particularly clearly seen in the case of indium compounds. For example, the unit cell volume in the family of indium hydrogen phosphates $M^IIn(HPO_4)_2$ ($M^I$ = K, Rb, $NH_4$, space group $P2_1/c$) increases gradually in the series $K-NH_4-Rb$. However, the unit cell parameters are sharply changed on going to caesium, which has the largest ionic radius of all the alkali metals under consideration, while the space group ($P2_1/c$) is retained. The $CsIn(HPO_4)_2$ compound is more similar in crystallographic characteristics to hydrogen phosphates $(H_3O)Fe(HPO_4)_2$, $\beta$-$(NH_4)V(HPO_4)_2$ and $\beta$-$RbV(HPO_4)_2$ than to $M^IIn(HPO_4)_2$ ($M^I$ = K, Rb, $NH_4$).

In the structure of $(H_3O)Fe(HPO_4)_2$,[67] the $FeO_6$ octahedra are linked to each other through four $PO_4$ tetrahedra. The block of the octahedra and tetrahedra forms a framework consisting of columns along the *a* axis. The cavities in the framework are occupied by the oxonium cations.§ The oxygen atom of the $H_3O^+$ cation is at distances of 2.90–3.14 Å from the seven nearest oxygen atoms of the $HPO_4$ groups. The structures of hydrogen phosphates $\beta$-$M^IV(HPO_4)_2$ ($M^I$ = $NH_4$, Rb)[61] and $CsIn(HPO_4)_2$ (see Ref. 56) differ from that of $(H_3O)Fe(HPO_4)_2$ (see Ref. 67) in that the $VO_6$ (as well as the $InO_6$) octahedra within the channels in these structures are linked to each other only by two $PO_4$ tetrahedra. On going from $\beta$-$RbV(HPO_4)_2$ to $CsIn(HPO_4)_2$, the oxygen polyhedron about the $M^{III}$ atom is enlarged. Thus, the coordination numbers of rubidium and caesium are 7 and 12, respectively.

The triclinic modification of $M^IM^{III}(HPO_4)_2$ ($M^I$ = Rb, $NH_4$; $M^{III}$ = Fe, V)[61,66] and $(NH_4)(Al_{1-x}Ga_x)(HPO_4)_2$ ($x$ = 0.36)[59] have mixed $\{M^{III}[HPO_4]_2\}_{3\infty}$ frameworks of the $M^{III}O_6$ octahedra and $PO_4$ tetrahedra. These skeleton frameworks contain large cavities occupied by monovalent cations. The sizes and shapes of the cavities allow mobile ions to migrate in different directions, which indicates that these compounds can exhibit ion-exchange properties.[68] The $M^{III}O_6$ octahedra share all vertices with six nearest $PO_4$ tetrahedra. Each tetrahedron shares three vertices with three adjacent octahedra, whereas the fourth proton-bearing vertex of each tetrahedron is not involved in the first coordination sphere of the $M^{3+}$ cations. The functional role of the fourth vertex consists in linking the tetrahedra through hydrogen bonding to form groups of three polyhedra each. The fact that the $V^{3+}$, $Fe^{3+}$, $Co^{3+}$ and $Ni^{3+}$ cations have similar radii [$r_{VI}(M^{III})$ = 0.64, 0.645, 0.61 and 0.60 Å, respectively] suggests the existence of the triclinic modification of the $M^IM^{III}(HPO_4)_2$ compounds with $M^I$ = Rb, $NH_4$ and $M^{III}$ = Co, Ni.

The $(NH_4)Fe(HPO_4)_2$ compound[68] exhibits antiferromagnetic properties and has two different magnetic subunits analogous to those found in $Li_3Fe_2(PO_4)_3$.[70] It should be noted that an increase in the ionic radius of the $M^{III}$ cation in the series Al–Ga–V–Fe in hydrogen phosphates with composition $(NH_4)M^{III}(HPO_4)_2$ is accompanied by a substantial deformation of the $FeO_6$ octahedra resulting in rotation of the $PO_4$ tetrahedra about $FeO_6$. This leads to doubling of the unit cell volume of the Fe-containing analogue (triclinic modification). The triclinic modification of the In-containing analogue was not found, which may be indicative of instability of this modification of hydrogen phosphates containing large $M^{III}$ cations.

The monoclinic modification of $M^IM^{III}(HPO_4)_2$ differs from their triclinic modification primarily in the mode of linking of the octahedra and tetrahedra in infinite columns along the *a* axis. For example, the columns in the structure of monoclinic $\beta$-$(NH_4)V(HPO_4)_2$ (Fig. 7 *a*) are linked in a framework through the $PO_4$ tetrahedra, whereas these columns in the more complex structure of triclinic $\alpha$-$(NH_4)V(HPO_4)_2$ (Fig. 7 *b*) are linked along the [100] direction due to the presence of an additional $VO_6$ octahedron. As a result, the structure $\beta$-$(NH_4)V(HPO_4)_2$ contains channels of one type occupied by the ordered $NH_4^+$ cations, whereas two types of channels occupied by the $NH_4^+$ ions are present in the structure of $\alpha$-$(NH_4)V(HPO_4)_2$ (see Fig. 7 *a*, *b*).

The structure of $RbFe(HPO_4)_2$ belonging to the trigonal system[60] (Fig. 7 *c*) has a fragment typical of the triclinic modification of the $M^IM^{III}(HPO_4)_2$ compounds. However, in the low-symmetry structure, the tetrahedra through which the octahedra are linked in columns, are 'sunk' into the cavities between the octahedra, whereas the arrangement of the tetrahedra around the $FeO_6$ octahedra in the trigonal structure corresponds to the symmetry $\bar{3}$.

The structure of $RbFe(HPO_4)_2$ contains the $Fe(1)_2Fe(2)(HPO_4)_{12}$ trimers involving two types of the octahedra, *viz*., $Fe(1)O_6$ and $Fe(2)O_6$. The trimers form helical columns along the *c* axis. Each $HPO_4$ group is linked to one

§ The presence of the $H_3O^+$ cation was confirmed by IR spectroscopy (a narrow absorption band at 3392 $cm^{-1}$).

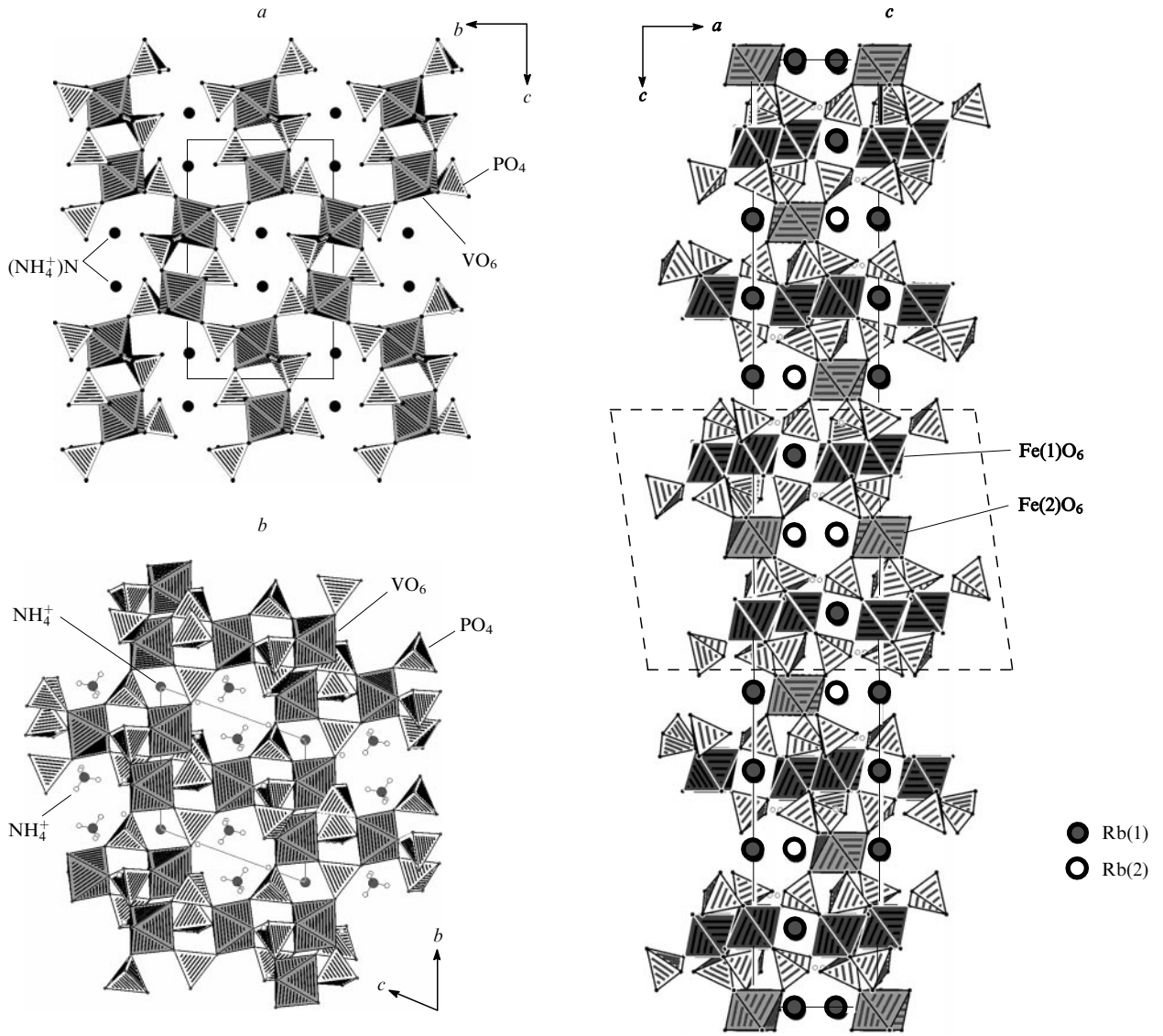



**Figure 7.** Structures of monoclinic β-$(NH_4)V(HPO_4)_2$ (*a*) and triclinic α-$(NH_4)V(HPO_4)_2$ (*b*) projected onto the *bc* plane and the structure of trigonal $RbFe(HPO_4)_2$ (*c*) projected onto the *ac* plane.

$Fe(1)O_6$ octahedron and one $Fe(2)O_6$ octahedron within the trimer and to one $Fe(1)O_6$ octahedron from the adjacent trimer so that the three-dimensional $[Fe(1)_2Fe(2)(HPO_4)_6]_{3\infty}$ framework is formed. The tunnels extended along the [100] and [110] directions are occupied by two types of rubidium cations with the coordination numbers of 12 and 9. As can be seen from the projection of the structure of $RbFe(HPO_4)_2$ onto the *ab* plane, the layers of the Fe(1) and Rb(1) atoms alternate with the layers of the Fe(2) and Rb(2) atoms and interleaved with the $HPO_4$ groups. All iron and rubidium atoms are located on threefold axes to form columns along the *c* axis with the $-$Fe(1)Fe(2)Fe(1)Rb(2)Rb(1).Rb(2)Fe(1)$-$ alternation. In $RbFe(HPO_4)_2$, the difference between the radii of the rubidium [$r_{XII}(Rb^+) = 1.73$ Å] and iron [$r_{VI}(Fe^{3+}) = 0.645$ Å] cations is ~1.09 Å. The pair of the caesium [$r_{XII}(Cs^+) = 1.88$ Å] and indium [$r_{VI}(In^{3+}) = 0.76$ Å] cations as well as the pair of rubidium and vanadium [$r_{VI}(V^{3+}) = 0.64$ Å] are characterised by similar values of $\Delta r$ and, hence, the trigonal modifications of $CsIn(HPO_4)_2$ and $RbV(HPO_4)_2$ would be expected to occur.

A decrease in $\Delta r_{(M^+ - M^{3+})}$ in the series Cs–Rb–K–Na (for one type of the $M^{3+}$ atoms) leads to a decrease in the coordination number of the alkali-metal cation. As a consequence, a new structural type can be formed. This assumption was confirmed by the structures of indium hydrogen phosphates $M^{I}In(HPO_4)_2$, where $M^{I}$ = K, Rb or $NH_4$, which we have established recently. In the framework structures of these compounds, the octahedra and tetrahedra are linked in infinite columns along the [100] and [001] directions. These structures differ from that of $CsIn(HPO_4)_2$ in the mode of linking of the columns to form a framework. In addition, the alkali-metal atoms in these structures adopt a smaller coordination number. Thus the coordination number of caesium in $CsIn(HPO_4)_2$ is 12, whereas the coordination number of potassium and rubidium in $M^{I}In(HPO_4)_2$ (M = K or Rb) is 9. In $CsIn(HPO_4)_2$, each column is linked to four analogous adjacent columns through four $PO_4$ tetrahedra, whereas there are eight such interactions in the structures of $M^{I}In(HPO_4)_2$ (M = K, Rb) and all tetrahedra are shared by columns (Fig. 8).

The $PO_4$ tetrahedra in $M^{I}In(HPO_4)_2$ (M = K or Rb) share two vertices with the $InO_6$ octahedra from one column and one vertex with the octahedron from the adjacent column. The fourth (protonated) oxygen vertex of each tetrahedron is directed inside the channel formed with the participation of three columns linked through the tetrahedra. These channels are occupied by the $M^{I}$ cations. The $InO_6$ octahedra in the structure of $KIn(HPO_4)_2$, unlike those in $RbIn(HPO_4)_2$, are strongly distorted. These structural features of $KIn(HPO_4)_2$ suggest that the formation of this structural type is highly improbable for the sodium analogue.

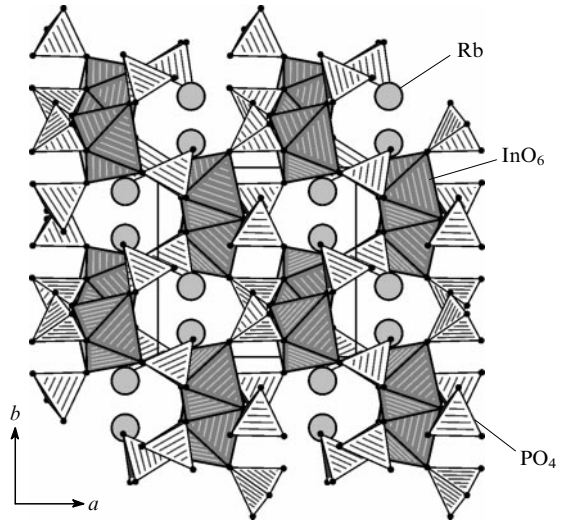



**Figure 8.** Structure of $RbIn(HPO_4)_2$ projected onto the *ab* plane.

Sodium for which $\Delta r_{(M^+ - M^{3+})}$ reaches the maximum value ($\sim 0.23$ Å) forms the $Na_2In_2(HPO_4)_4 \cdot H_2O$ [57] and $Na_4In_8(HPO_4)_{14}(H_2O)_6 \cdot 12\,H_2O$ [69] compounds with radically different structures.

The $Na_2In_2(HPO_4)_4 \cdot H_2O$ compound has the $[In_2(HPO_4)_4]_{3\infty}$ framework built from two types of the $InO_6$ octahedra and $PO_4$ tetrahedra. This framework can be described as consisting of the characteristic [In(1)In(2)$(HPO_4)_4$] structural blocks. The $InO_6$ octahedra of both types each share vertices with six $PO_4$ tetrahedra, which, in turn, each have three oxygen atoms in common with three adjacent octahedra. The remaining vertices of the $HPO_4$ polyhedra occupied by the protonated oxygen atoms are involved in formation of five hydrogen bonds. The octahedra and tetrahedra are packed in layers parallel to the *a* axis. The framework of $Na_2In_2(HPO_4)_4 \cdot H_2O$ contains two types of channels. The channels of one type are extended along the [100] direction and occupied by sodium cations and $H_2O$ molecules (Fig. 9 *a*). The channels of another type are extended along the [010] direction and are empty. It should be noted that the mode of binding of the In, P and O atoms in $Na_2In_2(HPO_4)_4 \cdot H_2O$ [57] is analogous to that observed in the structures of $Al_2O_3$ (corundum) and $Ti^{IV}Ti^{IV}(HPO_4)_4$.[71]

The structure of $Na_4In_8(HPO_4)_{14}(H_2O)_6 \cdot 12\,H_2O$ consists of the $[In_8(HPO_4)_{14}(H_2O)_6]$ layers formed by the $PO_4$ tetrahedra and the $In(1)O_6$ and $In(2)O_5O_W$ octahedra. The $[In_8(HPO_4)_{14}(H_2O)_6]$ layers are packed in the *ABAB* order according to the trigonal symmetry $P\bar{3}c1$, the channels along the [001] direction being lacking. The layers are linked to each other through the $In(1)O_6$ octahedra to form a framework with channels along the crystallographic *a* and *b* axis (Fig. 9 *b*). These channels have a 12-membered-ring shape in cross-section and include the $Na^+$ cations and water molecules. The water molecules fulfil two functions. Some water molecules are involved in the first coordination sphere about the In(2) cation and the remaining water molecules occupy the channels of the structure (zeolite-type water). The partial occupancies of the sodium positions and the nearest oxygen positions are directly associated with the presence of abnormally short bonds (2.06–2.19 Å) between these atoms. The Na–O interatomic distances in the $NaO_x$ polyhedron are close to the interatomic distances outside these polyhedra. This characteristic feature of the $Na_4In_8(HPO_4)_{14}(H_2O)_6 \cdot 12\,H_2O$ compound is also common to some hydrated sodium zeolites.[72]

The second group of complex hydrogen phosphates of the general formula $M^I_xM^{III}_y(HPO_4)_z(PO_4)_u \cdot n\,H_2O$ ($M^I$ = Rb, Cs; $M^{III}$ = V, Ga, In; $n = 0.5-2$) includes three compounds, *viz.*, $Rb_2Ga_4(HPO_4)(PO_4)_4 \cdot 0.5\,H_2O$, $CsIn_2(HPO_4)_2(PO_4)(H_2O)_2$ and

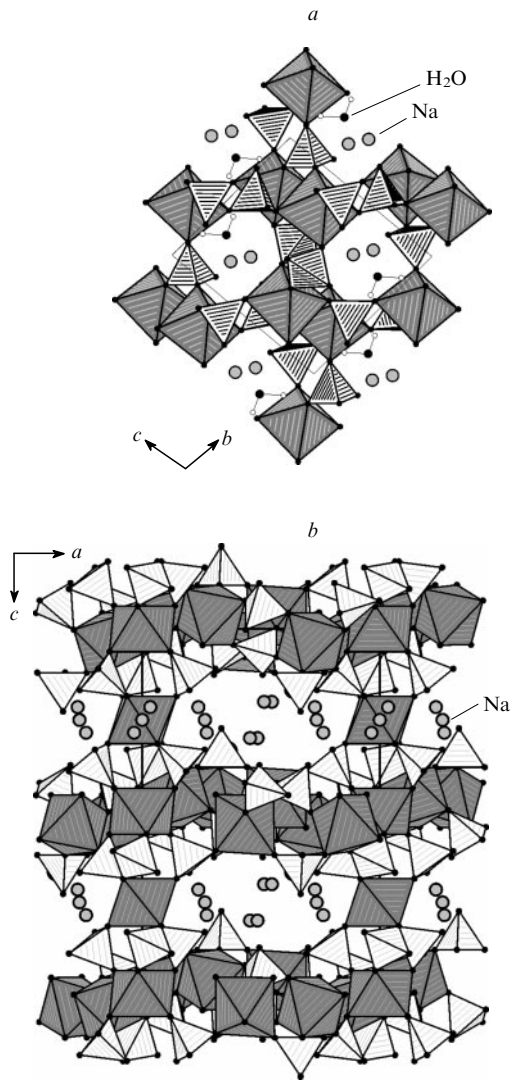



**Figure 9.** Structure of $Na_2In_2(HPO_4)_4 \cdot H_2O$ projected onto the *bc* plane (*a*) and structure of $Na_4In_8(HPO_4)_{14}(H_2O)_6 \cdot 12\,H_2O$ projected onto the *ac* plane (*b*).

$CsV_2(HPO_4)_2(PO_4)(H_2O)_2$. These compounds crystallise in two structural types (Table 6).

In monoclinic $Rb_2Ga_4(HPO_4)(PO_4)_4 \cdot 0.5\,H_2O$, [58] the $GaO_x$, $HPO_4$ and $PO_4$ polyhedra form an open-type structure with channels containing the rubidium cations and water molecules (Fig. 10 *a*). The presence of the $HPO_4$ groups and water of crystallisation in the structure was confirmed by IR spectroscopy. The Rb(1) and Rb(2) cations are located in the $M^IO_9$ and $M^IO_{10}$ polyhedra, respectively. Four crystallographically non-equivalent gallium atoms have different coordination environments (an octahedron, two tetrahedra and a trigonal bipyramid). All $GaO_x$ polyhedra share vertices with the phosphate tetrahedra, which, in turn, are coordinated (except for the OH vertices) by the gallium atoms. Two types of channels are formed along the [100] direction. The protonated oxygen vertices of the $PO_4$ tetrahedra are directed inside the channels of the first type occupied by the Rb(1) cations. The channels of the second type contain the Rb(2) cations and $H_2O$ molecules. The minimum O···O distances determining the sizes of the channels of the first and second types are 5.34 and 5.43 Å, respectively. The formation of an analogous structure is also highly probable for the RbAl analogue because the coordination numbers of 6, 5 and 4 are typical of aluminium.

The $CsIn_2(HPO_4)_2(PO_4)(H_2O)_2$ compound (centrosymmetrical structure) [63] has a rather complex structure. The octahedral environment about the In atoms is formed by five oxygen atoms of

**Table 6**. Crystallographic characteristics of the $M^{I}_{x}M^{III}_{y}(HPO_4)_z(PO_4)_u \cdot nH_2O$ and $M^{I}_{x}M^{III}_{y}(H_2PO_4)_z(HPO_4)_u \cdot nH_2O$ compounds.

| Compound | Crystal system | Space group | $Z$ | Unit cell parameters | | | | Ref. |
|---|---|---|---|---|---|---|---|---|
| | | | | $a$ /Å | $b$ /Å | $c$ /Å | $\beta$ /deg | |
| $Rb_2Ga_4(HPO_4)(PO_4)_4 \cdot 0.5\,H_2O$ | monoclinic | $P2_1$ | 2 | 5.061 | 21.643 | 8.207 | 91.8 | 58 |
| $CsV_2(HPO_4)_2(PO_4)(H_2O)_2$ | " | $P2_1/a$ | 4 | 10.004 | 17.812 | 6.370 | 97.0 | 62 |
| $CsIn_2(HPO_4)_2(PO_4)(H_2O)_2$ | " | $P2_1/c$ | 4 | 6.580 | 18.092 | 10.180 | 97.9 | 63 |
| $(H_3O)Al_3(H_2PO_4)_6(HPO_4)_2 \cdot 4\,H_2O$ | " | $C2/c$ | 4 | 16.722 | 9.437 | 17.126 | 90.9 | 73 |
| $(H_3O)Fe_3(H_2PO_4)_6(HPO_4)_2 \cdot 4\,H_2O$ | " | $C2/c$ | 4 | 16.797 | 9.528 | 17.609 | 90.6 | 74 |
| $KFe_3(H_2PO_4)_6(HPO_4)_2 \cdot 4\,H_2O$ | " | $C2/c$ | 4 | 17.01 | 9.604 | 17.50 | 90.9 | 75 |
| $(NH_4)Fe_3(H_2PO_4)_6(HPO_4)_2 \cdot 4\,H_2O$ | " | $C2/c$ | 4 | 16.845 | 9.611 | 17.647 | 90.9 | 76 |
| $(NH_4)_{0.33}Al_{0.89}(H_2PO_4)(HPO_4) \cdot 2\,H_2O$ | trigonal | $P31c$ | 6 | 8.905 | – | 16.488 | – | 77 |
| $(NH_4)Fe_3(H_2PO_4)_3[PO_3(OH)_{0.67}O_{0.33}]_3 \cdot 6\,H_2O$ | " | $P31c$ | 2 | 9.151 | – | 16.862 | – | 78 |

the $PO_4$ tetrahedra and one oxygen atom of the water molecule. The $HPO_4$ polyhedra share three vertices with the adjacent octahedra and their fourth protonated vertex is not involved in the first coordination sphere of the $In^{3+}$ cation. The $PO_4$ tetrahedron shares all vertices with the nearest $InO_6$ octahedra. The $InO_6$, $PO_4$ and $HPO_4$ polyhedra are linked to each other to form one-dimensional ribbons along the $c$ axis (Fig. 10 *b*). These ribbons are linked in a framework through the $HPO_4$ groups. The large cavities in the framework are occupied by caesium cations (the coordination number of caesium is 11).

Hydrogen phosphate $CsV_2(HPO_4)_2(PO_4)(H_2O)_2$ has an analogous structure.[62] However, the coordination polyhedron of caesium is enlarged (the coordination number of caesium is 13) due to the smaller ionic radius of vanadium. In this structure, the interactions between the ribbons somewhat resemble the interactions in the well-known structural type $M^{V}OPO_4$ with the difference that the $M^{V}O$ component is replaced by $M^{III}OH_2$ and additional phosphate groups are present between the ribbons. Taking into account the difference in the size of the vanadium and indium cations, it is reasonable to suggest that the structures characterised by an analogous topology of the framework must exist for the CsFe- and CsSc-containing compounds because the ionic radii of Fe and Sc are in the range between $r_{VI}(V^{3+})$ and $r_{VI}(In^{3+})$.

The third type of complex hydrogen phosphates includes compounds of the general formula $M^{I}_{x}M^{III}_{y}(H_2PO_4)_z(HPO_4)_u \cdot n\,H_2O$ ($M^{I}$ = K, $H_3O$, $NH_4$; $M^{III}$ = Al, Fe; $n$ = 2–6) containing two types of hydrogen phosphate anions, *viz*., $HPO_4^{2-}$ and $H_2PO_4^{-}$. The crystallographic characteristics of the monoclinic and trigonal structural types of these compounds are given in Table 6. These compounds are characterised by the ratio $M^{I} : M^{III} = 1 : 3$. Apparently, their stability is associated with the substantial difference in the radii of the $M^{I}$ and $M^{III}$ cations.

Hydrogen phosphates with composition $M^{I}M^{III}_{3}(H_2PO_4)_6 \cdot (HPO_4)_2 \cdot 4\,H_2O$ ($M^{I}$ = K, $H_3O$, $NH_4$) [73–77] and the ratio $H_2PO_4 : HPO_4 = 3 : 1$ were obtained for aluminium and iron. In the structures of these compounds, water of crystallisation is not involved in the coordination sphere about the $M^{III}$ cations. The structure of monoclinic phosphate with composition $KFe_3(H_2PO_4)_6(HPO_4)_2 \cdot 4\,H_2O$ (Fig. 11 *a*) [75] is characterised by a pronounced layered motif. The layers are composed of characteristic structural blocks, which are built from two different $FeO_6$ octahedra linked through the phosphate groups of two types, *viz*., $[HPO_4]^{2-}$ and $[H_2PO_4]^{-}$ (Fig. 11 *b*). The interlayer space is occupied by water molecules. The layers are related by the symmetry elements of the crystal lattice (space group $C2/c$) so that the channels are not formed along the [001] direction. The layers contain cavities occupied by potassium atoms to form the

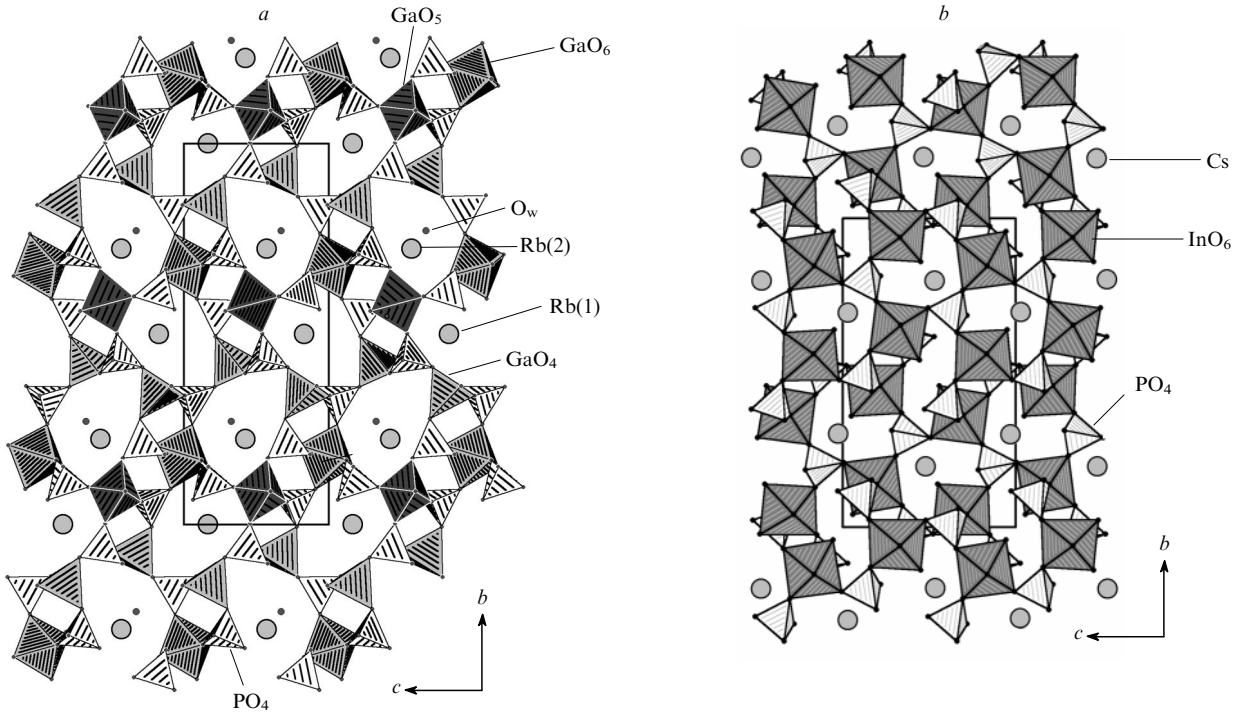



**Figure 10.** Structures of $Rb_2Ga_4(HPO_4)(PO_4)_4 \cdot 0.5\,H_2O$ (*a*) and $CsIn_2(HPO_4)_2(PO_4)(H_2O)_2$ (*b*) projected onto the *bc* plane.

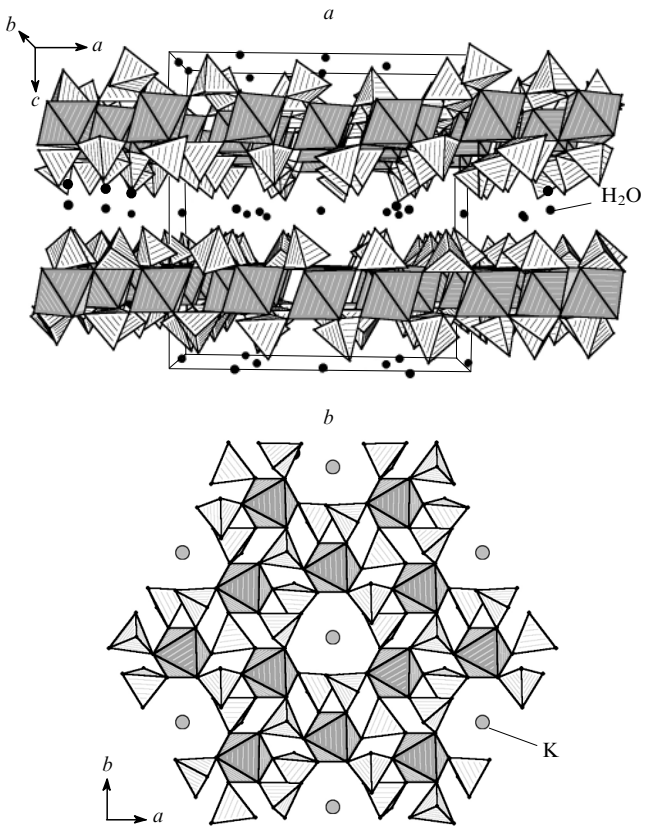



**Figure 11.** Structure of $KFe_3(H_2PO_4)_6(HPO_4)_2 \cdot 4H_2O$ projected along the [010] direction (*a*) and projected onto the *ab* plane (*b*).

$KO_{12}$ polyhedra. The layers are linked through hydrogen bonds between the oxygen atoms of the phosphate groups and water molecules, which impart additional stability to the structure. Taking into account the data on the structures of the $M^IFe_3(H_2PO_4)_6(HPO_4)_2 \cdot 4H_2O$ compounds, where $M^I$ = K, $H_3O$ or $NH_4$, and of their $(H_3O)Al$ analogue, compounds with such a composition would be expected to exist also for $M^{III}$ = Ga or V.

The $(NH_4)_{0.33}Al_{0.89}(H_2PO_4)(HPO_4) \cdot 2H_2O$ (see Ref. 77) and $(NH_4)Fe_3(H_2PO_4)_3[PO_3(OH)_{0.67}O_{0.33}]_3 \cdot 6H_2O$ (see Ref. 78) compounds are characterised by the presence of water molecules fulfilling different functions. The structures of these trigonal hydrogen phosphates differ in the number of formula units per unit cell (6 and 2, respectively).[77,78] Three crystallographically independent $M^{III}$ cations occupy the virtually non-distorted $MO_6$ octahedra in which the $M^{III}-O$ distance increases in parallel with the ionic radius of $M^{III}$. The structural formula $(NH_4)_{0.33}Al_{0.89} \cdot (H_2PO_4)(HPO_4)(H_2O) \cdot H_2O$ reflects the different role of the water molecules in the crystal motif of this compound. Three independent OH groups belonging to the $HPO_4$ [P(1)$O_4$ tetrahedron] and $H_2PO_4$ [P(2)$O_4$ tetrahedron] groups and two water molecules (coordinated to the Al atom and the $NH_4$ group) participate in hydrogen bonding. The $NH_4^+$ ions are surrounded by nine oxygen atoms most of which belong to the OH groups or $H_2O$ molecules.

Trigonal $NH_4Al$ and $NH_4Fe$ phosphates have framework structures. In the crystal structures, the $M^{III}(2)O_6$ and $M^{III}(3)O_6$ octahedra are located on threefold axes and share all their vertices with the phosphate tetrahedra. The $M^{III}(1)O_6$ octahedron has three vertices in common with the $PO_4$ tetrahedra and the remaining three vertices are occupied by the oxygen atoms of water molecules. In the structure of $NH_4Fe$ phosphate (Fig. 12 *a*,*b*),[78] the position of the protonated oxygen atom in the P(1) tetrahedron is statistically occupied by the hydrogen atom $(OH)_{2/3}O_{1/3}$.

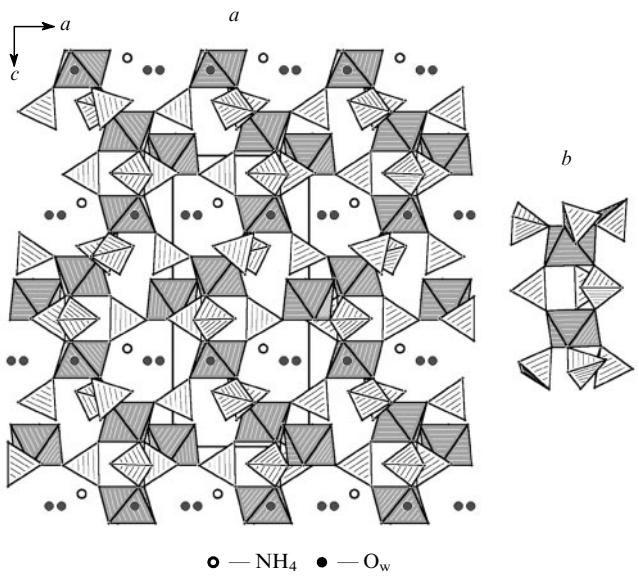



**Figure 12.** Structure of $(NH_4)Fe_3(H_2PO_4)[PO_3(OH)_{0.67}O_{0.33}]_3 \cdot 6H_2O$ projected onto the *ac* plane (*a*) and the structural block of two octahedra (*b*).

The structural block consisting of two octahedra, which are linked to nine tetrahedra through vertices (Fig. 12 *b*), is present in the crystal structures of many polytypic minerals, for example, of coquimbite, paracoquimbite and ferrinatrite $Na_3Fe(SO_4)_3(H_2O)_3$. In the latter compound, such fragments formed by the Fe octahedra and $SO_4$ tetrahedra are linked in chains parallel to the *c* axis. These chains are 'threaded' on threefold axes of the trigonal unit cell (space group $P\bar{3}$). Hence, the same repeated fragment is present in the crystal motifs of different classes of compounds. The degree of polymerisation of this fragment determines the structural diversity of compounds. It should be noted that if the octahedra with the coordinates (1/3; 2/3; *z*) located on a threefold axis are linked through tetrahedra to analogous octahedra with the coordinates (2/3; 1/3; *z*) located on another threefold axis, a large number of structures analogous to $NH_4Al$ and $NH_4Fe$ phosphates are generated. These structures can be assigned to zeolite-type compounds. Compounds in which the $M^I$-cation positions are vacant can also have analogous structures. In this case, the crystal-chemical formula can be written as $\square M^{III}(H_2PO_4)(HPO_4)(H_2O) \cdot H_2O$.[77]

The fourth type of hydrogen phosphates, *viz.*, $M^I_2M^{III}(H_2PO_4)(HPO_4)_2 \cdot H_3PO_4 \cdot 0.5H_2O$, is known only for gallium.[64] This compound has a unique composition because it contains protonated phosphate groups of all three types, *viz.*, $HPO_4^{2-}$, $H_2PO_4^-$ and $H_3PO_4$. The $Cs_2Ga(H_2PO_4)(HPO_4)_2 \cdot H_3PO_4 \cdot 0.5H_2O$ compound crystallises in the tetragonal system with a rare non-centrosymmetrical unit cell (space group $I4_1cd$, $a$ = 20.168, $c$ = 18.287 Å, $Z$ = 16). In this compound, the gallium atom is in a slightly distorted octahedral environment formed by four oxygen atoms of the $HPO_4$ groups and two oxygen atoms of the $H_2PO_4$ groups (Fig. 13 *a*). One $H_2PO_4$ group, two $HPO_4$ groups and the $GaO_6$ octahedron are involved in the typical $[Ga(H_2PO_4)(HPO_4)_2]^{2-}_{\infty}$ structural block. These blocks are linked in infinite columns along the [001] direction with the identity period involving four $GaO_6$ octahedra (due to the presence of a screw axis $4_1$, Fig. 13 *b*). Each column is linked to four adjacent columns through hydrogen bonds involving the $H_3PO_4$ molecules.

The crystal lattice contains large cavities occupied by water molecules and caesium cations. The structure contains two types of Cs atoms. The strongly distorted $Cs(2)O_{11}$ polyhedron is formed by the oxygen atoms of the phosphate groups of all three types and by the $H_2O$ molecule, which is involved in formation of

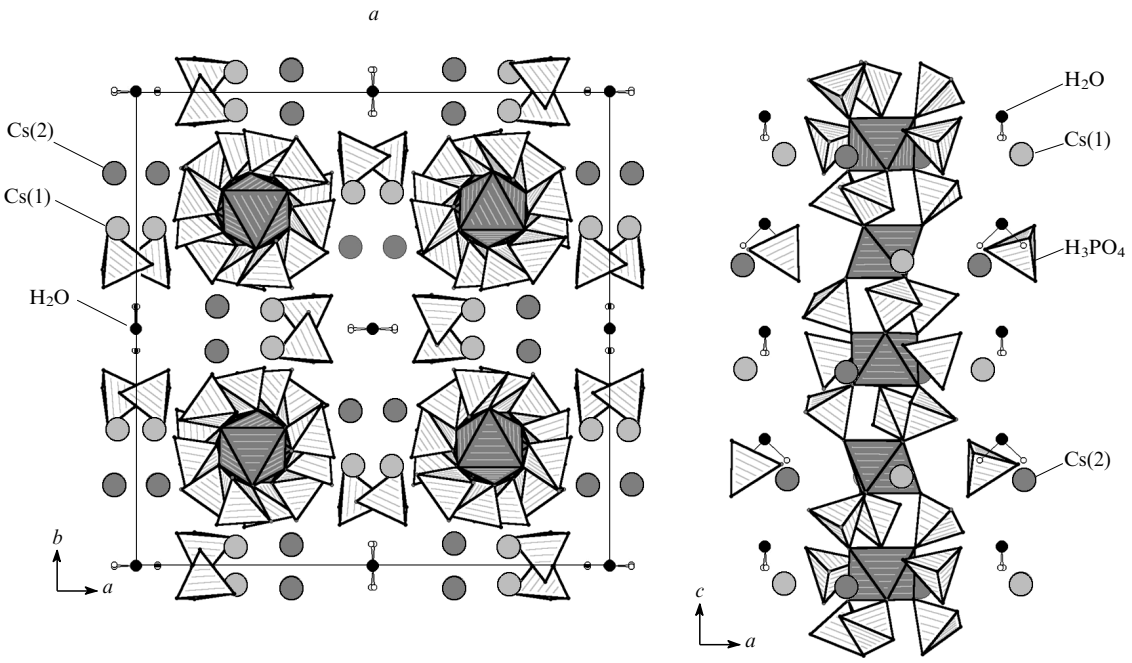



**Figure 13.** Structure of $Cs_2Ga(H_2PO_4)(HPO_4)_2 \cdot H_3PO_4 \cdot 0.5\,H_2O$ projected onto the *ab* plane (*a*) and the fragment of the $[Ga(H_2PO_4)(HPO_4)_2]_\infty$ column in combination with the $H_3PO_4$ and $H_2O$ molecules and $Cs^+$ cations (*b*).

the Cs(2)—$O_W$—Cs(2) chains. The $Cs(1)O_9$ polyhedra are less distorted and are not linked to the water molecules.

Analysis of the interatomic distances in the polyhedra of the $Cs_2Ga(H_2PO_4)(HPO_4)_2 \cdot H_3PO_4 \cdot 0.5\,H_2O$ structure showed that the gallium position can, in principle, be occupied by the Al, Fe and V atoms whose ionic radii are not much different from that of gallium. These replacements can lead to distortion of the unit-cell symmetry but the main $[M^{III}(H_2PO_4)(HPO_4)_2]^{2-}_\infty$ structural block must persist. By contrast, the replacement of caesium with rubidium or potassium must lead to degradation of the structure due to the tendency of smaller cations to have smaller coordination polyhedra.

The above-considered structural features of hydrogen phosphates containing mono- and trivalent cations, *viz*., the presence of the $HPO_4$ and $H_2PO_4$ groups and water molecules and the mode of their binding, are responsible both for the temperature range of stability of hydrogen phosphates and the possibility of their use in the synthesis of other classes of compounds.

Thermal decomposition of hydrogen phosphates $M^IM^{III}(HPO_4)_2 \cdot nH_2O$ ($M^I$ = Na, K, Rb, Cs) is accompanied by the formation of pyrophosphates $M^IM^{III}P_2O_7$. Decomposition of $RbFe(HPO_4)_2$ is accompanied by the removal of the water molecule in the temperature range of 350–550 °C to give crystalline $RbFeP_2O_7$. Thermal decomposition of $M^IIn(HPO_4)_2$ ($M^I$ = K, Rb, Cs) starts at about 280 °C and completes at 550–650 °C to form $M^IInP_2O_7$. Decomposition of $(NH_4)In.(HPO_4)_2$ at 800 °C affords a mixture of $In_4(P_2O_7)_3$ and $In(PO_3)_3$. Thermal decomposition of $(H_3O)Fe(HPO_4)_2$ proceeds in two steps. In the first step (at 670 °C), $H_2O$ is removed and hydrogen pyrophosphate is formed. The latter decomposes at 870 °C to give $Fe_2P_2O_7$ and $Fe(PO_3)_2$. Heating of $Na_2In_2.(HPO_4)_4 \cdot H_2O$ results in the loss of a water molecule (~365 °C) followed by crystallisation of a non-identified phase, which melts at 1208 °C.

Thermal decomposition of hydrogen phosphates of the second and third types is a complex process and does not afford single-phase products. In the case of $Rb_2Ga_4(HPO_4)(PO_4)_4 \cdot 0.5\,H_2O$, the removal of water of crystallisation followed by dehydration was observed at 250–600 °C. Dehydration of $(NH_4)_{0.33}Al_{0.89}(H_2PO_4)(HPO_4) \cdot 2\,H_2O$ proceeded successively. First, the water molecules and ammonium ions were eliminated at 320 °C and then the hydro- and dihydrogen phosphate anions

**Table 7**. Characterisation of different structural types of hydrogen phosphates containing $M^I$ and $M^{III}$ cations.

| Type of compound | Ratio $M^I : M^{III}$ | Type and ratio of phosphate groups | Crystal system | Space group | Structural blocks | Structural type |
|---|---|---|---|---|---|---|
| $M^I_xM^{III}_y(H_2PO_4)_z(HPO_4)_u \cdot n\,H_2O$ | 1 : 3 | $H_2PO_4 : HPO_4 = 3 : 1$ | monoclinic | $C2/c$ | $[M^{III}O_6]$ + $[HPO_4]$ and $[H_2PO_4]$ | layered |
| $M^I$ = K, $NH_4$, $H_3O$; $M^{III}$ = Al, Fe | | $H_2PO_4 : HPO_4 = 1 : 1$ | trigonal | $P\bar{3}1c$ | $[M^{III}O_{5w}]$ + $[HPO_4]$ and $[H_2PO_4]$ | framework |
| $M^I_xM^{III}_y(HPO_4)_z(PO_4)_u \cdot n\,H_2O$ | 1 : 2 | $HPO_4 : PO_4 = 2 : 1$ | monoclinic | $P2_1/c$ | $[M^{III}O_{5w}]$ + $[HPO_4]$ and $[PO_4]$ [a] | " |
| $M^I$ = Rb, Cs; $M^{III}$ = Ga, In, V | | $HPO_4 : PO_4 = 1 : 4$ | " | $P2_1/c$ | $[M^{III}O_{4,5,6}]$ + $[HPO_4]$ and $[PO_4]$ | " |
| $M^I_xM^{III}_y(HPO_4)_z \cdot n\,H_2O$ | 1 : 2 | $HPO_4$ | trigonal | $P\bar{3}c1$ | $[InO_6]$ and $[InO_5O_w]$ + $[HPO_4]$ | " |
| $M^I$ = Na; $M^{III}$ = In | | | | | | |
| $M^I_xM^{III}_y(HPO_4)_z \cdot n\,H_2O$ | 1 : 1 | $HPO_4$ | triclinic | $P\bar{1}$ | $[M^{III}O_6]$ + $[HPO_4]$ [b] | " |
| $M^I$ = Na, K, Rb, Cs, $NH_4$, $H_3O$; | | | monoclinic | $P2_1/c$ | | " |
| $M^{III}$ = Al, Ga, In, V, Fe | | | trigonal | $R\bar{3}c$ | $[M^{III}O_6]$ + $[HPO_4]$ [c] | " |
| $M^I_xM^{III}_y(H_2PO_4)_z(HPO_4)_u(H_3PO_4)_m \cdot$ | 2 : 1 | $H_2PO_4 : HPO_4 :$ | tetragonal | $I4_1cd$ | $[M^{III}O_6]$ + $[HPO_4]$, $[H_2PO_4]$ | chain |
| $n\,H_2O$ ($M^I$ = Cs; $M^{III}$ = Ga) | | $: H_3PO_4 = 1 : 2 : 1$ | | | and $[H_3PO_4]$ | |

[a] Ribbons, [b] columns, [c] helical columns.

decomposed. In the final step, $AlPO_4$ crystallised (tridymite modification).

A comparison of different procedures for the synthesis and a knowledge of the structural features of hydrogen phosphates containing mono- and trivalent cations lead to the conclusion that the steric factors play the major role in the formation of different types of complex hydrogen phosphates (Table 7). The presence of various organic additives and the use (in some cases) of fluoride ions as a mineraliser have less substantial effects on the compositions of the resulting compounds as compared to the influence of the $M^I : M^{III}$ ratio and the difference in the sizes of these cations. The effect of the $M^I$ and $M^{III}$ cations on stability of complex hydrogen phosphates in combination with the use of particular conditions for the formation of various protonated forms of phosphate groups in aqueous solutions provide the basis for the directed synthesis of new compounds.

## IV. Fluoride phosphates containing mono- and trivalent cations

Depending on the ratios of the cations ($M^I$ and $M^{III}$) and anions ($F^-$ and $PO_4^{3-}$), fluoride phosphates containing mono- and trivalent cations form several groups of compounds with compositions $M^IM^{III}FPO_4$, $M^I_3M^{III}_2F_3(PO_4)_2$, $M^I_5M^{III}F_2(PO_4)_2$ and $(M^I,M^{II},M^{III})_5F(PO_4)_3$ ($M^I$ = Li, Na, K, $NH_4$; $M^{II}$ are alkali-earth elements; $M^{III}$ are *p*-, *d*- or *f*-elements). Four types of REE sodium fluoride phosphates with different compositions were found in studies of the phase formation in the ternary systems $Na^+,M^{III}//F^-,PO_4^{3-}$ ($M^{III}$ = La, Nd, Gd, Er) by powder X-ray diffraction analysis.[79,80] Minerals belonging to fluoride phosphates are known, in particular, amblygonite $LiAlFPO_4$,[81,82] tavorite $LiFe(OH,F)PO_4$ (see Ref. 83) and lacroixite $NaAlFPO_4$ (see Ref. 84) as well as apatite-like deloneite $NaCa_3CeF(PO_4)_3$ and belovite $NaSr_3CeF(PO_4)_3$. In some fluoride phosphates, the fluoride ions are partially replaced with the hydroxide ions of a similar size. The OH : F ratio may vary; *cf.*, $Na_3Fe_2[(OH)_2F](PO_4)_2$ (see Ref. 85) and $M^IM^{III}F_{1-\delta}(OH)_\delta PO_4$ ($M^I$ = K, Rb, $NH_4$; $M^{III}$ = Al, Ga, In; $\delta \approx 0.3, 0.5$).[86]

### 1. Synthesis

Fluoride phosphates of different types, *viz.*, $M^IM^{III}FPO_4$ ($M^I$ = Na, K, $NH_4$; $M^{III}$ = Al, Cr, Fe, Ga, In, Y, Gd–Ho), $Na_3Fe_2[(OH)_2F](PO_4)_2$, $Na_3M^{III}_2F_3(PO_4)_2$ ($M^{III}$ = Al, V, Cr, Fe, Ga), $Na_5M^{III}F_2(PO_4)_2$ ($M^{III}$ = Al, Cr, Ga), and $(Na,M^{II},M^{III})_5.F(PO_4)_3$ ($M^{II}$ are alkali-earth metals; $M^{III}$ are REE), were synthesised in the solid state by crystallisation from flux or by the hydrothermal method.

The $NaM^{III}FPO_4$ compounds ($M^{III}$ = Gd, Tb, Dy) were prepared by heating stoichiometric amounts of $M^{III}PO_4$ ($M^{III}$ = Gd, Tb, Dy) and NaF in air at 550 °C ($M^{III}$ = Gd, Tb) or 500 °C ($M^{III}$ = Dy). Potassium fluoride phosphates $KM^{III}FPO_4$ ($M^{III}$ = Cr, Fe) were prepared by the reactions of chromium (or iron) oxide with $K_2O-P_2O_5$ melts in the presence of KF at 600–800 °C. In pure form, these compounds are formed in the $K_2O : P_2O_5$ range from 1 : 1 to 1 : 1.7 ($M^{III}$ = Cr) or from 1 : 1.5 to 1 : 2 ($M^{III}$ = Fe); otherwise the reactions afford the corresponding pyrophosphate $KM^{III}P_2O_7$.

The solid-phase synthesis of fluoride phosphates $Na_3M^{III}_2F_3(PO_4)_2$ containing aluminium, chromium or iron was carried out with the use of two-, three- or four-component mixtures ($NaF-M^{III}PO_4$, $M^{III}F_3-M^{III}PO_4-Na_3PO_4$, $NaF-M^{III}PO_4-NaCl-ZnCl_2$, $Na_2O-M^{III}_2O_3-P_2O_5-NaF$).[85,87–90] The reactions were carried out under an atmosphere of argon at $T$ = 600–880 °C. Aluminium (iron) sodium fluoride phosphates were prepared by recrystallisation of fluoride phosphate glasses formed upon heating of the $NaPO_3-M^{III}F_3$ or $NaF-M^{III}PO_4-M^{III}F_3$ mixtures ($M^{III}$ = Al, Fe) above the melting point followed by cooling in air to the crystallisation temperature. Aluminium-containing glass characterised by a large difference between the crystallisation and glass-transition temperatures is more stable than iron-containing glass.

Of fluoride phosphates of the $M^I_5M^{III}F_2(PO_4)_2$ family ($M^{III}$ = Al, Cr, Fe, Ga), only sodium-containing derivatives were prepared. The solid-phase synthesis of most of compounds with this composition was performed in the $M^{III}_2O_3-Na_2O-P_2O_5-NaF$ (or NaCl) system ($M^{III}$ = Cr, Fe, Ga) at $T \approx 750-1300$ °C by crystallisation from flux.[91–95] The aluminium derivative was prepared according to two procedures, *viz.*, by the solid-phase reaction in the $AlF_3-Al(OH)_3-NaH_2PO_4-Na_3PO_4$ system at $T$ = 1000 °C and precipitation from a solution.[96] In the latter case, $AlF_3 \cdot 3H_2O$ was added to an aqueous solution of $NaH_2PO_4$ at 80 °C. The suspension was kept at $T$ = 60 °C for several days after which crystallisation started.

Mixed sodium- and REE-containing fluoride phosphates were prepared with the use of two-, three- or four-component $Na^+,M^{III}//F^-,PO_4^{3-}$ mixtures ($M^{III}$ = La, Nd, Gd, Er). The mixtures were annealed under an inert or reductive atmosphere and also *in vacuo* at a temperature from 750 to 1150 °C.[79,80] When synthesising REE fluoride phosphates in air, the duration of annealing of the samples must be rigidly controlled because the time of annealing has a substantial effect on the composition of the final product. Thus, annealing of samples for 12–18 h (750 °C) gave rise to fluoride phosphate with specified composition. More prolonged heating (72 h) afforded REE oxofluorides and double phosphates $Na_3M^{III}(PO_4)_2$ ($M^{III}$ = REE).

Apatite-like REE fluoride phosphates were synthesised by the solid-phase method from $M^{II}CO_3$ ($M^{II}$ = Ca, Sr, Ba), ammonium hydrogen phosphate, REE oxide and an excess of NaF at ~1200 °C.[97–99] Phases with variable composition $Li_xM^{III}_xY_{1-x}F_{4x}(PO_4)_{1-x}$ ($M^{III}$ = Gd–Lu, Y; $0 \leqslant x \leqslant 0.45$) were prepared by heating stoichiometric amounts of double fluoride $LiM^{III}F_4$ and yttrium orthophosphate at 800 °C.[100]

Fluoride phosphates with different compositions can be obtained in the multicomponent $M^IF-M^{III}_2O_3-H_3PO_4-H_2O$ systems ($M^I$ = Li, Na, K, $NH_4$; $M^{III}$ = Al, Fe, Ga, In, Y, Ho, Er) under the hydrothermal conditions.[83,85,86,101,102] For example, $LiFe[(OH),F]PO_4$ (synthetic mineral tavorite)[83] and analogues of natural iron phosphates, such as triphylite $LiFePO_4$, sarcopside $Fe_3(PO_4)_2$ and zwieselite $Fe_2FPO_4$,[102] were obtained from the $LiF-Fe_2O_3-H_3PO_4-H_2O$ system at ≈ 300–500 °C and $p \approx 1.5$ kbar. Attempts to prepare gallium potassium fluoride phosphate $KGaFPO_4$, unlike analogous aluminium and iron compounds, failed although different modes of the solid-phase synthesis ($Ga_2O_3-NH_4H_2PO_4-KF$ mixture) and crystallisation from flux (anhydrous $Ga_2O_3-KPO_3-KF$ system) were used. Compounds in which the fluoride ions are partially replaced by the hydroxide groups, *viz.*, $M^IM^{III}F_{1-\delta}(OH)_\delta PO_4$ ($M^I$ = K, Rb, $NH_4$; $M^{III}$ = Al, Ga, In; $\delta \approx 0.3$; 0.5)[86,103,104] and $Na_3Fe_2[(OH)_2F](PO_4)_2$,[85] were prepared only under the hydrothermal conditions.

After the successful synthesis of a series of porous crystalline aluminosilicates (zeolites) and aluminophosphates, attempts were made to prepare porous fluoride phosphates of the general formula $A_aM^{III}_xF_y(PO_4)_z$ ($M^{III}$ = Ga, Fe, In; A is organic amine). It was expected that these compounds would find use as catalysts, molecular sieves or ion exchangers. In studies of the phase formation in the $NH_4F-M^{III}_2O_3-H_3PO_4-amine-H_2O$ ($M^{III}$ = Ga, Fe) and $NH_4F-Ce^{IV}(SO_4)_2-H_3PO_4-amine-H_2O$ systems at $T$ = 180 °C and $p$ = 18 bar, ammonium-containing fluoride phosphates $NH_4M^{III}FPO_4$ ($M^{III}$ = Ga, Fe)[105,106] and $NH_4Ce^{IV}F_2PO_4$ (see Ref. 107) were obtained. When $Ga_2O_3$ was used, ammonium-containing fluoride phosphate with unusual composition $(NH_4)_2Ga_2F_3(PO_4)(HPO_4)$ was obtained along with $NH_4GaFPO_4$.[106]

Polycrystalline samples of the $Na_3M^{III}_2F_3(PO_4)_2$ compounds ($M^{III}$ = V, Ga) were prepared under low-temperature hydrothermal conditions ($T$ = 180 °C, $p$ = 18 bar). However, the final products were contaminated by intermediates produced in the synthesis. The procedure used for the synthesis of sodium vana-

dium fluoride phosphate $Na_3V_2F_3(PO_4)_2$ (see Ref. 87) differs from a conventional method. Vanadium oxide $V_2O_5$ was dissolved in phosphoric acid and reduced with an aqueous solution of $N_2H_4$ until the solution turned green ($V^{3+}$ ions) and then NaF was added (the molar ratio $Na:V = 4.3:2$). The resulting solution was heated first at 180 °C and 18 bar and then at 700 °C and 2 kbar after which it was slowly cooled to room temperature with a rate of 10 °C per hour to obtain finally fluoride phosphate $Na_3V_2F_3(PO_4)_2$. The $Na_3Ga_2F_3(PO_4)_2$ compound [87] was not isolated in pure form (it contained impurities of $GaPO_4$ and $GaF_3$).

Aluminium fluoride phosphates $K_3Al_4F_9(PO_4)_2$ (see Ref. 108) and $(NH_4)Al_2F(PO_4)_2$ (see Ref. 109) were obtained by the hydrothermal method as by-products in the studies of the $M^IF-M^{III}_2O_3-H_3PO_4-H_2O$ systems.

## 2. Structure and properties

Sodium-containing fluoride phosphates with composition $NaM^{III}FPO_4$ are known only for $M^{III}$ = Al, REE. In the structures of the $NaM^{III}FPO_4$ compounds ($M^{III}$ = Y, Gd – Er), [110, 111] the $M^{III}$ atoms are located in the $[M^{III}O_6F_2]$ eight-vertex polyhedra (dodecahedra), the F atoms being in *cis* positions. The $M^{III}O_6F_2$ polyhedra are linked in infinite chains through common edges composed of two oxygen atoms. Every second polyhedron of one chain shares the edge composed of two fluorine atoms with the polyhedron form the adjacent chain giving rise to layers. These parallel layers are linked to each other through the $PO_4$ tetrahedra to form a framework (Fig. 14). The channels between the layers are occupied by sodium cations. The $NaO_8F_2$ coordination polyhedron is most preferable for sodium. The structural motif in the $NaM^{III}FPO_4$ compounds remains unchanged on going from Gd to Er and only the $PO_4$ tetrahedra are slightly rotated.

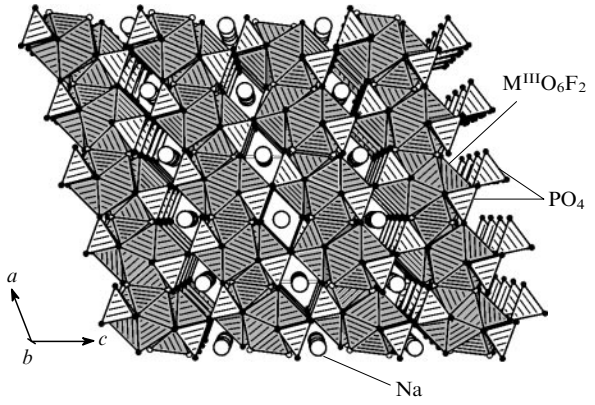



**Figure 14.** Fragment of the structure of $NaM^{III}FPO_4$ ($M^{III}$ = Y, Gd – Er).

Considering the crystal structures of this type of compounds and taking into account that REE of the second half of the series (Gd – Er) tend to adopt high coordination numbers (> 7), the formation of analogous sodium-containing fluoride phosphates would be highly improbable in the case of small trivalent REE cations (Yb, Lu) as well as in the case of In and Sc cations for which the coordination number of 6 is most typical. The exception is the mineral lacroixite $NaAlFPO_4$. [84] There is evidence for the formation of REE sodium fluoride phosphates with composition $Na_3M^{III}_2F_3(PO_4)_2$ ($M^{III}$ = Tm, Yb, Lu)¶ but the structures of these compounds remain to be established.

The $NaM^{III}FPO_4$ compounds ($M^{III}$ = Gd – Er) melt incongruently. According to the DTA data, their melting points decrease in the series Gd – Er from 903 to 837 °C. In the case of stepwise annealing in air in the temperature range of 500 – 850 °C, decomposition started already at 600 °C, proceeded through the intermediate formation of $M^{III}OF$, $Na_3PO_4$ and $M^{III}PO_4$ and afforded finally a mixture of double phosphate $Na_3M^{III}(PO_4)_2$ and oxide $M^{III}_2O_3$.

Potassium-containing fluoride phosphates $KM^{III}FPO_4$ are known for $M^{III}$ = Al, Cr, Fe, In. In the crystal structure of $KAlFPO_4$, [101, 112] the aluminium atoms are located in the $[AlO_4F_2]$ octahedra of two types, which differ in the positions of the F atoms (*trans* and *cis*). The structure of $KInFPO_4$, unlike $KAlFPO_4$, contains octahedra of only one type with a *cis* arrangement of the F atoms. In both $KM^{III}FPO_4$ compounds ($M^{III}$ = Al, In), the $M^{III}O_4F_2$ octahedra are linked in parallel helical chains through fluoride bridges and these chains are linked to each other to form a framework.

Fluoride phosphates $M^IM^{III}FPO_4$ ($M^{III}$ = Fe, Cr, Ga) [113 – 116] containing the large monovalent $K^+$ or $NH_4^+$ cations are isostructural to potassium titanyl phosphate $KTiOPO_4$ (KTP). [116] In the structures of $M^IM^{III}FPO_4$ with $M^I = K^+$ or $NH_4^+$, the $PO_4$ tetrahedra and $M^{III}O_4F_2$ octahedra are less distorted than the $TiO_6$ octahedra in $KTiOPO_4$. The $M^{III}O_4F_2$ octahedra are linked in chains extended in two mutually perpendicular directions (Fig. 15). These chains are linked to each other through the $PO_4$ tetrahedra to form a framework. The chains differ in that the $PO_4$ tetrahedra in these chains are oriented in opposite directions. The cavities in the framework are occupied by the potassium or ammonium cations.

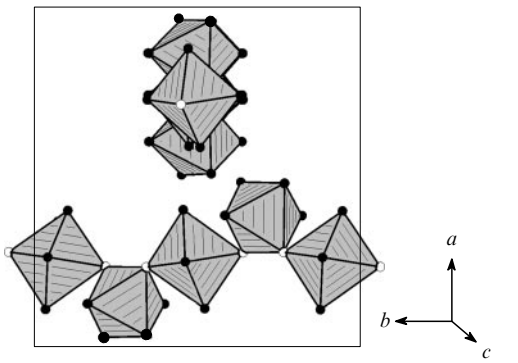



**Figure 15.** Chains of the $M^{III}O_4F_2$ octahedra in the structure of $M^IM^{III}FPO_4$ ($M^I$ = K, $NH_4$, $M^{III}$ = Cr, Fe, Ga).

Two types of potassium atoms in the structures of $KM^{III}FPO_4$ are in a complicated coordination environment formed by fluorine and oxygen atoms. The coordination numbers of the K(1) and K(2) atoms are 8 and 9, respectively. The structure of $KTiOPO_4$ contains K atoms of one type with the coordination number of 9. The coordination polyhedra about the potassium atoms have one edge (F – O) in common. The cavities occupied by the potassium atoms are linked in pairs and form two types of helical channels perpendicular to each other. The crystallographic characteristics of the $M^IM^{III}FPO_4$ compounds are given in Table 8.

In recent years, the structural features and physical properties of KTP-type compounds have attracted considerable attention, which is associated with a search for new promising nonlinear optical materials. Taking into account the results of dielectric measurements and studies of conductivity, it was suggested that the structures of KTP-type compounds are changed at 0 °C due to disordering in the potassium sublattice. An analogous phenomenon was found for fluoride phosphates $KM^{III}FPO_4$ ($M^{III}$ = Al, Fe). Like in the structure of $KTiOPO_4$, disordering in the potassium sublattice was observed in the structure of $KFeFPO_4$. As a result, two additional positions are present along with two statistically occupied potassium positions. The occupancies of these four positions are 0.9, 0.92, 0.1 and 0.08. At a temperature of about −100 °C, the K atoms are partially ordered, two main and one additional positions with the occupancies of 1.0, 0.94 and 0.06, respectively, being retained. Disordering in the potassium sublattice disappeared as the temperature was lowered to

¶ Our data.

**Table 8**. Crystallographic characteristics of the $M^{I}M^{III}FPO_4$ and $M^{I}M^{III}F_{1-\delta}(OH)_{\delta}PO_4$ compounds.

| Compound (mineral name) | Crystal system | Space group | $Z$ | Unit cell parameters | | | | Ref. |
|---|---|---|---|---|---|---|---|---|
| | | | | $a$ /Å | $b$ /Å | $c$ /Å | $\beta$ (or $\alpha$, $\beta$, $\gamma$) /deg | |
| $LiAlFPO_4$ (amblygonite) | triclinic | $P\bar{1}$ | 2 | 5.060 | 5.160 | 7.080 | $\alpha = 109.9$, $\beta = 107.5$, $\gamma = 97.9$ | 82 |
| | " | $C\bar{1}$ | 4 | 6.644 | 7.744 | 6.910 | $\alpha = 90.3$, $\beta = 117.3$, $\gamma = 91.0$ | 81 |
| $LiFe[(OH),F]PO_4$ (tavorite) | " | $P\bar{1}$ | 2 | 5.138 | 5.307 | 7.422 | $\alpha = 67.5$, $\beta = 67.7$, $\gamma = 82.0$ | 83 |
| $NaAlFPO_4$ (lacroixite) | monoclinic | $C2/c$ | 4 | 6.414 | 8.207 | 6.885 | 115.47 | 84 |
| $NaYFPO_4$ | " | $C2/m$ | 4 | 8.944 | 6.930 | 6.469 | 106.11 | 110 |
| $NaM^{III}FPO_4$ ($M^{III}$ = Tb–Er) | " | $C2/m$ | 4 | 9.000 (Tb)–8.943 (Er) | 6.985 (Tb)–6.923 (Er) | 6.506 (Tb)–6.468 (Er) | 105.98 (Tb)–106.21 (Er) | 111 |
| $KAlFPO_4$ | orthorhombic | $Pn2_1a$ | 8 | 12.522 | 10.149 | 6.226 | – | 101 |
| | " | $Pnna$ | 8 | 12.612 | 10.172 | 6.205 | – | 112 |
| $KCrFPO_4$ | " | $Pc2_1n$ | 8 | 6.346 | 10.555 | 12.776 | – | 115 |
| $KFeFPO_4$ | " | $P2_1nb$ | 8 | 10.656 | 12.885 | 6.370 | – | 113 |
| | " | $Pna2_1$ | 8 | 12.847 | 6.353 | 10.642 | – | 114 |
| $KInFPO_4$ | tetragonal | $P4_32_12$ | 8 | 9.351 | – | 11.101 | – | see [a] |
| $KInF_{0.7}(OH)_{0.3}PO_4$ | " | $P4_32_12$ | 8 | 9.345 | – | 11.096 | – | see [a] |
| $RbInF_{0.7}(OH)_{0.3}PO_4$ | " | $P4_32_12$ | 8 | 9.437 | – | 11.048 | – | see [a] |
| $NH_4InF_{0.7}(OH)_{0.3}PO_4$ | " | $P4_32_12$ | 8 | 9.447 | – | 11.103 | – | see [a] |
| $(NH_4)_{0.88}(H_3O)_{0.12}\cdot AlF_{0.67}(OH)_{0.33}PO_4$ | orthorhombic | $P2_12_12_1$ | 8 | 9.416 | 9.563 | 9.933 | – | 103 |
| $KGaF_{0.7}(OH)_{0.3}PO_4$ | " | $Pna2_1$ | 8 | 12.717 | 6.302 | 10.431 | – | 86 |
| $(NH_4)_{0.93}(H_3O)_{0.07}\cdot GaF_{0.5}(OH)_{0.5}PO_4$ | " | $P2_12_12_1$ | 8 | 9.593 | 9.742 | 9.981 | – | 104 |
| $(NH_4)FeFPO_4$ | " | $Pna2_1$ | 8 | 12.993 | 6.468 | 10.640 | – | 105 |
| $(NH_4)GaFPO_4$ | " | $Pna2_1$ | 8 | 12.921 | 6.440 | 10.415 | – | 106 |

[a] Our data.

–173 °C.[113, 114] Apparently, a more detailed study of this phenomenon will allow one to reveal correlations between the ionic conductivity and nonlinear optical properties of these compounds.

The $KM^{III}FPO_4$ compounds ($M^{III}$ = Cr, Fe) exhibit high thermal stability. The chromium compound is more stable and it melts congruently at a temperature above 1600 °C. For fluoride phosphate $KFeFPO_4$, a phase transition was found at $T = 850$ °C. At $T > 1150$ °C, this compound decomposes with the loss of oxygen to form complex iron(II) phosphates, *viz*., $KFePO_4$ and $K_2Fe_2P_2O_7F_2$ (as black melts).

The formation of complex fluoride hydroxide phosphates with composition $M^{I}M^{III}(OH)_{\delta}F_{1-\delta}PO_4$ is typical of such trivalent elements as Al, Fe, Ga and In in combination with lithium and large monovalent cations ($K^+$, $Rb^+$ and $NH_4^+$) (see Table 8). As examples we refer to synthetic tavorite $LiFe[(OH),F]PO_4$ (see Ref. 83) and the natural mineral amblygonite $LiAl[(OH),F]PO_4$.[81, 82] These compounds have framework structures. The $PO_4$ tetrahedra and $M^{III}O_6$ octahedra are the main structural elements of tavorite and amblygonite. These polyhedra are linked in chains along the [101] direction through the common (OH, F) vertices. These chains are linked in a three-dimensional framework through the $PO_4$ tetrahedra (Fig. 16 *a*). The framework is penetrated by a series of rather broad channels occupied by lithium atoms.

The environment about the lithium atom in the structures of tavorite and amblygonite deserves attention (Fig. 16 *b*). Thus, the structure of natural amblygonite contains two lithium positions with occupancies of 1/2, which are separated by a distance of 0.5 Å. These half-occupied positions are located in face-sharing five-vertex polyhedra which together form a distorted octahedron.

In the structure of montebrasite (OH-containing analogue of amblygonite), the nearest environment about the lithium atoms † is formed by five oxygen atoms. This is attributed to the fact that the oxygen atom belonging to the $AlO_6$ octahedron of one chain is involved in hydrogen bonding with the hydroxy group of the adjacent chain. In the structure of synthetic tavorite $LiFe[(OH),F]PO_4$, the coordination polyhedron about the lithium atom is the axially elongated strongly distorted square pyramid

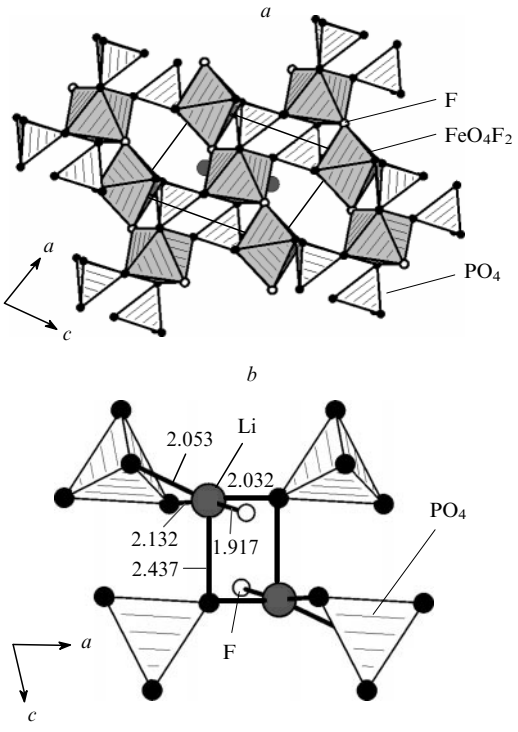



**Figure 16.** Structure of $LiFe[(OH),F]PO_4$ projected onto the *ac* plane (*a*) and the $[LiO_4(O,F)]$ polyhedra (*b*).

† The lithium atoms statistically occupy two positions separated by a distance of 0.24 Å.

$LiO_4F$ whose base is formed by the O and F atoms located at virtually equal distances from the Li atom (1.92 – 2.13 Å). The oxygen atom occupying the fifth vertex is at a distance of 2.44 Å from lithium.

The compositions of the known indium fluoride hydroxide phosphates correspond to the formula $M^{I}InF_{0.7}(OH)_{0.3}PO_4$ ($M^{I}$ = K, Rb, $NH_4$) (see Table 8). Apparently, the most stable structures are formed at the $F^-:OH^-$ ratio of 0.7:0.3. This conclusion is confirmed by the occurrence of analogous aluminium fluoride hydroxide phosphate $(NH_4)_{0.88}(H_3O)_{0.12}AlF_{0.67}.(OH)_{0.33}PO_4$,[103] and gallium fluoride hydroxide phosphate $KGaF_{0.7}(OH)_{0.3}PO_4$.[86] The $M^{I}InF_{0.7}(OH)_{0.3}PO_4$ compounds ($M^{I}$ = K, Rb, $NH_4$) are isostructural to $KInFPO_4$ and $RbIn(OH)PO_4$.[117] The $KGaF_{0.7}(OH)_{0.3}PO_4$ compound belongs to the $KTiOPO_4$ structural type.

In the structure of $M^{I}InF_{0.7}(OH)_{0.3}PO_4$, the fluoride and hydroxide ions statistically occupy one position. This replacement is quite reasonable and results from the similar sizes of these anions [$r(F^-)$ = 1.15 Å, $r(OH^-)$ = 1.18 Å]. The transformation of structurally similar fluorine-containing indium potassium phases $KInF_{1-\delta}(OH)_\delta PO_4$ ($\delta$ = 0 and 0.3) into hydroxide phosphate $KIn(OH)PO_4$ is accompanied by lowering of the symmetry of the crystal lattice from tetragonal to orthorhombic. Hence, even the partial replacement of the OH groups by the fluoride ions in the structure of $KIn(OH)PO_4$ leads to stabilisation of a more symmetrical structure, which is confirmed by X-ray diffraction analysis, electron diffraction study and the results of IR and Raman spectroscopy. Decomposition of $KInF_{0.7}(OH)_{0.3}PO_4$ in air is a complex process giving rise to fluoride $InF_3$ and indium oxofluoride InOF as intermediates, which are transformed into $K_3In(PO_4)_2$, $InPO_4$ and cubic $In_2O_3$.

The structure of the $(NH_4)_{0.93}(H_3O)_{0.07}GaF_{0.5}(OH)_{0.5}PO_4$ compound contains the $GaO_4(OH)$ trigonal bipyramid and the $GaO_4[F,(OH)]_2$ octahedron as the main building blocks linked to each other by two $PO_4$ tetrahedra.[106] These blocks are linked in layers. The channels extended along the [001] direction are occupied by the $NH_4^+$ cations. The replacement of one-half of fluoride ions in the $(NH_4)GaFPO_4$ compound by the hydroxide ions leads to a radical rearrangement of the fluoride phosphate structure. In the structure of the $(NH_4)_{0.93}(H_3O)_{0.07}GaF_{0.5}(OH)_{0.5}PO_4$ compound,[104] the bridging position linking the gallium cations is completely occupied by the hydroxy groups. The ammonium-containing compounds readily decompose to the corresponding orthophosphates $M^{III}PO_4$.

Polymorphism was found in most of representatives of fluoride phosphates with composition $Na_3M_2^{III}F_3(PO_4)_2$ ($M^{III}$ = Al, V, Cr, Fe) and several (up to three) polymorphic modification (α, β, γ) were revealed.[87] The relationships between the unit cell parameters of the α, β and γ modifications are shown in Fig. 17. The high-temperature α modifications of Al, V, Cr and Fe fluoride phosphates are isostructural, whereas the β modifications stable at low temperatures are structurally different (β′ and β″) (Table 9). The unit cell volumes of the the β′ modifications are four times larger than those of the α modifications of the same compounds. The β′ polymorphic modification is typical of Al, Cr(III) and Ga fluoride phosphates. The unit cell volumes for the β″ modification of vanadium(III) and iron(III) fluoride phosphates are twice as large as those for the α modifications. The γ modification was found only for an iron compound.

The β and α modifications differ primarily in the arrangement of the sodium atoms. In the high-temperature tetragonal unit cell of the β′ modification (space group *I*4/*mmm*), the alkali-metal atoms are shifted only slightly as compared to the sodium positions in the unit cell of the α modification, whereas substantial shifts (by 0.3 – 0.5 Å) are observed in the tetragonal structures of the β′ and β″ modifications (space group $I4_2/mbc$ and $I4_2/mnm$, respectively). The volume of the orthorhombic unit cell of the γ modification ($T$ = −190 °C) of $Na_3Fe_2F_3(PO_4)_2$ (space group *Pbam*) is twice as large as the unit cell volume of the β″ modification. The γ and β″ modifications of $Na_3Fe_2F_3(PO_4)_2$ differ primarily in the positions occupied by sodium cations and distortion of the polyhedra in the structures. The transformation γ → β″ is accompanied by deformation of the $[Fe_2F_3O_8]^{3-}$ polyhedron and displacement of the $Na^+$ cation by 0.7 Å.

The tetragonal α modification of the $Na_3M_2^{III}F_3(PO_4)_2$ compounds ($M^{III}$ = Al, Fe, Cr) consists of the $M^{III}O_4F_2$ octahedra and the isolated $PO_4$ tetrahedra as the structural blocks (Fig. 18 *a*). The octahedra are linked in pairs through the fluoride bridges. These doubled octahedra $M_2^{III}O_8F_3$ are linked in a mixed framework through the phosphate tetrahedra. The sodium atoms occupy the channels. The characteristic structural feature of these compounds is the statistical distribution of the alkali-metal atoms in the unit cell. Due to triple disorder, there are three modes of coordination of the sodium ions, all these atoms being located approximately on a circle with a diameter of 1.9 – 2.2 Å (Fig. 18 *b*).

At room temperature, the β′-$Na_3Al_2F_3(PO_4)_2$ compound crystallises in the tetragonal system (space group $P4_2/mbc$) but exhibits a superstructure.

The partial replacement of the fluoride ions in the $Na_3Fe_2F_3(PO_4)_2$ compound by the hydroxy groups leads to the formation of $Na_3Fe_2[(OH)_2F](PO_4)_2$ (see Ref. 85) isostructural to β′-$Na_3V_2F_3(PO_4)_2$ (see Table 9). In the structure of $Na_3Fe_2[(OH)_2F](PO_4)_2$, the $[Fe_2O_8F_3]$ bioctahedra are deformed resulting in a doubling of the unit cell volume as compared to that of $Na_3Fe_2F_3(PO_4)_2$.

Ammonium-containing gallium fluoride phosphate $(NH_4)_2Ga_2F_3(PO_4)(HPO_4)$ [106] (see Table 9) was assigned to the 'pseudo-KTP' type related to the KTP type ($KTiOPO_4$) (Fig. 19 *a*). In compounds of the 'pseudo-KTP' type, only three of four oxygen atoms of each $PO_4$ tetrahedron are involved in the octahedral environment about gallium to form the $GaO_4F_2$ and

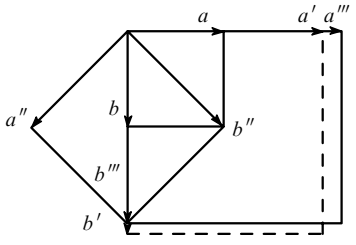



**Figure 17.** Relationship between the unit cell parameters of the α, β and γ modifications $M_3^{I}M_2^{III}F_3(PO_4)_2$.[87] The *a* and *b* parameters correspond to the α modification, *a*′ and *b*′ correspond to the β′ modification, *a*″ and *b*″ correspond to the β″ modification and *a*‴ and *b*‴ correspond to the γ modification.

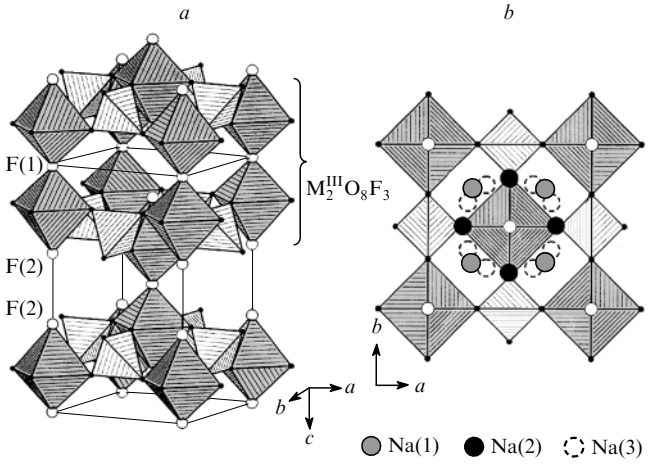



**Figure 18.** Structure $Na_3Al_2F_3(PO_4)_2$. Overall view (*a*); a one-layer fragment projected onto the *ab* plane (*b*).

**Table 9**. Synthesis conditions and crystallographic characteristics of the $Na_3M^{III}_2F_3(PO_4)_2$ ($M^{III}$ = Al, V, Cr, Fe), $Na_3Fe_2(OH)_2F(PO_4)_2$ and $(NH_4)_2Ga_2F_3(PO_4)(HPO_4)$ compounds.

| Compound | Method of synthesis | Synthesis conditions | | $T_m$ ($T_{tr}$) /°C | Crystal system | Space group | $Z$ | Unit cell parameters | | | Ref. |
|---|---|---|---|---|---|---|---|---|---|---|---|
| | | $T$ /°C | $p$ /bar | | | | | $a$ /Å | $b$ /Å | $c$ /Å | |
| β′-$Na_3Al_2F_3(PO_4)_2$ | hydrothermal | 650 | 2000 | 43 (β→α) | tetragonal | $P4_2/mbc$ | 4 | 12.406 | – | 10.411 | 87 |
| α-$Na_3Al_2F_3(PO_4)_2$ | " | 300 | 80 | – | " | $I4/mmm$ | 2 | 6.211 | – | 10.407 | 88 |
| | solid-phase (from NaCl flux) | 700 | – | 726 (sh.) | " | $I4/mmm$ | 2 | 6.206 | – | 10.418 | 87 |
| β″-$Na_3V_2F_3(PO_4)_2$ | hydrothermal | 650 | 2000 | – | " | $P4_2/mnm$ | 4 | 9.047 | – | 10.705 | 87 |
| β′-$Na_3Cr_2F_3(PO_4)_2$ | solid-phase (under Ar) | 700 | – | 55 (β→α) | " | $I4/mmm$ | 4 | 12.666 | – | 10.608 | 87 |
| α-$Na_3Cr_2F_3(PO_4)_2$ | solid-phase (from flux) | 950 | – | 1045 (sh.) | " | $I4/mmm$ | 2 | 6.341 | – | 10.613 | 89 |
| γ-$Na_3Fe_2F_3(PO_4)_2$ | – | – | – | 27 (γ→β) | orthorhombic | $Pbam$ | 8 | 12.756 [a] | 12.803 [a] | 10.602 [a] | 87 |
| β″-$Na_3Fe_2F_3(PO_4)_2$ | solid-phase (from NaCl flux) | 700 | – | – | tetragonal | $I4/mmm$ | 4 | 9.037 | – | 10.668 | 87 |
| α-$Na_3Fe_2F_3(PO_4)_2$ | hydrothermal | 300 | 80 | 746 (sh.) | " | $I4/mmm$ | 2 | 6.399 | – | 10.679 | 90 |
| $Na_3Fe_2(OH)_2F(PO_4)_2$ | " | 200 | 20 | – | " | $P4_2/mnm$ | 4 | 9.050 | – | 10.679 | 85 |
| $Na_3Ga_2F_3(PO_4)_2$ | " | 180 | 18 | 701 (sh.) | " | $I4/mmm$ | 2 | 6.291 | – | 10.646 | 87 |
| $(NH_4)_2Ga_2F_3(PO_4)(HPO_4)$ | hydrothermal (with guanidine) | 180 | 18 | – | orthorhombic | $Pna2_1$ | 4 | 12.497 | 7.702 | 9.846 | 106 |

[a] Data obtained at $T = -190$ °C.

**Table 10**. Synthesis conditions and crystallographic characteristics of the $Na_5M^{III}F_2(PO_4)_2$ ($M^{III}$ = Al, Ga, Cr, Fe) and $Na_{5-x}Fe(O_\delta F_{1-\delta})(PO_4)_2$ compounds.

| Compound | Method of synthesis | $T$ /°C | Crystal system | Space group | $Z$ | Unit cell parameters | | | Ref. |
|---|---|---|---|---|---|---|---|---|---|
| | | | | | | $a$ /Å | $b$ /Å | $c$ /Å | |
| $Na_5AlF_2(PO_4)_2$ | solid-phase (from flux) | 730 | trigonal | $P\bar{3}$ | 3 | 10.468 | – | 6.599 | 91 |
| | from aqueous solution | 60 | " | $P\bar{3}$ | 3 | 10.483 | – | 6.607 | 96 |
| | solid-phase | 1000 | " | $P\bar{3}$ | 3 | | | | 96 |
| $Na_5GaF_2(PO_4)_2$ | solid-phase (from flux) | 730 | " | $P3$ | 3 | 10.560 | – | 6.660 | 91 |
| $Na_5CrF_2(PO_4)_2$ | the same | 850 – 700 | " | $P3$ | 3 | 10.576 | – | 6.669 | 92 |
| $Na_5FeF_2(PO_4)_2$ | " | 850 – 700 | orthorhombic | $Pbca$ | 16 | 11.643 | 21.777 | 13.750 | 93 |
| $Na_{4.6}Fe(O_{0.6}F_{0.4})(PO_4)_2$ | " | 750 | " | $Ibam$ | 8 | 15.514 | 14.809 | 7.116 | 94 |
| $Na_{4.5}Fe(O, F)(PO_4)_2$ (see [a]) | " | 750 | " | $Bmcm$ | 4 | 15.520 | 7.410 | 7.119 | 95 |
| $Na_{4.5}Fe(O,F)(PO_4)_2$ (see [b]) | " | 750 | " | $Bmcm$ | 4 | 15.645 | 7.433 | 7.144 | 95 |

[a] Modulated phase I stable at $T = 0$ °C. [b] Modulated phase II stable at $T = 350$ °C.

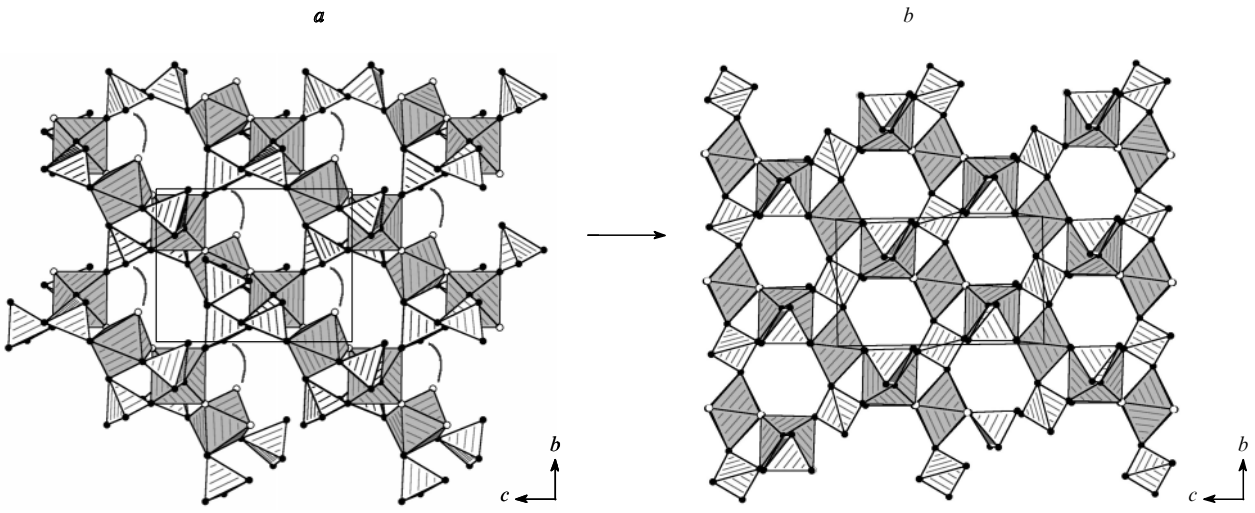



**Figure 19.** Relationship between the 'pseudo-KTP'-type structure of $(NH_4)_2Ga_2F_3(PO_4)(HPO_4)$ (*a*) and the KTP-type structure of $(NH_4)GaF(PO_4)$ (*b*). Layered fragments are shown. The ammonium groups are omitted.

$GaO_3F_3$ octahedra, as distinct from compounds of the KTP type in which all oxygen atoms of the $PO_4$ tetrahedra are involved in the $M^{III}O_6$ octahedra. The structure of the 'pseudo-KTP' type can be transformed into the structure of the KTP type by rotation of the corresponding $PO_4$ tetrahedra and $GaO_3F_3$ octahedra (see Fig. 19). In the KTP-type structures, the channels extended along the [100] direction have regular hexagonal cross-sections, whereas the channels along the [010] direction have distorted hexagonal cross-sections (Fig. 19 *b*). The framework structure of the $(NH_4)_2Ga_2F_3(PO_4)(HPO_4)$ compound is more distorted as compared to the structure of $(NH_4)GaFPO_4$.

Fluoride phosphates $Na_5M^{III}F_2(PO_4)_2$ with $M^{III}$ = Al, Cr, Ga [91, 92] crystallise in the trigonal system (Table 10), whereas an analogous iron compound is characterised by lower symmetry (orthorhombic). The $Na_5M^{III}F_2(PO_4)_2$ compounds can be assigned to layered structures. These structures contain corrugated layers parallel to the *ab* plane. The layers are built from the $M^{III}O_4F_2$ octahedra and the $PO_4$ tetrahedra (Fig. 20 *a*,*b*). One-third of all sodium atoms are located in these layers. The sodium atoms occupy from 6 (in the aluminium-containing compound) to 9 (in the chromium- and gallium-containing compounds) and 10 (in the iron-containing compounds) crystallographically independent positions most of which are statistically occupied. In the structures of these compounds, the alkali-metal atoms are located only in the centres of octahedra, which are formed either by oxygen atoms or together by fluorine and oxygen atoms ($NaO_6$, $NaO_5F$, $NaO_4F_2$, $NaO_3F_3$). For iron, not only fluoride phosphate with composition $Na_5FeF_2(PO_4)_2$ but also oxofluoride phosphates with variable composition $Na_{5-x}Fe(O,F)(PO_4)_2$ ($x$ = 0.4 and 0.5) are known. Modulations of the atomic positions were revealed in the structures of the latter compounds.[93–95] The reversible phase transition from one modulated phase to another (I→II) observed at $T$ = 257 °C is associated with slight displacements of the atoms and a change in the direction of the modulation vector. The investigation of polymorphism in $Na_{4.5}Fe(O,F)(PO_4)_2$ (see Ref. 95) depending on the temperature ($T$ < 1000 °C) and pressure ($p = 1\times10^5 - 1.2\times10^{10}$ Pa) revealed the presence of one (at $T \approx 260$ °C, $p$ = 101.3 kPa) and two [at $p_1$ = 1.39(8) GPa and $p_2$ = 4.52(32) GPa] polymorphic transformations, respectively. The modulation effect in the structure of $Na_{4.6}Fe(O_{0.6}F_{0.4})(PO_4)_2$ has no influence on the ionic transport ($\sigma_0 \approx 1.17\times10^4 - 1.88\times10^4$ S cm$^{-1}$, $E_a$ = 0.33 eV) and dielectric properties.

The difference in occupancies of the same positions by sodium atoms in the isotypic structures of fluoride phosphates $Na_3M^{III}_2F_3(PO_4)_2$ and $Na_5M^{III}F_2(PO_4)_2$ ($M^{III}$ = Al, Fe, Ga) is indicative of the possible ionic conductivity. At $T$ = 0 °C, the measured specific conductivity ($\sigma$) of the $Na_5M^{III}F_2(PO_4)_2$ compounds ($M^{III}$ = Al, Ga) is approximately equal to $10^{-7}$ S cm$^{-1}$ and it increases by only three orders of magnitude (to $\sigma \approx 10^{-4}$ S cm$^{-1}$) as the temperature is raised to 327 °C.[91] As mentioned above, the $Na^+$ ions can migrate only in some of the

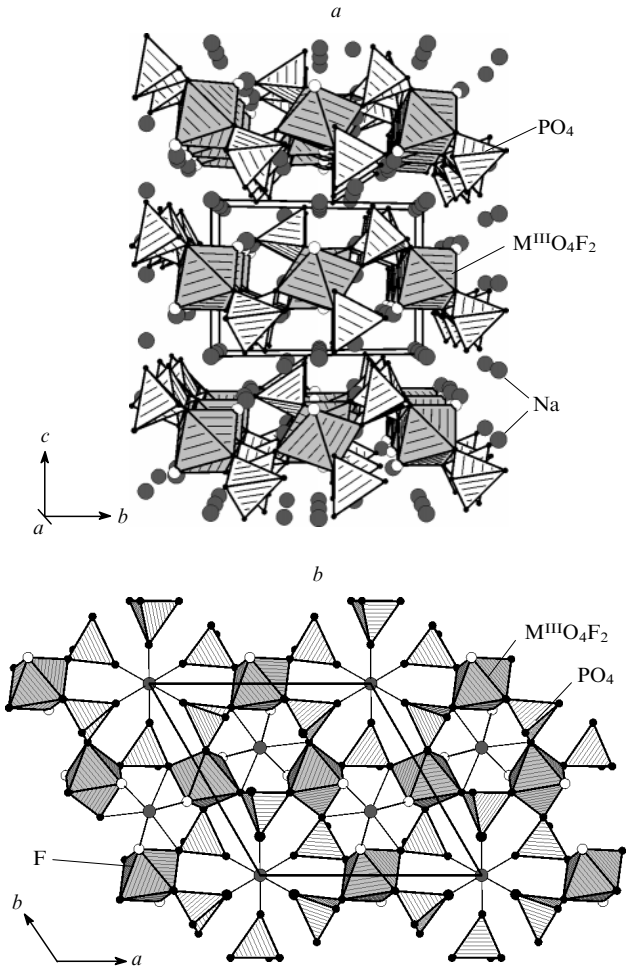



**Figure 20.** Structure of $Na_5M^{III}F_2(PO_4)_2$ ($M^{III}$ = Al, Cr, Ga) projected along the [001] direction (*a*) and the one-layer fragment projected onto the *ab* plane (*b*).

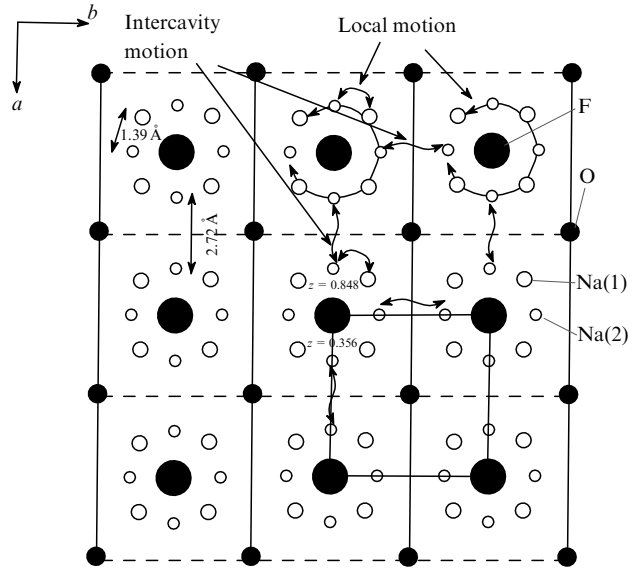



**Figure 21.** Structure of $Na_3Al_2F_3(PO_4)_2$ projected onto the *ab* plane. Different trajectories of motion of the $Na^+$ ions are shown.

channels in the structures of $Na_3M^{III}_2F_3(PO_4)_2$. The $Na_3Al_2F_3(PO_4)_2$ compound is characterised by a rather high activation energy (0.80 eV at 500 °C), which prevents the wide use of this fluoride phosphate as a ionic conductor. This compound is inferior to the recognised sodium conductors, such as compounds of the NASICON type ($E_a \approx 0.35$ eV) or Na – β-$Al_2O_3$ ($E_a \approx 0.14$ eV).

Based on the analysis of the sizes and geometry of the cavities occupied by the sodium atoms, several possible trajectories of motion of alkali cations in the structure were proposed, *viz*., the migration from one cavity to another through a distance of 2.72 Å and/or the local motion around a circle within each cavity. These trajectories are schematically shown in Fig. 21.‡

Fluoride phosphate $K_3Al_4F_9(PO_4)_2$ (see Ref. 108) crystallises in another structural type characterised by the presence of the $[Al_4F_9O_8]_n$ chains (Fig. 22 *a*). The structural block of the chain is formed by four vertex-sharing $AlO_2F_4$ octahedra with the *cis* arrangement of the oxygen atoms (Fig. 22 *b*). In the perpendicular direction, the chains are linked to each other through the $PO_4$ tetrahedra to form a three-dimensional framework whose channels are occupied by the potassium ions (Table 11). A change in

‡ From J-M Le Meins, O Bohnke, G Courbion *Solid. State Ion.* **111** 67 (1998).

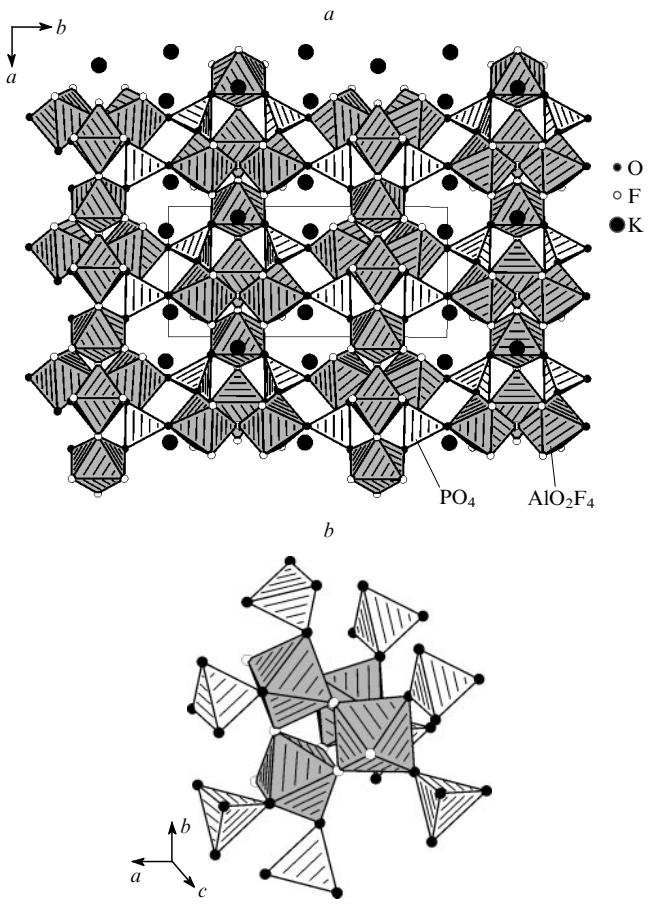



**Figure 22.** Structure of $K_3Al_4F_9(PO_4)_2$ projected onto the *ab* plane (*a*) and the mode of linkage of the $AlO_2F_4$ octahedra in the chain (*b*).

the Al : F : P ratio from 1 : 1 : 1 corresponding to the $KAlFPO_4$ compound to 2 : 4.5 : 1 corresponding to the $K_3Al_4F_9(PO_4)_2$ compound is associated with a more complex mode of linkage of the octahedra in the chains in the latter compound.

The data on apatite-type compounds containing $M^I$, $M^{II}$ and $M^{III}$ cations instead of (or along with) calcium are concerned primarily with sodium derivatives of particular REE (see Table 11). The parent compound of this family, *viz*., potassium fluoride phosphate $Ca_{10}F_2(PO_4)_6$ (fluoroapatite), crystallises in the hexagonal system (space group $P6_3/m$) (Fig. 23 *a*).[118] In the unit cell of $Ca_{10}F_2(PO_4)_6$, six $PO_4$ tetrahedra are located on mirror planes ($z$ = 1/4 and 3/4). The calcium cations occupy two crys-

**Table 11**. Synthesis conditions and crystallographic characteristics of apatite-type fluoride phosphates.

| Compound | Method of synthesis | $T$ /°C | Crystal system | Space group | $Z$ | Unit cell parameters | | | | Ref. |
|---|---|---|---|---|---|---|---|---|---|---|
| | | | | | | $a$ /Å | $b$ /Å | $c$ /Å | $\beta$ /deg | |
| $K_3Al_4F_9(PO_4)_2$ | hydrothermal [a] | 180 | monoclinic | $P2_1/m$ | 2 | 6.721 | 13.856 | 7.276 | 105.9 | 108 |
| $(NH_4)Al_2F(PO_4)_2$ | " | 180 | orthorhombic | $P2_12_12_1$ | 4 | 9.456 | 9.621 | 9.965 | – | 109 |
| $Li_xM^{III}Y_{1-x}(PO_4)_{1-x}F_{4x}$ ($M^{III}$ = Gd – Lu, Y; $0 \leqslant x \leqslant 0.45$) (zircon type) | solid-phase ($LiMF_4 - YPO_4$) | 800 | tetragonal | $I4_1/amd$ | 2 | 6.958 – 6.900 | – | 6.188 – 6.055 | – | 100 |
| $Na_2Ba_6La_2F_2(PO_4)_6$ | solid-phase | 1000 | hexagonal | $P\bar{6}$ | 2 | 9.939 | – | 7.442 | – | 97 |
| $Na_3Ba_4Nd_3F_2(PO_4)_6$ | " | 1000 | trigonal | $P\bar{3}$ | 1 | 9.786 | – | 7.281 | – | 97 |
| $Na_2Ca_6Sm_2F_2(PO_4)_6$ | " | 1200 | hexagonal | $P6_3/m$ | 1 | 9.390 | – | 6.895 | – | 98 |
| $Na_2Ca_6Eu_2F_2(PO_4)_6$ | " | 1200 | " | $P6_3/m$ | 1 | 9.385 | – | 6.893 | – | 99 |
| $(NH_4)Ce^{IV}F_2(PO_4)$ | hydrothermal [a] | 180 | monoclinic | $P2_1/m$ | 2 | 6.660 | 5.875 | 7.177 | 114.31 | 107 |

[a] The pressure was 18 bar.

tallographically independent positions. The Ca(1) cations lie on threefold axes in the positions (1/3, 2/3, $z$) and form the $CaO_9$ polyhedra in which six Ca—O distances have close values and are substantially shortened (2.43–2.47 Å) as compared to the remaining three distances (2.83 Å). The Ca(2) cations are located on the planes $m$ in the positions ($x$, $y$, 1/4) and form the $Ca(2)O_8F$ polyhedra in which six O atoms are at distances of 2.36–2.53 Å, the F atom is located at a distance of 2.26 Å and two substantially remote O atoms are at distances of 3.27 Å. Two $F^-$ ions lie on the $6_3$ axis.

In apatite-type structures, impurity cations (in particular, REE) are differently distributed over two crystallographically non-equivalent calcium positions (Fig. 23 *b*).§ In the structure of Nd-doped fluoroapatite, the positions occupied by neodymium atoms depend on the mechanism of replacement.[97] When neodymium was introduced as trifluoride $NdF_3$, the Ca(1) and Ca(2) positions were equally replaced by Nd. By contrast, the use of $Nd_2O_3$ as a source of REE led to the structure in which neodymium atoms occupy predominantly the Ca(2) position. In the hexagonal structure of $Na_2Ba_6La_2F_2(PO_4)_6$, the $La^{3+}$ and $Na^+$ ions statistically occupy both positions, *viz.*, Ca(1) and Ca(2). In the trigonal structure of $Na_3Ba_4Nd_3F_2(PO_4)_6$, two-third of all $Nd^{3+}$ and $Na^+$ ions occupy the Ca(1) positions, whereas the remaining atoms are disordered in the Ca(2) positions.

Fluoride phosphates with composition $Na_2Ca_6M^{III}_2F_2(PO_4)_6$ ($M^{III}$ = Sm, Eu),[98, 99] like non-doped fluoroapatite, crystallise in the hexagonal system. The $Eu^{3+}$ ions occupy the Ca(1) positions by approximately 75% and the alkali-metal ions are located only in the Ca(2) positions, whereas the opposite situation is observed in the structure of the samarium compound. In the latter structure, the sodium atoms are located only in the Ca(1) positions, whereas the REE ions replace the Ca(2) atoms by 78.5%. In fluoroapatite-type structures, the REE atoms have different coordination numbers (7 and 9).

The REE compounds, which crystallise in the apatite structural type, can be used as catalysts, ion-exchange phases and luminescent materials. The $Na_2Ca_6Tb_{1.75}Y_{0.25-x}Eu_xF_2(PO_4)_6$ compound was found to exhibit luminescence properties.[119] The introduction of europium leads to weakening of radiation by the $Tb^{3+}$ cations, which is indicative of the charge transfer from $Tb^{3+}$ to $Eu^{3+}$.

§ Figure 23 *b* was published by P K Rastsvetaeva, A P Khomyakov *Kristallographiya* **41** 831 (1996); [*Crystallogr. Rep. (Engl. Transl.)* **41** 789 (1996)].

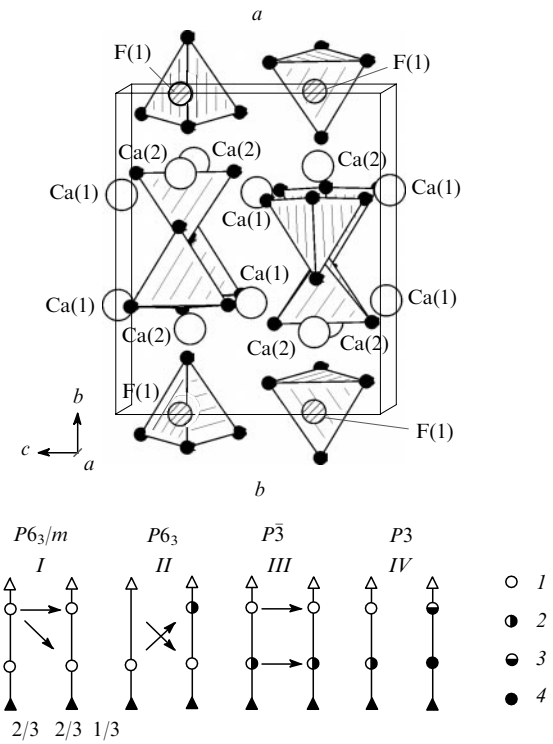



**Figure 23.** Structure of $Ca_5F(PO_4)_3$ projected along the [100] direction (*a*) and the schematic representation of the arrangement of the cations (*1–4*) in the Ca(1) positions in the hexagonal and trigonal apatite-type structures (*I–IV*) (*b*).
(*I*) $Ca_5F(PO_4)_3$; (*II*) $Sr_5F(PO_4)_3$; (*III*) $NaSr_3CeF(PO_4)_3$; (*IV*) $NaCa_3.CeF(PO_4)_3$.

Hence, there are several types of fluoride phosphates containing mono- and trivalent cations, which differ in composition and structure (Table 12). Compounds belonging to the same type are either isostructural or structurally related. Variations in the type and ratio of the ions in the cation sublattice as well as a change of the anion composition in complex phosphates containing mono- and trivalent cations by partially replacing the $PO_4$ tetrahedral groups with anions of different nature ($F^-$) lead not only to the formation of compositionally different compounds with different $M^I : M^{III} : PO_4^{3-}$ ratios but also to a radical rearrangement of the

**Table 12**. Characterisations of the structures of different types of complex fluoride phosphates with $M^I$ and $M^{III}$ cations.

| Type of compound | Ratio $M^I : M^{III}$ | Crystal system | Space group | Building blocks | Structural type |
|---|---|---|---|---|---|
| $M^I_3M^{III}_4F_9(PO_4)_2$ ($M^I$ = K, $M^{III}$ = Al) | 3 : 4 | monoclinic | $P2_1/m$ | $[M^{III}_4O_8F_9]_\infty$ (chains) + $[PO_4]$ | framework |
| $M^I_{2+x}M^{II}_{6-2x}M^{III}_{2+x}F_2(PO_4)_6$ ($x$ = 0, 1) ($M^I$ = Na; $M^{III}$ = Sm, Nd, Eu) | (2 : 4) – (3 : 3) | trigonal<br>hexagonal | $P\bar{3}$<br>$P\bar{6}$, $P6_3/m$ | $[M^{III}O_xF_y]$ (isolated polyhedra) + $[PO_4]$ | " |
| $M^IM^{III}F(PO_4)$ ($M^I$ = Na; $M^{III}$ = Y, Gd – Er) | 1 : 1 | monoclinic | $C2/m$ | $[M^{III}O_6F_2]_{2\infty}$ (layers) + $[PO_4]$ | " |
| $M^IM^{III}F(PO_4)$ ($M^I$ = Li, Na, K, $NH_4$, Rb; $M^{III}$ = In, Ga, Sc, Al, Fe, Cr) | 1 : 1 | triclinic<br>tetragonal<br>orthorhombic | $P\bar{1}$, $C\bar{1}$<br>$P4_32_12$<br>$P2_12_12_1$, $Pc2_1n$, $Pnna$, $Pna2_1$ | $[M^{III}O_4F_2]_\infty$(chains) + $[PO_4]$ | " |
| $M^I_3M^{III}_2F_3(PO_4)_2$ ($M^I$ = Na; $M^{III}$ = Ga, Al, Fe, Cr, V) | 3 : 2 | tetragonal<br><br>orthorhombic | $I4/mmm$, $P4_2/mnm$, $P4_2/mbc$, $I4/mmm$<br>$Pbam$ | $[M^{III}_2O_8F_3]$ (bioctahedra) + + $[PO_4]$ | " |
| $M^I_5M^{III}F_2(PO_4)_2$ ($M^I$ = Na; $M^{III}$ = Ga, Al, Fe, Cr) | 5 : 1 | trigonal<br>orthorhombic | $P3$, $P\bar{3}$<br>$Pbca$, $Ibam$, $Bmcm$ | $[M^{III}_4F_2]$ (octahedra) + $[PO_4]$ | layered |

structure from layered (typical only of fluoride phosphates with a high content of alkali cations, $M^I : M^{III} = 5 : 1$) to framework consisting of ($[M_2^{III}O_8F_3]$ and $[M_4^{III}O_8F_9]$) island fragments, chains or layers built from the $M^{III}O_xF_y$ polyhedra.

## V. Hydroxide phosphates containing mono- and trivalent cations

Like fluoride-containing analogues, hydroxide phosphates are characterised by complex compositions combining tri- and monovalent cations. The similarity between the effective ionic radii of the $F^-$ and $OH^-$ anions and the formation of bonds between these anions and the $M^{III}$ cations of comparable strength are responsible for the occurrence of the $M^IM^{III}(OH)PO_4$ compounds compositionally similar to $M^IM^{III}FPO_4$. However, hydroxide phosphates with compositions untypical of fluoride phosphates are also known:

$M_4^IM^{III}(OH)(PO_4)_2$, $M_3^IM^{III}(OH)(HPO_4)(PO_4)$,

$M_{1.5}^I[M_2^{III}O_{0.5}(OH)_{0.5}(PO_4)_2(H_2O)] \cdot x\,H_2O$,

$M^IM_2^{III}(OH)(PO_4)_2 \cdot 2\,H_2O$ and $M^IM_3^{III}(OH)_4(PO_4)_2 \cdot 2\,H_2O$.

Some compounds of the $M^IM^{III}(OH)PO_4$ group as well as a series of phases with composition $M^IM_2^{III}(OH)(PO_4)_2 \cdot 2\,H_2O$ were found as minerals. Complex hydroxide phosphates of all these types are known for $M^{III}$ cations with small ionic radii (Al, Ga, In, V, Fe, Mn).

### 1. Synthesis

The mineral tavorite $LiFe(OH,F)PO_4$ is the Fe-containing analogue of montebrasite $LiAl(OH)PO_4$ (see Ref. 81) belonging to the group of amblygonite $LiAl(OH,F)PO_4$. The ideal compositions of tavorite and amblygonite are described by the formulas $LiFe(OH)PO_4$ (see Ref. 120) and $LiAlFPO_4$ (see Ref. 81), respectively. Being a rare mineral from lithium pegmatites, tavorite is unstable under natural conditions. Various paragenetic associations are typical of minerals of the leucophosphite group of the general formula $M^IM_2^{III}(OH)(PO_4)_2 \cdot 2\,H_2O$, where $M^I = K$, $NH_4$ and $M^{III} = Al$, Fe. Leucophosphite $KFe_2(OH).(PO_4)_2 \cdot 2\,H_2O$ [121, 122] by itself is a product formed by the action of organic solutions derived from bat guano with iron oxides in serpentine rocks or is generated in late stages of the hydrothermal transformation of triphylite in pegmatites. Tinsleyite [123] (Al analogue of leucophosphite) was found together with $KFe_2(OH).(PO_4)_2 \cdot 2\,H_2O$ in pegmatites. Spheniscidite $(NH_4)Fe_2(OH).(PO_4)_2 \cdot 2\,H_2O$ [124, 125] is formed by the actions of ammonium phosphate solutions of penguin guano with mica and chlorite minerals. Cyrilovite $NaFe_3(OH)_4(PO_4)_2 \cdot 2\,H_2O$,[126] which is the Fe-containing final member of the series of minerals belonging to the group of wardite $Na(Al,Fe)_3(OH)_4(PO_4)_2 \cdot 2\,H_2O$, is fragmentary present in pegmatites and can occupy cavities of oxidation zones of ferrous precipitates.

Most of the compounds under consideration were synthesised under hydrothermal conditions (Table 13).[117, 122, 125, 127–135] The simultaneous action of pressure and temperature leads to a substantial increase in solubility of the compounds under study in active aqueous media and is favourable for the preparation of complex $M^{III}$ hydroxide phosphates as highly crystalline powders and well-faceted crystals, which cannot, in principle, be grown by alternative methods. Unlike Al- and Fe-containing phases of the $M^IM^{III}(OH)PO_4$ type, their indium analogues do not form minerals of their own. Single crystals of hydroxide phosphates $KIn(OH)PO_4$ (see Ref. 127) and $RbIn(OH)PO_4$ (see Ref. 117) were obtained under drastic conditions (900 and 550 °C, respectively) followed by stepwise cooling. It should be noted that these phases are stable at pH 7–8. Attempts to prepare polycrystalline

**Table 13**. Hydrothermal synthesis of complex hydroxide phosphates with $M^{III}$ cations.

| Composition | Compound | Starting reagents (molar ratio), pH | Conditions of synthesis | | | Ref. |
|---|---|---|---|---|---|---|
| | | | $T$ /°C | $p$ /bar | $\tau$ /h | |
| $M^IM^{III}(OH)PO_4$ | $LiMn(OD)PO_4$ | $MnPO_4 \cdot D_2O$, $LiNO_3$ (Li : Mn = 2 : 1) | 200 | 20 | 504 | 134 |
| | $KIn(OH)PO_4$ | $In_2O_3$, $K_2HPO_4$(sol.) | 900 [a] | 3000 | 12 | 127 |
| | $RbIn(OH)PO_4$ | $In_2O_3$, 2.5 M $Rb_2HPO_4$, 3 M $RbH_2PO_4$ (Rb : P = 1.5) | 550 [b] | 2200 | 8 | 117 |
| | $NH_4In(OH)PO_4$ | $In_2O_3$, $NH_4H_2PO_4$, $NH_4OH$(sol.) ($NH_4$ : In : P = 8.1 : 1 : 2.41) | 200 | 20 | 168 | 135 |
| $M^IM_2^{III}(OH)(PO_4)_2 \cdot 2\,H_2O$ | $KFe_2(OH)(PO_4)_2 \cdot 2\,H_2O$ (leucophosphite) | $FePO_4 \cdot n\,H_2O$, 2.5 M $K_3PO_4$, pH 2 | 150 | – | 336 | 122 |
| | $(NH_4)V_2(OH)(PO_4)_2 \cdot 2\,H_2O$ | $VCl_4$, $H_3PO_4$, $H_2O$, 1,3-diaminopropane (1 : 7.4 : 1004 : 8.6) | 200 | – | 87 | 128 |
| | $(NH_4)Fe_2(OH)(PO_4)_2 \cdot 2\,H_2O$ (spheniscidite) | FeO(OH), $H_3PO_4$, HF, $H_2O$, 1,3-diaminopropane (2 : 2 : 2 : 3 : 80) | 200 | – | 24 | 125 |
| | $K_{1.5}[Al_2P_2O_{8.5}(OH)_{0.5}(H_2O)] \cdot x\,H_2O$ | $Al(OH)_3$, $KH_2PO_4$ (K : Al = 3 : 2; 3 : 4; 1 : 1; 3 : 2) | 175–225 | – | – | 129 |
| | $Rb_{1.5}[Al_2P_2O_{8.5}(OH)_{0.5}(H_2O)] \cdot x\,H_2O$ | $Al(OH)_3$, $RbH_2PO_4$ (Rb : Al = 3 : 2; 3 : 1) | 225 | – | – | 129 |
| $M^IM^{III}(OH)(PO_4)_2$ | $Na_4Al(OH)(PO_4)_2$ | $Al(NO_3)_3 \cdot 9\,H_2O$, $H_3PO_3$, NaOH, 1,4-diazabicyclo[2.2.2]octane, $H_2O$, pH 10 | 200 | 20 | 96 | 132 |
| | $Na_4Ga(OH)(PO_4)_2$ | $Ga_2O_3$, $NH_4H_2PO_4$, NaOH | 400 | – | 96 | see [c] |
| | | (Na : Ga : P = 3 : 1 : 2.4), pH 12 | 160 | 18 | 96 | see [c] |
| $M_3^IM^{III}(OH)(HPO_4)(PO_4)$ | $Na_3Al(OH)(HPO_4)(PO_4)$ | $Al(OH)_3$, $Na_2HPO_4 \cdot 2\,H_2O$, $NaH_2PO_4 \cdot 2\,H_2O$ (Na : P = 1.5) | 600 [d] | – | 20 | 133 |
| | $Na_3Ga(OH)(HPO_4)(PO_4)$ | $Ga_2O_3$, $Na_2HPO_4 \cdot 2\,H_2O$, $NaH_2PO_4 \cdot 2\,H_2O$ (Na : P = 1.5) | 600 [d] | – | 20 | 133 |

[a] Slow cooling to 500 °C for 32 h; [b] slow cooling to 250 °C for 60 h; [c] unpublished data; [d] slow cooling to 500 °C for 66 h.

samples of $MIn(OH)PO_4$ (M = K, Rb) in pure form failed. These samples contained unconsumed $In_2O_3$ even when the synthesis was carried out for 2–3 weeks. Under these conditions, the sodium analogue $NaIn(OH)PO_4$ is not formed.

The hydrothermal synthesis of hydroxide phosphates of the leucophosphite group is characterised by a wide variety of the starting reagents. In a number of studies aimed at preparing porous organometallic phosphate compounds, hydroxide phosphates with composition $M^IM^{III}_2(OH)(PO_4)_2 \cdot 2H_2O$ were synthesised.[125, 128] Ammonium leucophosphite was prepared not only by the hydrothermal method with the use of aqueous solutions but also by the low-temperature synthesis from hydrogel ($T$ = 150 °C, $\tau$ = 45 h, pH of the final solution was 6.52).[124] The $M^I_{1.5}[M^{III}_2O_{0.5}(OH)_{0.5}(PO_4)_2(H_2O)] \cdot x H_2O$ compounds[129] ($M^I$ = K, Rb), which are structurally similar to compounds of the leucophosphite group, are generated from mixtures of $Al(OH)_3$ and $M^IH_2PO_4$ in the temperature range of 175–225 °C. The $NaAl(OH)PO_4$ and $(NH_4)Al_2(OH).(PO_4)_2 \cdot 2H_2O$ compounds were prepared with the use of $NaH_2PO_4$ and $(NH_4)H_2PO_4$, respectively.[130, 131] Hydroxide phosphates of this types are stable in weakly acidic and neutral media at pH 2.5–7.5.

The $M^I_4M^{III}(OH)(PO_4)_2$ compounds ($M^I$ = Na; $M^{III}$ = Al, Ga)[132] are formed as transparent elongated prismatic crystals in an alkaline medium (pH 10–12) under mild hydrothermal conditions in the presence of an excess of alkali cations (Na : Al $\geqslant$ 3). The structurally related $M^I_3M^{III}(OH)(HPO_4)(PO_4)$ compounds ($M^I$ = Na; $M^{III}$ = Al, Ga)[133] were prepared from weakly alkaline media at high temperatures (600 °C) using stepwise cooling. The $Na_3Al(OH)(HPO_4)(PO_4)$ and $Na_3Ga(OH)(HPO_4)(PO_4)$ compounds crystallise as colourless prisms and thin platelet-like crystals, respectively.

## 2. Structures and properties

There is an obvious structural analogy between all hydroxide phosphates, except for compounds belonging to the $M^IM^{III}(OH)PO_4$ group. The crystal chemistry of the latter compounds radically changes depending on the nature of the $M^I$ and $M^{III}$ cations.

Recent studies dealing with the determination of the crystal structures of complex hydroxide phosphates were aimed primarily at refining the assignment of a particular compound to the structural type (with a typical alternation of the cations and anions) and revealing the crystal-chemical features of the structures of the compounds synthesised.

Minerals with composition $M^IM^{III}(OH)PO_4$, where $M^I$ = Li, Na and $M^{III}$ = Al, Fe, are isomorphous. These compounds are characterised by high mobility of alkali atoms in the channels of the structures. The structural feature of this group of complex phosphates is the presence of chains built from the vertex-sharing $FeO_6$ or $AlO_6$ octahedra linked by OH groups (Table 14). Mixed frameworks containing such chains are also typical of kizerite ($MgSO_4 \cdot 2H_2O$), titanite ($CaTiOSiO_4$) and isostructural minerals (space group $C2/c$).[81]

In a manganese analogue of tavorite, *viz*., $LiMn(OH)PO_4$,[134] strong distortion of the $MnO_4(OH)_2$ octahedra gives rise to a substantial ferromagnetic component although this compound belongs to antiferromagnetics. The elongated Mn–O bonds (O are the oxygen atoms of the $PO_4$ groups) make the main contribution to the direction of the vector of the magnetic moment. As a result, the vectors of the magnetic moments of the $MnO_4(OH)_2$ octahedra belonging to the same chain are parallel, co-directed and virtually perpendicular to the M–OH–M bond. This direction of the vectors of the magnetic moments is responsible for the ferromagnetic properties of the $LiMn(OH)PO_4$ compound.[134]

On going from iron- and manganese-containing compounds [$r_{VI}(Fe^{3+})$ = 0.645 Å, $r_{VI}(Mn^{3+})$ = 0.65 Å] to indium compounds [$r_{VI}(In^{3+})$ = 0.79 Å], the structural type changes attended with an increase in the symmetry from triclinic to orthorhombic and tetragonal (see Table 14). An increase in the ionic radius of alkali metal on going from potassium to rubidium also leads to an increase in the symmetry from orthorhombic to tetragonal. Complex indium hydroxide phosphates containing different monovalent cations have compositions in which the ratio $M^I : M^{III} : PO_4^{3-}$ = 1 : 1 : 1 is retained. The structure of orthorhombic indium hydroxide phosphate $KIn(OH)PO_4$ is based on helical chains of the $InO_4(OH)_2$ octahedra sharing *cis* vertices.[127] These chains are extended along the $c$ axis (Fig. 24 *a*). The polyhedra about the potassium cations ($KO_7$) can be described as distorted trigonal antiprisms. In the structures of $NH_4In$ and RbIn hydroxide phosphates, the presence of screw axes $4_3$ leads to an ordered arrangement of the polyhedra in helical chains so that the channels of virtually square cross-section are formed along the [001] direction (Fig. 24 *b*). The $NH_4^+$ and $Rb^+$ ions are surrounded by nine oxygen atoms each.

In the structures of the $M^IIn(OH)PO_4$ compounds ($M^I$ = Rb and $NH_4$), the indium octahedra are almost non-distorted. Thus, the difference in the In–O bond lengths is 0.003 Å and 0.059 Å in $(NH_4)In(OH)PO_4$ (see Ref. 135) and $RbIn(OH)PO_4$ (see Ref. 117), respectively. The crystallographically independent indium atoms alternate along the helical chains and are linked to each other through the bridging oxygen atoms of the hydroxy groups, which are not involved in hydrogen bonding with the nearest environment. The presence of independent OH groups in the structures was confirmed by IR spectroscopy ($\nu \approx 3520$ cm$^{-1}$). Each $PO_4$ tetrahedron shares two vertices with the $InO_6$ octahedra belonging to the same chain and shares two other vertices with the octahedra from the adjacent chain. The chains are linked through the tetrahedra to form a framework whose large cavities are occupied by single-charged cations. The framework of the $KIn(OH)PO_4$ compound is similar to that of $\gamma$-$NaTiOPO_4$.[136] The difference is observed in the positions of the alkali cations located in the tunnels of these structures.

The fact that indium and scandium have similar ionic radii [$r_{VI}(Sc^{3+})$ = 0.745 Å] as well as the fact that $KIn(OH)PO_4$ and $RbIn(OH)PO_4$ belong to different structural types indicate that related hydroxide phosphate $KSc(OH)PO_4$ may occur. Apparently, the sodium-containing analogue with composition $NaIn(OH)PO_4$ that is structurally similar to $KIn(OH)PO_4$ does not occur. In this case, the steric factor is of considerable importance because the difference in the sizes of the potassium and sodium cations is much larger than that in the sizes of the potassium and rubidium cations.

**Table 14**. Crystallographic characteristics of the $M^IM^{III}(OH)PO_4$ compounds.

| Compound (mineral name) | Crystal system | Space group | $Z$ | Unit cell parameters | | | | Ref. |
|---|---|---|---|---|---|---|---|---|
| | | | | $a$ /Å | $b$ /Å | $c$ /Å | α, β, γ /deg | |
| $LiAl(OH)PO_4$ (montebrasite) | triclinic | $C\bar{1}$ | 4 | 6.713 | 7.708 | 7.019 | 91.31, 117.93, 91.77 | 81 |
| $LiFe(OH)PO_4$ (tavorite) | " | $P\bar{1}$ | 2 | 5.340 | 7.283 | 5.110 | 109.29, 97.86, 106.32 | 120 |
| $LiMn(OD)_{0.442}(OH)_{0.558}PO_4$ | " | $C\bar{1}$ | 4 | 6.719 | 8.187 | 7.123 | 89.5, 117.7, 86.4 | 134 |
| $KIn(OH)PO_4$ | orthorhombic | $P2_12_12_1$ | 8 | 9.277 | 9.339 | 11.245 | – | 127 |
| $RbIn(OH)PO_4$ | tetragonal | $P4_32_12$ | 8 | 9.400 | – | 11.179 | – | 117 |
| $(NH_4)In(OH)PO_4$ | " | $P4_32_12$ | 8 | 9.423 | – | 11.177 | – | 135 |

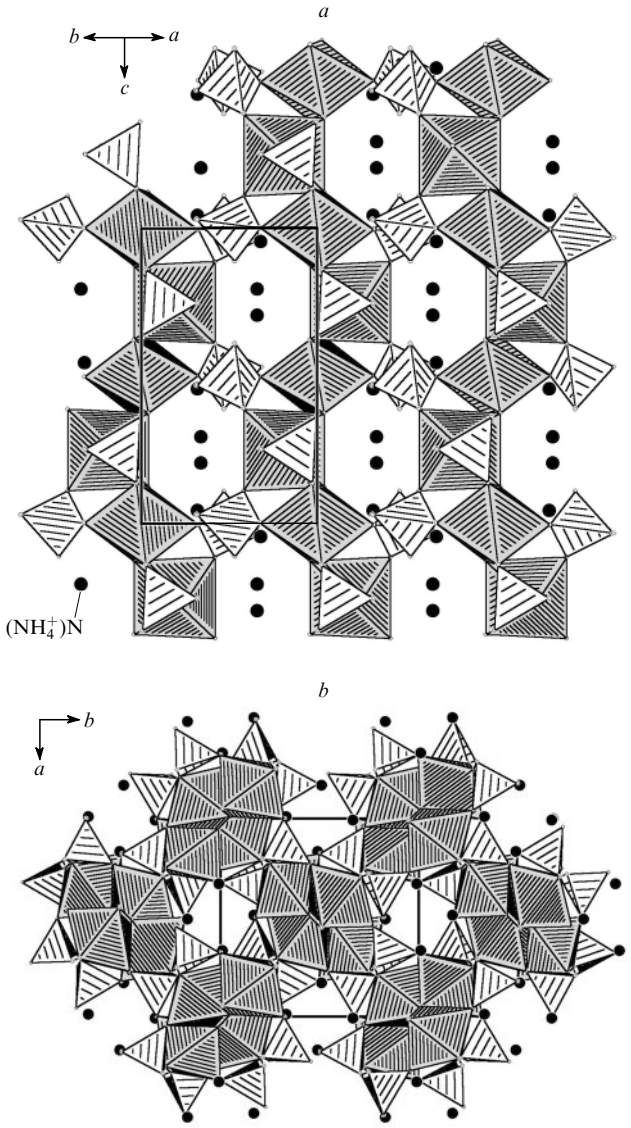



**Figure 24.** Chains of the $(OH)_2$ octahedra in the structure of $(NH_4)In(OH)PO_4$ along the [110] direction (*a*) and the structure of $(NH_4)In(OH)PO_4$ projected onto the *ab* plane (*b*).

Hence, analysis of the structural types in the morphotropic series $M^IM^{III}(OH)PO_4$ demonstrates that the structures of these compounds are characterised by the presence of chains or ribbons, which are built from octahedra of the trivalent cations linked to each other through the OH vertices.

Taking into account the structural and compositional similarity, the $M^IIn(OH)PO_4$ compounds ($M^I$ = K, Rb and $NH_4$) can be compared with phases related to $KTiOPO_4$. It is known that the $TiO_6$ octahedra in the structure of $KTiOPO_4$ are substantially distorted with alternation of short and long bonds along the $-O-Ti(1)-O-Ti(2)-O-$ chain. The differences between the long and short Ti(1)–O and Ti(2)–O bonds are 0.275 and 0.363 Å, respectively.[116] These differences in the bond lengths are of importance in determining the nonlinear optical properties of the KTP-type $A^IB^{IV}OX^VO_4$ compounds. However, weak distortion of the $M^{III}O_6$ and $M^{III}O_xF_y$ octahedra in the structures of complex indium phosphates, such as $M^IIn(OH)PO_4$ ($M^I$ = K, Rb, $NH_4$), $KInFPO_4$ and $M^IInF_{1-\delta}(OH)_\delta PO_4$ ($M^I$ = K, Rb, $NH_4$), and in the structures of $M^IM^{III}F_{1-\delta}(OH)_\delta PO_4$ ($M^I$ = K, $NH_4$; $M^{III}$ = Ga, Fe) is responsible for the fact that these compounds do not exhibit nonlinear optical properties.

Two minerals, *viz*., wardite $NaAl_3(OH)_4(PO_4)_2\cdot 2H_2O$ [137] and cyrilovite $NaFe_3(OH)_4(PO_4)_2\cdot 2H_2O$,[126] belong to hydroxide phosphates with composition $M^IM^{III}_3(OH)_4(PO_4)_2\cdot 2H_2O$. These compounds crystallise in the tetragonal system (space group $P4_12_12$, $Z = 4$). The unit cell parameters of wardite ($a = 7.030$, $c = 19.040$ Å) are close to those of cyrilovite ($a = 7.313$, $c = 19.315$ Å). The structures of these minerals are composed of the layers located perpendicular to the [001] direction. The layers consist of infinite chains of the alternating *cis*-linked $M(1)O_6$ and $M(2)O_6$ octahedra extended along the *a* and *b* axes (Fig. 25). In the $M(1)O_6$ octahedron, the $M^{3+}$ cation is surrounded by three oxygen atoms of the $PO_4$ tetrahedra, two oxygen atoms of the OH groups and the oxygen atom of the water molecule. In the $M(2)O_6$ octahedron, the $M^{3+}$ cation is surrounded by two oxygen atoms of the $PO_4$ groups and four oxygen atoms of the OH group. The $M(1)O_6$ octahedron is linked to two nearest $M(2)O_6$ octahedra through bridging hydroxy groups. The $M(2)O_6$ octahedron, in turn, is linked to four nearest strongly distorted $M(1)O_6$ octahedra through four hydroxy bridges. The cavities in the layers are occupied by sodium ions (coordination number is 8). The $PO_4$ tetrahedra share three vertices with three octahedra in the layer and one vertex with an octahedron from the adjacent layer, three vertices being involved in the $M(1)O_6$ octahedron and one vertex being involved in the $M(2)O_6$ octahedron.

In the mixed framework of the octahedra and tetrahedra, two types of channels are extended along the [100] and [010] directions. These channels are occupied by zeolite-type water molecules. The presence of water of crystallisation and bridging OH group in the structures was confirmed by IR spectroscopy. Analysis of the interatomic distances in the $M^{III}O_6$ polyhedra in the $NaM^{III}_3(OH)_4(PO_4)_2\cdot nH_2O$ compounds and the radii of the $M^{III}$ cations demonstrated that the octahedral positions can be occupied not only by the Al and Fe cations but also by the gallium and vanadium cations with no changes in the crystal structure. The occurrence of potassium analogues is highly improbable because of the small sizes of the cavities in the layers.

Minerals of the leucophosphite of the general formula $M^IM^{III}_2(OH)(PO_4)_2\cdot 2H_2O$ ($M^I$ = K, $NH_4$; $M^{III}$ = Al, Fe) form a continuous series of low-temperature solid solutions. Three minerals of this series are known, *viz*., leucophosphite $KFe_2(OH)(PO_4)_2\cdot 2H_2O$, tinsleyite $KAl_2(OH)(PO_4)_2\cdot 2H_2O$ and spheniscidite $(NH_4,K)(Al,Fe)_2(OH)(PO_4)_2\cdot 2H_2O$. Besides, the related synthetic KAl, $NH_4Al$, $NH_4Ga$ and $NH_4V$ analogues [138–141] belong to this group (Table 15).

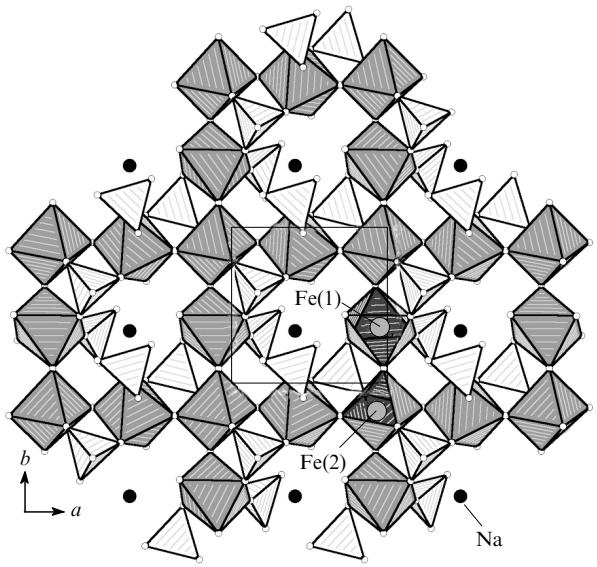



**Figure 25.** Structure of $NaFe_3(OH)_4(PO_4)_2\cdot 2H_2O$ projected onto the *ab* plane.

**Table 15**. Crystallographic characteristics of minerals of the leucophosphite group of the general formula $M^{I}M^{III}_{2}(OH)(PO_4)_2 \cdot 2H_2O$ and the $M^{I}_{4}M^{III}(OH)(PO_4)_2$ and $M^{I}_{3}M^{III}(OH)(HPO_4)(PO_4)$ compounds.

| Compound (mineral) | Crystal system | Space group | $Z$ | Unit cell parameters | | | | Ref. |
|---|---|---|---|---|---|---|---|---|
| | | | | $a$ /Å | $b$ /Å | $c$ /Å | $\beta$ /deg | |
| $KAl_2(OH)(PO_4)_2 \cdot 2H_2O$ | orthorhombic | $P2_12_12_1$ | 4 | 9.205 | 9.707 | 9.828 | – | 138 |
| $KAl_2(OH)(PO_4)_2 \cdot 2H_2O$ (tinsleyite) | monoclinic | $P2_1/n$ | 4 | 9.602 | 9.532 | 9.543 | 103.16 | 123 |
| $K_{1.5}\{Al_2O_{0.5}(OH)_{0.5}(PO_4)_2(H_2O)\} \cdot xH_2O$ | " | $P2_1/n$ | 4 | 9.495 | 9.5589 | 9.4384 | 101.74 | 129 |
| $(NH_4)Al_2(OH)(PO_4)_2 \cdot 2H_2O$ | " | $P2_1/n$ | 4 | 9.553 | 9.577 | 9.614 | 103.6 | 130 |
| | " | $P2_1/n$ | 4 | 9.617 | 9.572 | 9.556 | 103.6 | 131 |
| $KFe_2(OH)(PO_4)_2 \cdot 2H_2O$ (leucophosphite) | " | $P2_1/n$ | 4 | 9.782 | 9.658 | 9.751 | 102.2 | 121 |
| | " | $P2_1/n$ | 4 | 9.756 | 9.664 | 9.769 | 102.4 | 122 |
| $(NH_4)Fe_2(OH)(PO_4)_2 \cdot 2H_2O$ (spheniscidite) | " | $P2_1/n$ | 4 | 9.819 | 9.737 | 9.874 | 102.8 | 124 |
| | " | $P2_1/n$ | 4 | 9.823 | 9.738 | 9.872 | 102.8 | 125 |
| $(NH_4)V_2(OH)(PO_4)_2 \cdot 2H_2O$ | " | $P2_1/n$ | 4 | 9.803 | 9.688 | 9.858 | 102.91 | 128 |
| $(H_3O)Ga_2(OH)(PO_4)_2 \cdot 2H_2O$ | " | $P2_1/n$ | 4 | 9.68 | 9.64 | 9.77 | 102.7 | 139 |
| $(NH_4)Ga_2(OH)(PO_4)_2 \cdot 2H_2O$ | " | $P2_1/n$ | 4 | 9.689 | 9.703 | 9.788 | 102.80 | 140 |
| $LiNa_2HAl(OH)(PO_4)_2$ | orthorhombic | $Pbcb$ | 4 | 6.948 | 14.089 | 14.065 | – | 141 |
| $Na_4Al(OH)(PO_4)_2$ | " | $Pbcm$ | 8 | 15.279 | 14.660 | 6.947 | – | 132 |
| $Na_4Ga(OH)(PO_4)_2$ | " | $Pbcm$ | 8 | 15.407 | 14.661 | 7.049 | – | see [a] |
| $Na_3Al(OH)(HPO_4)(PO_4)$ | monoclinic | $C2/m$ | 4 | 15.277 | 7.054 | 7.041 | 96.73 | 133 |
| $Na_3Ga(OH)(HPO_4)(PO_4)$ | " | $C2/m$ | 4 | 15.432 | 7.164 | 7.057 | 96.64 | 133 |

[a] Our unpublished data.

The compounds of this groups are characterised by the presence of the $M^{III}_{4}(OH)_2(H_2O)_2(PO_4)_4$ island fragment formed from four octahedra of two types, *viz*., $M(1)O_4(OH)_2$ and $M(2)O_4(OH)(H_2O)$. The central core of this fragment consists of two edge-sharing $M(1)O_6$ octahedra¶ with two anchored hydroxo groups. The $M(1)O_6$ octahedra share edges containing two OH vertices with two $M(2)O_6$ octahedra (Fig. 26 *a*,*b*). The fragments consisting of four $M^{III}O_6$ octahedra are linked in a framework through the isolated $PO_4$ tetrahedra. The channels of the structure are occupied by monovalent cations and water molecules.

In each independent $M^{III}O_6$ octahedron, four oxygen atoms are at short distances from the $M^{3+}$ ion (these distances differ by only 0.03 – 0.04 Å), whereas two oxygen atoms are far remote from $M^{III}$. This distortion of the octahedra results from the fact that the oxygen atoms of the OH groups and water molecules must satisfy the valence balance rule. The octahedral coordination of the $M^{III}$ cations is retained but the $M^{III}-O$ distances change as the ionic radius increases in the series Al – Ga – V – Fe. Analysis of the interatomic $M^{III}-O$ distances in the $M^{III}O_6$ octahedra and the $M^{I}:M^{III}$ ratio showed that the compounds of all the above-mentioned trivalent cations ($M^{III}$ = Al, Fe, V, Ga) in combination with rubidium can also crystallise in the structural type $M^{I}M^{III}_{2}(OH)(PO_4)_2 \cdot 2H_2O$. It is quite possible that In-containing analogues can also crystallise in this structural type. In all compounds with $M^{I} = NH_4$, the $NH_4^+$ cations are surrounded by four oxygen atoms giving rise to a tetrahedron within which two $N-H\cdots O$ hydrogen bonds occur (Fig. 26 *b*).

The water molecules in the structure of $M^{I}M^{III}_{2}(OH)(PO_4)_2 \cdot 2H_2O$ fulfil different functions. One $H_2O$ molecule is involved in the first coordination sphere of the $M^{III}(2)O_6$ octahedron, whereas another water molecule is of a zeolite type and is not coordinated to any cation. As a result, the structural formula of these hydroxide phosphates can be written as follows $M^{I}\{M^{III}_{2}(OH)(PO_4)_2(H_2O)\} \cdot H_2O$.

It should be noted that the structures of all the above-considered minerals and their synthetic analogues are derived from the structure of $GaPO_4 \cdot 2H_2O$.[139] In this structure, the positions of the hydroxonium ions correspond to the positions of the monovalent $K^+$ and $NH_4^+$ cations according to the structural formula $H_3O\{Ga_2(OH)[PO_4]_2(H_2O)\} \cdot H_2O$. The replacement of

¶ The presence of the edge-sharing $M^{III}O_6$ octahedra in these structures is responsible for the magnetic properties of iron-containing representatives of this group.

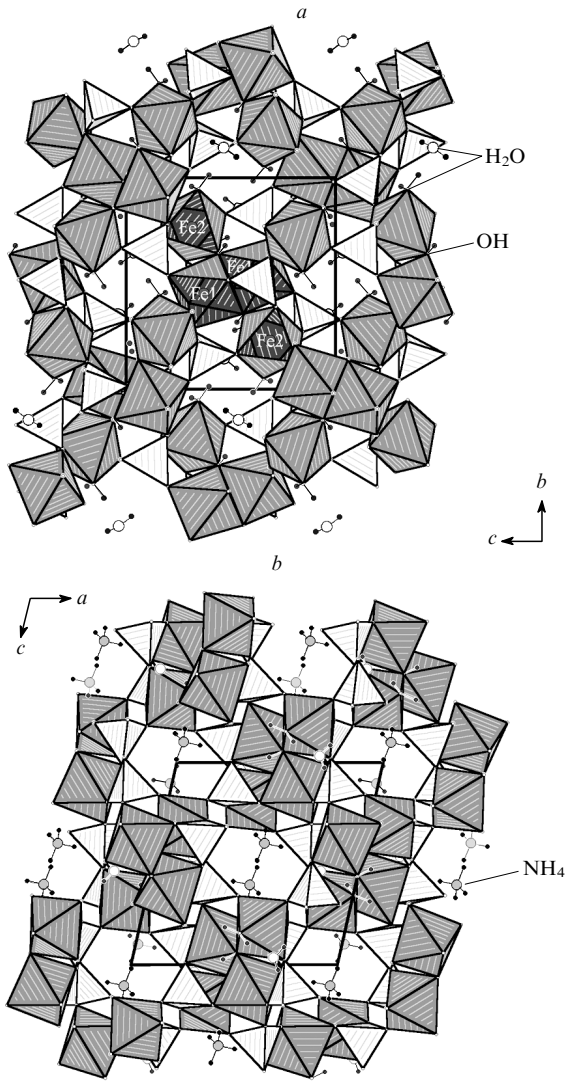



**Figure 26.** Structure of $(NH_4)Fe_2(OH)(PO_4)_2 \cdot 2H_2O$ projected onto the *bc* (*a*) and *ac* planes (*b*). The centrosymmetrical island fragments of the Fe octahedra are displayed (*a*); the positions of the $NH_4^+$ cations in the channels of the structure are shown (*b*).

one-half of the hydroxide ions in the $M^{I}\{M^{III}_{2}(OH)(PO_4)_2(H_2O)\}\cdot H_2O$ compounds by the oxide ions gives rise to compounds with compositions $M^{I}_{1.5}\{M^{III}_{2}O_{0.5}(OH)_{0.5}(PO_4)_2(H_2O)\}\cdot x\,H_2O$ ($M^{I}$ = K, Rb; $M^{III}$ = Al).[129]

The presence of the $M^{III}_{2}O_4$ groups is common to hydroxide phosphates $M^{I}M^{III}_{2}(OH)(PO_4)_2\cdot 2\,H_2O$ and their topological analogues deprived of OH groups, such as $(NH_4)Mo_2.P_2O_{10}\cdot H_2O$[142] and $RbMo_2P_2O_{10}\cdot(1-x)\,H_2O$.[143] In the $Al_3(PO_4)_3\cdot H_2O\cdot en$ and $Ga_3(PO_4)_3\cdot H_2O\cdot en$ compounds (en is ethylenediamine), the $M^{III}_{2}O_4$ groups are involved in trigonal bipyramids and the organic cations (protonated ethylenediamine molecules) occupy the channels.[144] Due to the specific ion-conducting properties, these compounds can be used as molecular sieves.[145]

Hydroxide phosphates with composition $Na_4M^{III}(OH)(PO_4)_2$ ($M^{III}$ = Al, Ga) and the ratio $M^{I}:M^{III}=4:1$ are also known (see Table 15). Let us consider the structures of these compounds using an aluminium compound as an example. The main structural elements of the $Na_4Al(OH)(PO_4)_2$ compound are the infinite $[Al(OH)(PO_4)_2]_\infty$ chains extended along the [001] direction (Fig. 27 *a*). In these chains, the $AlO_4(OH)_2$ octahedra are *trans*-linked to each other through the bridging oxygen atoms of the hydroxy groups (Fig. 27 *b*). The adjacent octahedra in the chains are linked by two $PO_4$ groups. Each $PO_4$ group shares two vertices with the adjacent octahedra in the chain. The $[Al(OH)(PO_4)^{4-}_{2}]_\infty$ chains are held together primarily through interactions between two non-shared vertices of the phosphate groups and the sodium atoms located in the channels between the $[Al(OH)(PO_4)^{4-}_{2})]_\infty$ chains. The sodium atoms located between the $PO_4$ tetrahedra in *cis* positions with respect to the hydroxyl hydrogen atoms have a lesser effect on binding of the chains. The $PO_4$ tetrahedra and $AlO_6$ octahedra are only slightly distorted.

In the structure of $Na_4Al(OH)(PO_4)_2$, the sodium atoms have different coordination numbers depending on their positions with respect to the $[Al(OH)(PO_4)^{4-}_{2}]_\infty$ chains. Four of seven independent sodium atoms are involved in the $NaO_6$ octahedra. One $NaO_{4+2}$ polyhedron is formed by four oxygen atoms located in the first coordination sphere (the Na–O distances are ~ 2.495 Å) and two oxygen atoms at distances of 2.72–2.99 Å. Finally, the coordination environment about two sodium atoms are five-vertex polyhedra with four short Na–O bonds (~ 2.3 Å) and one abnormally large distance (~ 2.88 Å).

In the mineral tancoite $LiNa_2HAl(OH)(PO_4)_2$,[141] the arrangement of the chains is analogous to that observed in the structure of $Na_4Al(OH)(PO_4)_2$. The slight differences in the positions of the Li and H atoms in the structure of tancoite as compared to the positions of the sodium atoms replacing these atoms in the structure of $Na_4Al(OH)(PO_4)_2$ cause changes in the symmetry of the structure, *viz*., the parameter *a* is decreased, whereas the parameter *c* is doubled.

Taking into account the similarity of the ionic radii of aluminium, gallium and iron, gallium- and iron-containing analogues of $Na_4Al(OH)(PO_4)_2$ with the same structure would be expected to occur. Actually, we have recently prepared isostructural hydroxide phosphate $Na_4Ga(OH)(PO_4)_2$.

The structures of the $Na_3M^{III}(OH)(HPO_4)(PO_4)$ compounds ($M^{III}$ = Al, Ga) are similar to that of $Na_4Al(OH)(PO_4)_2$ with the only difference that the sodium atoms are partially replaced by the hydrogen atoms of the $HPO_4$ groups (Fig. 28 *a*).[133] The adjacent octahedra in the $[Al(OH)(HPO_4)(PO_4)^{3-}]_\infty$ chains are linked through the bridging HO groups and by the $HPO_4$ and $PO_4$ groups (Fig. 28 *b*). The structure is additionally stabilised by hydrogen bonds involving the $HPO_4$ groups from the adjacent chains. The sodium atoms in the structure have different coordination environments, *viz*., $NaO_5$, $NaO_6$ and $NaO_8$. The coordination polyhedron about the sodium atom with the coordination number of 8 is a distorted cube with four short, two medium and two long Na–O distances. The average $M^{III}$–O and P–O bond lengths are comparable with the analogous distances in $Na_4Al(OH)(PO_4)_2$. For $Na_3Al(OH)(HPO_4)(PO_4)$, these bond lengths are 1.911 and 1.536 Å, respectively.

The chains consisting of the $[M(EO_4)_2X]$ groups (X is a non-specific ligand), which were found in the structures of $M^{I}_{4}M^{III}(OH)(PO_4)_2$ and $M^{I}_{3}M^{III}(OH)(HPO_4)(PO_4)$, are typical of a large group of phosphate, sulfate and silicate minerals.[132] For example, in the structures of the minerals jahnsite $CaMnMg_2.[Fe(OH)(PO_4)_2]_2\cdot 8\,H_2O$,[146] segelerite $CaMg[Fe(OH)(PO_4)_2]\cdot 4\,H_2O$ and overite $CaMg[Al(OH)(PO_4)_2]\cdot 4\,H_2O$ (see Ref. 147), the $[M(EO_4)_2X]$ chains are linked in layers through the $M^{II}O_2(H_2O)_4$ octahedra.

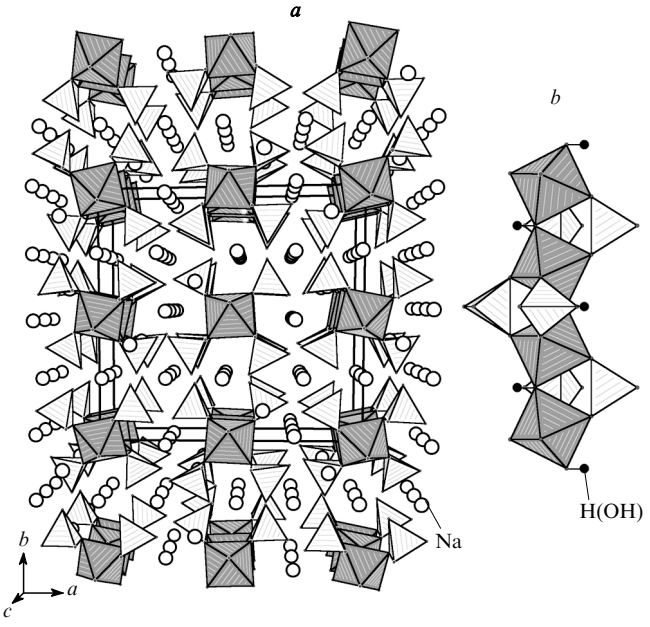



**Figure 27.** Structure of $Na_4Al(OH)(PO_4)_2$ projected along the [001] direction (*a*) and the $[Al(OH)(PO_4)^{4-}_{2}]_\infty$ chain (*b*).

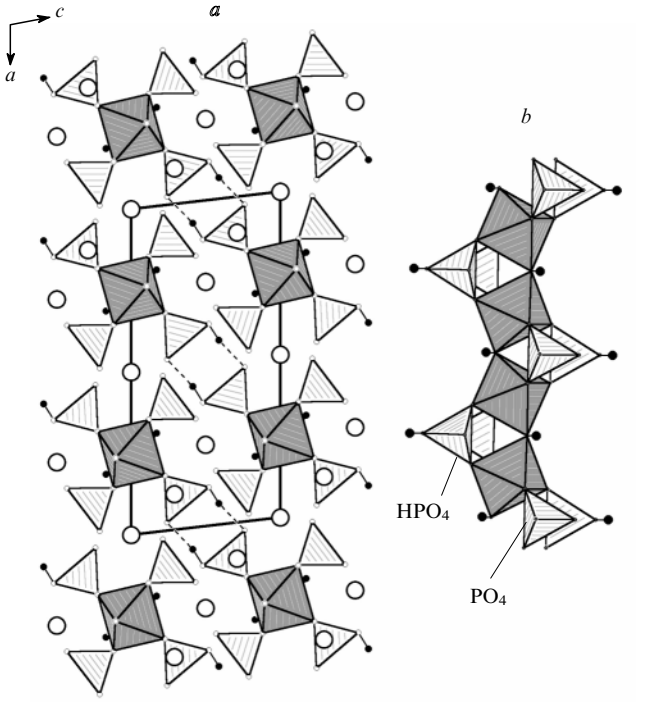



**Figure 28.** Structure of $Na_3Al(OH)(HPO_4)(PO_4)$ projected onto the *ac* plane (*a*) and the $[Al(OH)(HPO_4)(PO_4)^{3-}]_\infty$ chain (*b*).

Thermal stability of hydroxide phosphates containing mono- and trivalent cations depends on the mode of binding of water molecules in these structures. Thus, hydroxide phosphates $M^{I}In(OH)PO_4$ ($M^{I}$ = K, Rb) lose water of crystallisation in the temperature range of 500–700 °C. Decomposition of hydroxide phosphate $KIn(OH)PO_4$ affords $K_3In(PO_4)_2$, $InPO_4$ and $In_2O_3$. Hydroxide phosphate $(NH_4)In(OH)PO_4$ decomposes in two steps at 180–490 °C and 535–690 °C. Crystallisation of $InPO_4$ starts at 620 °C. Dehydration of leucophosphite $KFe_2(OH).(PO_4)_2 \cdot 2H_2O$ occurs in two steps at 300–575 °C. First, the zeolite-type water is removed and then the $H_2O$ molecules located in the first coordination sphere about the iron atoms are eliminated. Dehydration of $NaFe_3(OH)_4(PO_4)_2 \cdot n H_2O$ proceeds in one step. The temperature ranges of the removal of the zeolite-type water and water of crystallisation overlap (the maximum temperatures corresponding to the removal of these water molecules are 428 and 447 °C, respectively) and complete dehydration is achieved at 600 °C. In the case of the $NH_4V$ analogue of leucophosphite, water of crystallisation is eliminated at a substantially lower temperature (in the range of 45–110 °C) and decomposition of the compound is completed at 320 °C. Dehydration of $Na_3Al(OH)(HPO_4)(PO_4)$ proceeds in one step with a maximum at ~438 °C and ends in the formation of double aluminium phosphate $Na_3Al(PO_4)_2$.

A comparison of the data on the structures of complex hydroxide phosphates containing mono- and trivalent cations revealed the main structural features of these compounds. The coordination polyhedra about the $M^{III}$ cations are without exception octahedra. The $M^{III}O_6$ octahedra are linked in infinite chains through the bridging hydroxy groups. Depending on the ratio between the $M^{I}$ and $M^{III}$ cations, the chains are either linked to each other through the phosphate tetrahedra or are held together by hydrogen bonds and $M^{I}\cdots O$ interactions† to form framework, layered or chain structures (Table 16).

For the above-considered compounds, two compositions with the ratios $M^{I}:M^{III} = 1:2$ or 1 : 1 (in the case of the medium and large monovalent $K^+$, $Rb^+$, $NH_4^+$ cations) are preferential. The compositions with 1 : 3 or 3 : 1 (4 : 1), where $M^{III}$ cations are either excessive or deficient with respect to $M^{I}$ cations, are typical only of sodium-containing aluminium and gallium hydroxide phosphates, both the OH and $HPO_4$ groups being involved in compounds with the ratio $M^{I}:M^{III} = 3:1$. It should be noted that water molecules play an important role in the formation of structures containing an excess of $M^{III}$ cations with respect to $M^{I}$. The $H_2O$ molecules are involved in the formation of the first coordination sphere about the $M^{III}$ cations and occupy the channels and cavities in the structures as 'guests', which are not bound to any cations.

† Considering the size factor, only sodium can serve as such monovalent cation.

## VI. Other complex phosphates containing mono- and trivalent cations

In addition to fluoride phosphates and hydroxide phosphates containing mono- and trivalent cations, other complex mixed-anion compounds are known. In such compounds, the $PO_4^{3-}$ anion is combined with $VO_4^{3-}$, $MoO_4^{2-}$, $SO_4^{2-}$ or $S_2O_3^{2-}$. It is expected that mixed-anion phosphates will exhibit improved properties (such as sorption ability, luminescence, *etc.*) as compared to monoanion phases. The replacement of the tetrahedral $PO_4$ group in the anion sublattices of complex phosphates by other groups enables one to vary not only the total negative charge of the compound, which makes it possible to change the number of cations, but also the size characteristics of the cavities in framework structures and of interlayer spaces in layered phases. Such structural changes may allow one to influence the catalytic properties and ionic mobility of compounds as well as ion exchange processes involving these compounds.[148–152]

The partial replacement of the $PO_4^{3-}$ anions in compounds with composition $K_3M^{III}(PO_4)_2$ ($M^{III}$ = Y, La, Eu, Gd, Yb) by $VO_4^{3-}$ gives rise to continuous or limited solid solutions based on one of the structural types (arcanite or glaserite) typical of non-substituted double phosphates $K_3M^{III}(PO_4)_2$ or vanadates $K_3M^{III}(VO_4)_2$. The lack of new compounds is associated with a small difference in the sizes of the $PO_4^{3-}$ and $VO_4^{3-}$ anions. The formation of limited or continuous solid solutions is determined by the dissimilarity or similarity of the structural types of the starting double phosphates and vanadates.[28]

Phosphate vanadates $K_3M^{III}(PO_4)_x(VO_4)_{2-x}$ ($M^{III}$ = Sc, Y, La–Lu; $x = 0-2$) exhibit sorption properties with respect to $H_2O$, $CO_2$ and organic compounds. The degree of sorption of $H_2O$ and $CO_2$ from the gas phase depends on the $PO_4^{3-}:VO_4^{3-}$ ratio whose increase leads to preferential sorption of water molecules from a mixture of $H_2O$ and $CO_2$.[153] The degree of sorption correlates linearly with the conductivity and dielectric characteristics of the water-containing $K_3M^{III}(PO_4)_x(VO_4)_{2-x}$ phases.

Complex phosphate vanadates $K_3M^{III}_{1-y}Eu_y(PO_4)_x(VO_4)_{2-x}$ ($M^{III}$ = Sc, Y, La, Gd; $x = 0-2$; $y = 0-1$) possess luminescent properties, which depend both on the concentration of the activator $Eu^{3+}$ ions and the $PO_4^{3-}:VO_4^{3-}$ ratio. The formation of solid solutions, which crystallise in the same structural type, is evidenced by the similarity of their luminescence spectra. These spectra are characterised by the absence of complete concentration quenching of luminescence as the concentration of activator ions is increased. The maximum intensity of luminescence was observed at the $Eu^{3+}$ concentration corresponding to $y = 0.3$.

**Table 16**. Characterisations of the structures of different types of complex hydroxide phosphates with $M^{I}$ and $M^{III}$ cations.

| Type of compound | Ratio $M^{I}:M^{III}$ | Crystal system | Space group | Building blocks | Structural type |
|---|---|---|---|---|---|
| $M^{I}M^{III}_3(OH)_4(PO_4)_2 \cdot 2H_2O$ ($M^{I}$ = Na, $M^{III}$ = Al, Fe) | 1 : 3 | tetragonal | $P4_12_12$ | $[M^{III}O_2(OH)_4]$ ù $[M^{III}O_3(OH)_2O_w]$ (chains) + $[PO_4]$ | framework |
| $M^{I}M^{III}_2(OH)(PO_4)_2 \cdot 2H_2O$ ($M^{I}$ = K, $NH_4$, $M^{III}$ = Al, Fe, Ga, V) | 1 : 2 | monoclinic | $P2_1/n$ | $[M^{III}_4(OH)_2(H_2O)_2(PO_4)_4]_{3\infty}$ (island fragments) | " |
| $M^{I}M^{III}(OH)PO_4$ ($M^{I}$ = Li, Na, K, $NH_4$, Rb; $M^{III}$ = Al, Fe, Mn, In) | 1 : 1 | triclinic<br>orthorhombic<br>tetragonal | $P\bar{1}$, $C\bar{1}$<br>$P2_12_12_1$<br>$P4_32_12$ | $[M^{III}O_4(OH)_2]_\infty$ (chains) + $[PO_4]$ | " |
| $M^{I}_3M^{III}(OH)(HPO_4)(PO_4)$ ($M^{I}$ = Na, (Li, Na), $M^{III}$ = Al, Ga) | 3 : 1 | monoclinic | $C2/m$ | $[M^{III}O_4(OH)_2]_\infty$ (chains) + + $[PO_4]$ and $[HPO_4]$ | chain |
| $M^{I}_4M^{III}(OH)(PO_4)_2$ ($M^{I}$ = Na, $M^{III}$ = Al, Ga) | 4 : 1 | orthorhombic | $Pbcm$ | $[M^{III}O_4(OH)_2]_\infty$ (chains) + $[PO_4]$ | " |

Phosphate vanadates $K_3M^{III}_{1-y}Eu_y(PO_4)_x(VO_4)_{2-x}$ ($M^{III}$ = Sc, Y, Gd) possessing bright red luminescence are promising photoluminescent and cathode-luminescent materials.[154–156]

Complex molybdate phosphate $Na_2Y(PO_4)(MoO_4)$ [157] was prepared by crystallisation from flux in the study of the $Y_2O_3-(NH_4)_2HPO_4-Na_2MoO_4$ system. This compound crystallises in the monoclinic system (space group $C2/c$, $Z = 8$, unit cell parameters $a = 13.928$, $b = 18.016$, $c = 6.847$ Å, $\beta = 119.62$ °). The structure of $Na_2Y(PO_4)(MoO_4)$ contains chains (along the $c$ axis) of the edge-sharing $YO_8$ dodecahedra. The chains are linked in corrugated layers parallel to the $ac$ plane through the $PO_4$ (shared edges) and $MoO_4$ (shared vertices) tetrahedra (Fig. 29 *a*). The sodium atoms are located in the interlayer space (Fig. 29 *b*). Molybdate phosphates of this type are unknown for REE.

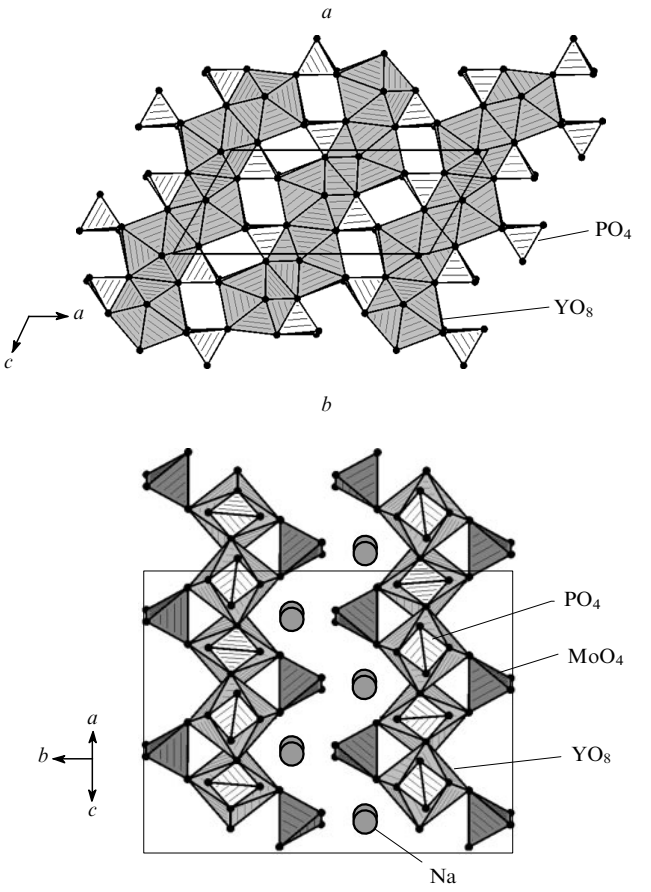



**Figure 29.** Structure of $Na_2Y(PO_4)(MoO_4)$ projected onto the $ac$ plane (*a*) ($MoO_4$ tetrahedra are omitted) and the arrangement of the Na atoms in the structure (*b*).

Quite recently, sodium lanthanum phosphate thiosulfate with composition $Na_2La(PO_4)(S_2O_3)$ was prepared by the reaction of $La_2O_3$ with $Na_3PO_3S$ in an excess of $Na_2S_4$.[158] This compound crystallises in the monoclinic system (space group $P2_1/c$, $Z = 4$, unit cell parameters $a = 13.779$, $b = 5.336$, $c = 9.356$ Å, $\beta = 89.97$ °). In the crystal structure of $Na_2La(PO_4)(S_2O_3)$, the $LaO_7S_2$ polyhedra are linked in chains through the apical sulfur atoms of the thiosulfate groups. The chains are linked in layers by the $PO_4$ and $S_2O_3$ tetrahedra (Fig. 30 *a*, *b*). The negatively charged $[La(PO_4)(S_2O_3)]^{2-}$ fragment is the major building block of each layer. The $[La(PO_4)(S_2O_3)]_n$ layers are parallel to the $bc$ plane. The terminal sulfur atoms of the thiosulfate ions are located within these layers. The structure contains three types of sodium atoms. The Na(1) and Na(2) atoms are located in the interlayer space occupying the centres of the octahedra, which are formed by the oxygen atoms belonging only either to the phosphate [Na(1)] or

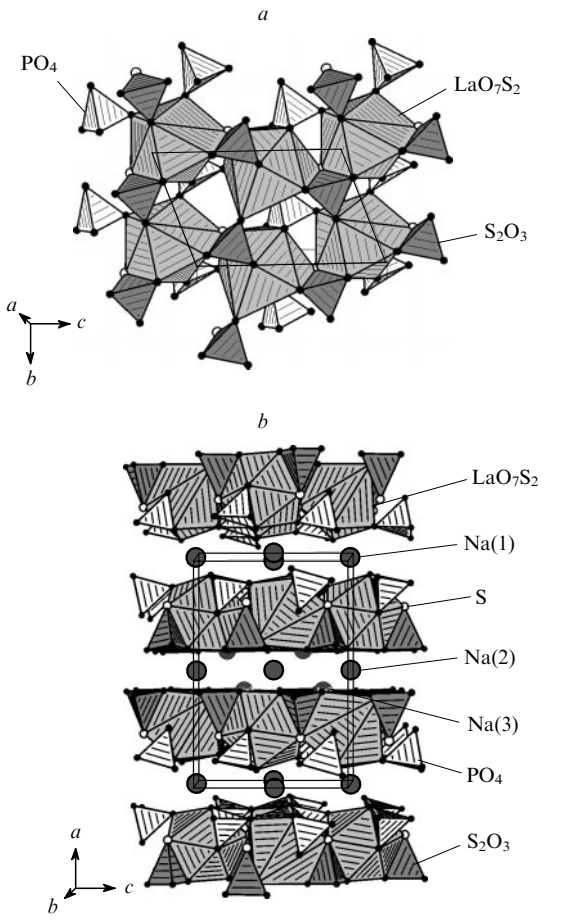



**Figure 30.** Structure of $Na_2La(PO_4)(S_2O_3)$ projected onto the $bc$ plane (*a*) and the chains of the $LaO_7S_2$ polyhedra linked through the $PO_4$ and $S_2O_3$ tetrahedra (*b*).

thiosulfate [Na(2)] groups. The Na(3) atoms are in an octahedral environment formed by the oxygen atoms belonging to four $S_2O_3^{2-}$ anions and one $PO_4^{3-}$ anion.

A new structural type for the $Na_2La(PO_4)(S_2O_3)$ compound would be expected to occur by analogy with the $Na_2Y(PO_4)$. $(MoO_4)$ compound combining the $PO_4^{3-}$ and $MoO_4^{2-}$ anions. However, analysis of the polyhedra demonstrated that the structure of $Na_2La(PO_4)(S_2O_3)$ is derived from glaserite $K_3Na(SO_4)_2$. The difference is that one-half of positions, which are occupied by the alkali-metal cations in the structures of glaserite-like double phosphates [for example, in $K_3M^{III}(PO_4)_2$, where $M^{III}$ = Lu, Sc], are vacant in the structure of $Na_2La(PO_4)(S_2O_3)$. These changes in the cation composition lead to the appearance of a superstructure in $Na_2La(PO_4)(S_2O_3)$ resulted from doubling of the unit cell parameter $a$ corresponding to the parameter $c$ in the glaserite structure. In addition, the incorporation of the $S_2O_3^{2-}$ ion into complex phosphate has a substantial effect on thermal stability of the $Na_2La(PO_4)(S_2O_3)$ compound. Thus, the decomposition temperature of the $Na_2La(PO_4)(S_2O_3)$ compound is 313 °C, whereas this temperature for $Na_3La(PO_4)_2$ is much higher (1000 °C). The data from powder X-ray diffraction analysis and the results of IR and Raman spectroscopy for the decomposition product of $Na_2La(PO_4)(S_2O_3)$ (after TGA) demonstrated that sodium lanthanum phosphate thiosulfate decomposes to form a compound of unknown composition containing the $PO_4^{3-}$ and $SO_4^{2-}$ ions in the anion sublattice.

Recently, a series of new phases with composition $Li_{3-x}Fe_2(PO_4)(SO_4)_2$ were prepared.[159] In these compounds, $x$ depends on the content of iron in oxidation states 2+ and 3+. The redox potential of the $LiFe_2(PO_4)(SO_4)_2$ compound (3.4 eV) is higher than that of its monoanion precursor $Li_3Fe_2(PO_4)_3$

(2.8 eV), and this compound is a promising electrodic material for recharging lithium batteries.

The above-considered examples demonstrate that the $M^I_xM^{III}_y(PO_4)(EO_4)_2$ compounds possess new or improved properties (important for technical applications) as compared to monoanion complex phosphates. The total negative charge of the anionic portion of the compound can be changed by replacing the $PO_4$ groups in the anion sublattices of complex phosphates by the tetrahedral $EO_4$ groups (E = V, Mo, S), which allows one to change the number of cations and size characteristics of the cavities of framework structures and of the interlayer spaces in layered phases.

## VII. Conclusion

A comparison of the crystal structures of different groups of complex phosphates containing mono- and trivalent cations not only reveals the similarity of formal characteristics (composition, simplest structural polyhedra) among these compounds but also enables one to establish their structural features depending on the size factors (ionic radii of the $M^I$ and $M^{III}$ cations), nature of the cations and anions, combinations of different anions, presence of water molecules and OH groups and hydrogen bonding.

Compositions with the ratio $M^{III}:PO_4^{3-}$ or $M^{III}:(PO_4^{3-} + EO_4^{2-})$ equal to 1 : 2, for example, $M^I_3M^{III}(PO_4)_2$, $M^IM^{III}(HPO_4)_2$ and $M^I_2M^{III}(PO_4)(EO_4)$, are typical of simple double phosphates, hydrogen phosphates and phosphates whose anionic portions contain the $PO_4$ groups together with other $EO_4$ tetrahedra ($EO_4 = MoO_4$, $S_2O_3$). Simple hydroxide phosphates and fluoride phosphates have related structures corresponding to the formulas $M^IM^{III}(OH)PO_4$ and $M^IM^{III}FPO_4$. A limited number of compositions and structural types are known for simple double phosphates. A complication of the anionic portion of double phosphates and the presence of water molecules in these compounds lead to the formation of complex phosphates of different types (fluoride phosphates, hydrogen phosphates containing different $H_nPO_4^{3-n}$ anions and hydroxide phosphates), which differ both in composition and structure. In most representatives of complex phosphates containing mono- and trivalent cations, the ionic radius of the $M^{III}$ cation is no larger than 0.8 Å (Al, V, Fe, Cr, Sc, Ga, In). Compounds containing REE or Y are known only for double phosphates and fluoride phosphates.

Changes in the ionic radii of the $M^I$ and $M^{III}$ cations (particularly, in the REE series) both in compositionally different and analogous groups of compounds are accompanied by a change in the structural type. In the case of sodium derivatives, which are most prone to polymorphism, the structural changes associated with a change in the size of the $M^{III}$ cation and synthesis conditions are most pronounced (see Fig. 1 and Table 3).

The structures of complex phosphates of all the above-considered types are built from the $M^{III}O_x$, $M^{III}O_x(H_2O)_y$ or $M^{III}O_{x-y}[F,(OH)]_y$ polyhedra ($x = 6-8$ and $y = 2-4$) and the $PO_4$ or $H_nPO_4$ polyhedra (the $EO_4$ tetrahedra can partially replace the $PO_4$ tetrahedra). The polyhedra about the $M^{III}$ cations with the ionic radii $r \leqslant 0.8$ Å are octahedra distorted to a greater or lesser extent. The vertices of the octahedra are occupied by the oxygen atoms of the $PO_4$, $H_nPO_4$, $EO_4$ or OH groups or water molecules. In the case of fluoride phosphates, the F atoms can also be involved in the coordination polyhedra. In the structures of double REE phosphates and fluoride phosphates, the REE atoms adopt the coordination numbers of 7, 8 and 9.

The partial replacement of the $PO_4^{3-}$ anions by the $H_nPO_4^{3-n}$ ($n = 1, 2$), $EO_4^{n-}$, $F^-$ or $OH^-$ anions and changes in the ratios $r(M^I):r(M^{III})$, $M^I:M^{III}$ and $M^{III}:PO_4$ ($H_nPO_4^{3-n}$, $n = 0-2$) lead to the formation of more complex structural ensembles based on either framework or layered constructions. Layered structures are typical of compounds with a high content of the $M^I$ (or $M^I + H^+$) cations with respect to the $M^{III}$ cations. This relationship is observed in most of the group of compounds considered above, *viz.*, in double phosphates $M^I_3M^{III}(PO_4)_2$, fluoride phosphates $M^I_5M^{III}F_2(PO_4)_2$, hydrogen phosphates $M^IM^{III}_3(H_2PO_4)_6.(HPO_4)_2$ and phosphates containing an $EO_4$ tetrahedron along with the $PO_4$ tetrahedron, for example, in $Na_2Y(PO_4)(MoO_4)$ and $Na_2La(PO_4)(S_2O_3)$. One-dimensional motifs are observed in compounds characterised by a high content of alkali-metal cations and the presence of hydroxy groups, for example, in $M^I_3M^{III}(OH)(HPO_4)(PO_4)$ and $M^I_4M^{III}(OH)(PO_4)_2$.

A decrease in the $M^I:M^{III}$ ratio results in the formation of framework structures typical of most of representatives of these groups of compounds, in particular, of $M^I_3M^{III}_2(PO_4)_3$, $M^IM^{III}(HPO_4)_2$, $M^IM^{III}(OH)(PO_4)$, $M^IM^{III}FPO_4$ and $M^I_3M^{III}_2F_3(PO_4)_2$. In framework structures, the $M^{III}O_x$ or $M^{III}O_{x-y}[F,(OH)]_y$ polyhedra are linked to each other through either tetrahedral groups (in double and hydrogen phosphates) or fluoride and hydroxy groups (in fluoride phosphates and hydroxide phosphates, respectively).

The character of the structures depends substantially on the presence of the $H_nPO_4^{3-n}$ cations, OH groups and $H_2O$ molecules in the coordination sphere about the $M^{III}$ cation, which is associated with the involvement of these groups and molecules in the formation of rather strong hydrogen bonds.

Complex phosphates can be used in the design of polyfunctional materials. Compounds of REE and Sc containing the $PO_4^{3-}$ anions together with the $VO_4^{3-}$ anions are of particular interest. The formation of solid solutions based of double REE- and Sc-containing phosphates and vanadates allows one to vary the luminescent, sorption and other properties of the materials rather accurately by changing the $PO_4^{3-}:VO_4^{3-}$ ratio. Phosphate vanadates selective absorb $H_2O$, $CO_2$ and various organic molecules from the gas phase. Europium-doped compounds of this type containing Sc, Y and REE possess luminescent properties. It is also highly probable that REE fluoride phosphates and phosphate vanadates will exhibit catalytic properties. Phosphate vanadates of REE can be used also in the construction of nonlinear optical materials.

Phosphates with composition $M^I_3M^{III}_2(PO_4)_3$ ($M^I$ = Li, Na; $M^{III}$ = Sc, In, Fe) are ionic conductors. Some representatives of hydrogen phosphates possess proton conductivity. A number of these compounds (with zeolite-type structures) are of interest as new ion exchange phases. The fact that most of the complex phosphates belong to dielectric compounds provides the basis for the preparation of dielectric materials for different purposes.

* * *

When this review was already in preparation, new data on the synthesis, crystal structures and properties of two groups of complex phosphates, *viz.*, $M^IM^{III}(HPO_4)_2$ and $M^IM^{III}_2(OH).(PO_4)_2\cdot 2H_2O$, were reported. Thus, we have expected that indium hydrogen phosphates $M^IIn(HPO_4)_2$ ($M^I$ = Li, Na, Ag, Rb),[160] scandium hydrogen phosphates $M^ISc(HPO_4)_2$ ($M^I$ = K, Rb, $NH_4$) and iron hydrogen phosphate β-$RbFe(HPO_4)_2$ would occur, and this assumption was confirmed. All these compounds, except for $KSc(HPO_4)_2$ (space group *Pnma*), crystallise in the monoclinic system (space group $P2_1/c$). The above-listed hydrogen phosphates either widen the range of representatives of the known structural type β-$RbV(HPO_4)_2$ (see Ref. 62), for example, $\beta_1$-$RbIn(HPO_4)_2$, β-$RbFe(HPO_4)_2$ and $M^ISc(HPO_4)_2$, where $M^I$ = K, Rb, $NH_4$, or form unique framework structures, for example, $M^IIn(HPO_4)_2$, where $M^I$ = Li, Na, Ag. Our assumption that the structural group of the mineral leucophosphite must involve also rubidium hydroxide phosphate $RbGa_2(OH).(PO_4)_2\cdot 2H_2O$ was also confirmed.[161]

## References

1. P P Mel'nikov, L N Komissarova *Koord. Khim.* **12** 1299 (1986) [a]
2. I A Bondar', N V Vinogradova, L N Dem'yanets *Soedineniya RZE. Silikaty, Fosfaty, Arsenaty, Vanadaty* (Compounds of REE. Silicates, Phosphates, Arsenates and Vanadates) (Moscow: Nauka, 1983)

3. I V Tananaev, V P Orlovskii *Zh. Neorg. Khim.* **31** 1923 (1986) [b]
4. T A Slivko, I N Smirnova, F M Spiridonov, G V Zimina, N N Chudinova *Zh. Neorg. Khim.* **47** 202 (2002) [b]
5. I Szczygiel, T Znamierowska *J. Solid State Chem.* **95** 260 (1991)
6. G V Zimina, I N Smirnova, S I Kudryashova, F M Spiridonov, I F Poletaev *Zh. Neorg. Khim.* **35** 2134 (1990) [b]
7. W Jungowska, T Znamierowska *J. Solid State Chem.* **95** 265 (1991)
8. B N Litvin, V A Masloboev *Redkozemel'nye Fosfaty* (Rare-Earth Phosphates) (Leningrad: Nauka, 1989)
9. P P Mel'nikov, L N Komissarova *Dokl. Akad. Nauk SSSR* **256** 878 (1981) [c]
10. A I Kryukova, I A Korshunov, E P Moskvichev, V A Mitrofanova, N V Vorob'eva, G N Kazantsev, O V Skiba *Zh. Neorg. Khim.* **21** 2560 (1976) [b]
11. A I Kryukova, I A Korshunov, V A Mitrofanova, N V Vorob'eva, G N Kazantsev, O V Skiba *Zh. Neorg. Khim.* **22** 2301 (1977) [b]
12. L N Komissarova, P P Mel'nikov, Sh B Ibragimov, E G Zaugol'nikova *Dokl. Akad. Nauk SSSR* **295** 911 (1987) [c]
13. C Parent, G Demazeau, R Salmon, G Le Flem *Rev. Chim. Miner.* **16** 548 (1979)
14. K-H Lii *Eur. J. Solid State Inorg. Chem.* **33** 519 (1996)
15. C E Bamberger, P R Robinson, R L Sherman *Inorg. Chim. Acta* **34** L203 (1979)
16. T A Butuzova, Candidate Thesis in Chemical Sciences, Moscow State University, Moscow, 1983
17. M Toumi, L Smiri-Dogguy, A Bulou *Eur. J. Inorg. Chem.* 1545 (1999)
18. K Okada, U Ossaka *Acta Crystallogr., Sect. B, Struct. Crystallogr.* **36** 919 (1980)
19. M T Robinson *J. Phys. Chem.* **62** 925 (1958)
20. J K Nimmo *Acta Crystallogr., Sect. B, Struct. Crystallogr.* **37** 431 (1981)
21. B I Lazoryak *Usp. Khim.* **65** 307 (1996) [*Russ. Chem. Rev.* **65** 287 (1996)]
22. V A Efremov, P P Melnikov, L N Komissarova *Rev. Chim. Miner.* **22** 666 (1985)
23. R D Shannon *Acta Crystallogr., Sect. A, Fund. Crystallogr.* **32** 751 (1976)
24. V A Morozov, B I Lazoryak, A P Malakho, K V Pokholok, S N Polyakov, T P Terekhina *J. Solid State Chem.* **160** 377 (2001)
25. V B Kalinin, S Yu Stefanovich, in *Khimiya Tverdogo Tela (Itogi Nauki i Tekhniki)* [Solid State Chemistry (Advanced in Sciences and Engineering Series)] (Moscow: Izd. VINITI, 1992) p. 51
26. V A Efremov, P P Mel'nikov, L N Komissarova *Koord. Khim.* **17** 467 (1981) [a]
27. H Y-P Hong, S R Chinn *Mater. Res. Bull.* **11** 421 (1976)
28. L N Komissarova, A P Bobylev, A N Kirichenko, G Ya Pushkina, F M Spiridonov *Zh. Neorg. Khim.* **47** 684 (2002) [b]
29. M G Zhizhin, A A Filaretov, A V Olenev, V V Chernyshev, F M Spiridonov, L N Komissarova *Kristallografiya* **47** 800 (2002) [e]
30. F Mazzi, L Ungaretti *Neues Jahrb. Miner. Monatsh.* **2** 49 (1994)
31. M G Zhizhin, L N Komissarova, V A Morozov, F M Spiridonov *Phosph. Res. Bull.* **11** 102 (2000)
32. M G Zhizhin, V A Morozov, A P Bobylev, A M Popov, F M Spiridonov, L N Komissarova, B I Lazoryak *J. Solid State Chem.* **149** 99 (2000)
33. R Salmon, C Parent, M Vlasse, G Le Flem *Mater. Res. Bull.* **13** 439 (1978)
34. R Salmon, C Parent, M Vlasse, G Le Flem *Mater. Res. Bull.* **14** 85 (1979)
35. A Arakcheeva, G Chapuis, M Zhizhin, in *Aperiodic Structures: Satellite Meeting of 20th European Crystallographic Meeting* (Krakow: EJB, 2001) p. 296
36. M Pintard-Scrépel, F d'Yvoire, J Durand *Acta Crystallogr., Sect. C, Cryst. Struct. Commun.* **39** 9 (1983)
37. B A Maksimov, L A Muradyan, E A Genkina, V I Simonov *Dokl. Akad. Nauk SSSR* **288** 634 (1986) [c]
38. E A Genkina, L A Muradyan, B A Maksimov *Kristallografiya* **31** 595 (1986) [d]
39. D Tran Qui, S Hamdoune *Acta Crystallogr., Sect. C, Cryst. Struct. Commun.* **43** 397 (1987)
40. C Masquelier, C Wurm, J Rodriguez-Carvajal, J Gaubicher, L Nazar. *Chem. Mater.* **12** 525 (2000)
41. T Suzuki, K Yoshida, K Uematsu, T Kodama, K Toda, Z-G Ye, M Ohashi, M Sato *Solid State Ion.* **115** 89 (1998)
42. E A Genkina, L A Muradyan, B A Maksimov, B V Merinov, S E Sigarev *Kristallografiya* **32** 74 (1987) d
43. N Fanjat, J L Soubeyroux *J. Magn. Magn. Mater.* **104** 933 (1992)
44. V A Efremov, V B Kalinin *Kristallografiya* **23** 703 (1978) [d]
45. K-H Lii, J Ye *J. Solid State Chem.* **131** 131 (1997)
46. E A Genkina, V B Kalinin, B A Maksimov, A M Golubev *Kristallografiya* **36** 1126 (1991) [d]
47. B I Lazoryak, V B Kalinin, S Yu Stefanovich, V A Efremov *Dokl. Akad. Nauk SSSR* **250** 861 (1980) [c]
48. J Winand, A Rulmont, P Tarte *J. Mater. Sci.* **25** 4008 (1990)
49. J Goodenough, H Hong, J Kafalas *Mater. Res. Bull.* **11** 203 (1976)
50. D Antenucci, G Miehe, P Tarte, W W Schmahl, A-M Fransolet *Eur. J. Miner.* **5** 207 (1993)
51. M Kloss, B Finke, L Schwarz, D Haberlandl *J. Lumin.* **72** 684 (1997)
52. M Vlasse, C Parent, R Salmon, G Le Flem, P Hagenmuller *J. Solid State Chem.* **35** 318 (1980)
53. C Parent, P Bochu, A Daoudi, G Le Flem *J. Solid State Chem.* **42** 190 (1982)
54. L N Zorina, Zh A Ezhova, V P Orlovskii, E M Koval', N P Soshchin *Izv. Akad. Nauk SSSR, Neorg. Mater.* **15** 1116 (1979) [e]
55. Y Miyajima, T Miyoshi, J Tamaki, M Matsuoka, Y Yamamoto, C Masquelier, M Tabuchi, Y Saito, H Kageyama *Solid State Ion.* **124** 201 (1999)
56. A A Filaretov, M G Zhizhin, A V Olenev, A A Gurkin, A P Bobylev, B I Lazoryak, L N Komissarova, V P Danilov *Zh. Neorg. Khim.* **47** 1930 (2002) [b]
57. J-X Mi, Y-X Huang, S-Y Mao, X-D Huang, Z-B Wei, Z-L Huang, J-T Zhao *J. Solid State Chem.* **157** 213 (2001)
58. K-H Lii *Inorg. Chem.* **35** 7440 (1996)
59. S M Stalder, A P Wilkinson *J. Mater. Chem.* **8** 261 (1998)
60. K-H Lii, L-S Wu *J. Chem. Soc., Dalton Trans.* 1577 (1994)
61. R C Haushalter, Z W Wang, M E Thompson, J Zubieta *Inorg. Chim. Acta.* **232** 83 (1995)
62. R C Haushalter, Z W Wang, M E Thompson, J Zubieta *Inorg. Chem.* **32** 3700 (1993)
63. S S Dhingra, R C Haushalter *J. Solid State Chem.* **112** 96 (1994)
64. N Anisimova, N Chudinova, R Hoppe, M Serafin *Z. Anorg. Allg. Chem.* **623** 39 (1997)
65. S Dick, U Gossner, A Weiss, C Robl, G Grossmann, G Ohms, M Mueller *J. Solid State Chem.* **132** 47 (1997)
66. Z Bircsak, W T A Harrison *Acta Crystallogr., Sect. C, Cryst. Struct. Commun.* **54** 1195 (1998)
67. I Vencato, E Mattievich, L deF Moreira, Y P Mascarenhas *Acta Crystallogr., Sect. C, Cryst. Struct. Commun.* **45** 367 (1989)
68. O V Yakubovich *Kristallografiya* **38** 43 (1993) [d]
69. M P Attfield, A K Cheetham, S Natarajan *Mater. Res. Bull.* **35** 1007 (2000)
70. A Goni, L Lezama, A Espina, C Trobajo, J R Garcia, T Rojo *J. Mater. Chem.* **11** 2315 (2001)
71. S Ekambaram, C Serre, G Ferey, S C Sevov *Chem. Mater.* **12** 444 (2000)
72. D H Olsen *J. Phys. Chem.* **74** 2758 (1970)
73. D Brodalla, R Kniep *Z. Naturforsch., B Chem. Sci.* **35** 403 (1980)
74. W P Bosman, P T Beurskens, J M Smits, H Behm, J Mintjens, W Meisel, J C Fuggle *Acta Crystallogr., Sect. C, Cryst. Struct. Commun.* **42** 525 (1986)
75. N Anisimova, N Chudinova, M Serafin *Z. Anorg. Allg. Chem.* **623** 1708 (1997)
76. A Mgaidi, H Boughzala, A Driss, R Clerac, C Coulon *J. Solid State Chem.* **144** 163 (1999)
77. O V Yakubovich, M S Dadashov *Kristallografiya* **33** 848 (1988) [d]
78. P B Moore, T Araki *Am. Miner.* **64** 587 (1979)
79. G V Zimina, I N Smirnova, M Yu Gorkovenko, F M Spiridonov, L N Komissarova, N I Kaloev *Zh. Neorg. Khim.* **39** 1567 (1994) [b]
80. G V Zimina, I N Smirnova, M Yu Gorkovenko, F M Spiridonov, L N Komissarova *Zh. Neorg. Khim.* **40** 1578 (1995) [b]
81. L A Groat, M Raudsepp, F C Hawthorne, T S Ercit, B L Sherriff, J S Hartman *Am. Miner.* **75** 992 (1990)
82. V I Simonov, N V Belov *Kristallografiya* **3** 428 (1958) [d]
83. E A Genkina, Yu K Kabalov, B A Maksimov, O K Mel'nikov *Kristallografiya* **29** 50 (1984) [d]
84. S Lathi *Am. Miner.* **70** 849 (1985)

85. O V Yakubovich, M A Simonov, O K Mel'nikov *Kristallografiya* **29** 484 (1984) [d]
86. W T A Harrison, M L F Phillips, G D Stucky *Chem. Mater.* **7** 1849 (1995)
87. J-M Le Meins, M-P Crosnier-Lopez, A Hemon-Ribaud, G Courbion *J. Solid State Chem.* **148** 260 (1999)
88. O V Yakubovich, O K Mel'nikov *Kristallografiya* **41** 663 (1996) [d]
89. N S Slobodyanik, P G Nagornyi, Z I Kornienko, A A Kapshuk, V V Mitkevich *Zh. Neorg. Khim.* **34** 2473 (1989) [b]
90. O V Yakubovich, O K Mel'nikov, V S Urusov *Dokl. Akad. Nauk SSSR* **342** 615 (1995) [c]
91. D M Poojary, A Clearfield, V A Timofeeva, S E Sigaryov *Solid State Ion.* **73** 75 (1994)
92. P G Nagornyi, A A Kapshuk, Z I Kornienko, V V Mitkevich, S M Tret'yak *Zh. Neorg. Khim.* **35** 839 (1990) [b]
93. R K Rastsvetaeva, B A Maksimov, V A Timofeeva *Dokl. Akad. Nauk* **350** 499 (1996) [c]
94. A M Golubev, B A Maksimov, N E Klokova, O K Mel'nikov, V A Timofeeva, N I Sorokina, V I Simonov *Kristallografiya* **34** 1574 (1989) [d]
95. B Maximov, M Sirota, S Werner, H Schulz *Acta Crystallogr., Sect. B, Struct. Crystallogr.* **55** 259 (1999)
96. J Arlt, M Jansen, H Klassen, G Schimmel, G Heymer *Z. Anorg. Allg. Chem.* **547** 179 (1987)
97. M Mathew, I Mayer, B Dickens, L W Schroeder *J. Solid State Chem.* **28** 79 (1979)
98. M Toumi, L Smiri-Dogguy, A Bulou *J. Solid State Chem.* **149** 308 (2000)
99. I Mayer, S Cohen *J. Solid State Chem.* **48** 17 (1983)
100. D Zambon, M El-Ghozzi, D Avignant, N Ben Said, I Mansouri *J. Chim. Phys.* **88** 1963 (1991)
101. O L Slovokhotova, G D Ilyushin, N S Triodina, O K Mel'nikov, L N Dem'yanets, R G Gerr, V G Tsirel'son *Zh. Neorg. Khim.* **32** 103 (1991) [b]
102. O V Yakubovich, M A Simonov, E N Matvienko, N V Belov *Dokl. Akad. Nauk SSSR* **238** 576 (1978) [c]
103. F Taulelle, T Loiseau, J Maquet, J Livage, G Fgrey *J. Solid State Chem.* **105** 191 (1993)
104. G Férey, T Loiseau, P Lacorre, F Taulelle *J. Solid State Chem.* **105** 179 (1993)
105. T Loiseau, Y Calage, P Lacorre, G Ferey *J. Solid State Chem.* **111** 390 (1994)
106. T Loiseau, C Paulet, N Simon, V Munch, F Taulelle, G Ferey *Chem. Mater.* **12** 1393 (2000)
107. R Yu, D Wang, T Takei, H Koizumi, N Kumada, N Kinomura *J. Solid State Chem.* **157** 180 (2001)
108. W Massa, O V Yakubovich, O V Karimova, L N Dem'yanets *Acta Crystallogr., Sect. C, Cryst. Struct. Commun.* **51** 1246 (1995)
109. L Yu, W Pang *Gaodeng Xuexiao Huaxue Xuebao* **12** 1137 (1991)
110. M G Zhizhin, A V Olenev, F M Spiridonov, L N Komissarova, O G D'yachenko *J. Solid State Chem.* **157** 8 (2001)
111. M A Strelkov, M G Zhizhin, F M Spiridonov, A P Bobylev, L N Komissarova *Zh. Neorg. Khim.* **46** 1629 (2001 [b]
112. S J Kirkby, A J Lough, G A Ozin *Z. Kristallogr.* **210** 956 (1995)
113. E L Belokoneva, O V Yakubovich, V G Tsirel'son, V S Urusov *Dokl. Akad. Nauk SSSR* **310** 1129 (1990) [c]
114. E L Belokoneva, O L Slovokhotova, M Yu Antipin, V G Tsirel'son, Yu T Struchkov *Dokl. Akad. Nauk* **322** 520 (1992) [c]
115. N S Slobodyanik, P G Nagornyi, Z I Kornienko, A A Kapshuk *Zh. Neorg. Khim.* **36** 1390 (1991) [b]
116. G D Stucky, M L F Phillips, T E Gier *Chem. Mater.* **1** 492 (1989)
117. K-H Lii *J. Chem. Soc., Dalton Trans.* 815 (1996)
118. P E Machie, R A Young *J. Appl. Crystallogr.* **6** 26 (1973)
119. M Tachihante, D Zambon, J-C Cousseins *Eur. J. Solid State Inorg. Chem.* **33** 713 (1996)
120. *Powder Diffraction File Card 42-1412, JCPDS* International Center of Diffraction Data, Swartmore, PA
121. P B Moore *Am. Miner.* **57** 397 (1972)
122. S Dick, T Zeiske *J. Solid State Chem.* **133** 508 (1997)
123. P Dunn *Am. Miner.* **69** 374 (1984)
124. O V Yakubovich, M S Dadashov *Kristallografiya* **37** 1403 (1992) [d]
125. M Cavellec, D Riou, G Ferey *Acta Crystallogr., Sect. C, Cryst. Struct. Commun.* **50** 1379 (1994)
126. D Cozzupoli, O Grubessi, A Mottana, P F Zanazzi *Miner. Petrol.* **37** 1 (1987)
127. J A Hriljac, C P Grey, A K Cheetham, P D VerNooy, C C Torardi *J. Solid State Chem.* **123** 243 (1996)
128. V Soghomonian, L A Meyer, R C Haushalter, J Zubieta *Inorg. Chim. Acta* **275**–**276** 122 (1998)
129. R N Devi, K Vidyasagar *J. Chem. Soc., Dalton Trans.* 3841 (1999)
130. J Parise *Acta Crystallogr., Sect. C, Cryst. Struct. Commun.* **40** 1641 (1984)
131. J J Pluth, J V Smith, J M Bennett, J P Cohen *Acta Crystallogr., Sect. C, Cryst. Struct. Commun.* **40** 2008 (1984)
132. M P Attfield, R E Morris, I Burshtein, C F Campana, A K Cheetham *J. Solid State Chem.* **118** 412 (1995)
133. K-H Lii, S-L Wang *J. Solid State Chem.* **128** 21 (1997)
134. M A G Aranda, S Bruque, J P Attfield, F Palacio, R B Von Dreele *J. Solid State Chem.* **132** 202 (1997)
135. A A Filaretov, M G Zhizhin, L N Komissarova, V P Danilov, V V Chernyshev, B I Lazoryak *J. Solid State Chem.* **166** 362 (2002)
136. P G Nagornyi, A A Kapshuk, N V Stus', N S Slobodyanik *Kristallografiya* **35** 634 (1990) [d]
137. L Fanfani, A Nunzi, P F Zanazzi *Miner. Mag.* **37** 598 (1970)
138. S Dick, G Grossmann, G Ohms, M Mueller *Z. Naturforsch., B Chem. Sci.* **52** 1447 (1997)
139. R C L Mooney *Acta Crystallogr.* **20** 526 (1966)
140. T Loiseau, G Ferey *Eur. J. Solid State Inorg. Chem.* **31** 575 (1994)
141. F C Hawthorne *Tschermaks Mineral. Petrogr. Mitt.* **31** 121 (1983)
142. H E King, L A Mundi, K G Strohmaier, R C Haushalter *J. Solid State Chem.* **92** 1 (1991)
143. A Leclaire, M M Borel, A Grandin, B Raveau *J. Solid State Chem.* **108** 177 (1994)
144. J B Parise *Inorg. Chem.* **24** 4312 (1985)
145. M S Dadashov, Candidate Thesis in Geological and Mineralogical Sciences, Moscow State University, Moscow, 1986
146. P B Moore, T Araki *Am. Miner.* **59** 964 (1974)
147. P B Moore, T Araki *Am. Miner.* **62** 692 (1977)
148. H Monma *J. Catal.* **75** 200 (1982)
149. H Owada, K Yamashita, T Umegaki, T Kanazawa *Solid State Ion.* **35** 401 (1989)
150. L Hench *J. Am. Ceram. Soc.* **74** 1487 (1991)
151. A Laghzizil, A Bouhaouss, P Barboux, R Morineau J Livage *Solid State Ion.* **67** 137 (1993)
152. A Laghzizil, S El Hajjaji, A Bouhaouss, M Ferhat *Solid State Ion.* **126** 245 (1999)
153. A N Kirichenko, S N Bessonov, V I Yurchenko, A P Bobylev, L N Komissarova *Neorg. Mater.* **35** 877 (1999) [e]
154. A N Kirichenko, E N Otkidach, F M Spiridonov, V F Kharsika, L N Komissarova *Zh. Neorg. Khim.* **44** 1061 (1999) [b]
155. V F Kharsika, L N Komissarova, A N Kirichenko, E N Murav'ev, V P Orlovskii, A P Chernyaev *Neorg. Mater.* **37** 981 (2001) [e]
156. V F Kharsika, L N Komissarova, A N Kirichenko, E N Murav'ev, V P Orlovskii, A P Chernyaev *Neorg. Mater.* **37** 1130 (2001) [e]
157. M Ben Amara, M Dabbabi *Acta Crystallogr., Sect. C, Cryst. Struct. Commun.* **43** 616 (1987)
158. M G Zhizhin, F M Spiridonov, L N Komissarova, P K Dorhout, in *The 20th European Crystallographic Meeting (Book of Abstracts), Krakow, 2001* S8.M1.P2
159. A K Padhi, V Manivannan, J B Goodenough *J. Electrochem. Soc.* **145** 1518 (1998)
160. A A Filaretov, L N Komissarova, V P Danilov, in *XXXVIII Vserossiisk. Nauch. Konf. po Problemam Matematiki, Informatiki, Fiziki, Khimii i Metodam Prepodavaniya Estestvennonauchnykh Distsiplin (Tez. Dokl.)* [XXXVIIIth All-Russian Scientific Conference on Mathematics, Information Science, Physics and Chemistry Problems and on the Methods of Teaching of Natural Sciences (Abstracts of Reports)] (Moscow: Peoples' Friendship University of Russia, 2002) p. 27
161. L Beitone, T Loiseau, G Ferey *Acta Crystallogr. Sect. C, Cryst. Struct. Commun.* **58** 103 (2002)

[a] — *Russ. J. Coord. Chem. (Engl. Transl.)*
[b] — *Russ. J. Inorg. Chem. (Engl. Transl.)*
[c] — *Dokl. Chem. (Engl. Transl.)*
[d] — *Crystallogr. Rep. (Engl. Transl.)*
[e] — *Inorg. Mater. (Engl. Transl.)*